PERFORMANCE EVALUATION OF MODIFIED-RECYCLED AGGREGATE CONCRETE

BY

RAYHAN MD. FAYSAL

A Thesis Presented to the
DEANSHIP OF GRADUATE STUDIES

KING FAHD UNIVERSITY OF PETROLEUM & MINERALS
DHAHRAN, SAUDI ARABIA

In Partial Fulfillment of the
Requirements for the Degree of

MASTER OF SCIENCE

In

CIVIL ENGINEERING

JUNE 2019

KING FAHD UNIVERSITY OF PETROLEUM & MINERALS

DHAHRAN- 31261, SAUDI ARABIA

DEANSHIP OF GRADUATE STUDIES

This thesis, written by Rayhan Md. Faysal under the direction of his thesis advisor and approved by his thesis committee, has been presented and accepted by the Dean of Graduate Studies, in partial fulfillment of the requirements for the degree of MASTER OF SCIENCE IN CIVIL ENGINEERING.

Dr. Shamsad Ahmad
(Advisor)

Dr. Salah U. Al-Dulaijan
Department Chairman

Dr. Mohammed Maslehuddin
(Member)

Dr. Salam A. Zummo
Dean of Graduate Studies

Dr. Saheed Kolawole Adekunle
(Member)

26/6/2019
Date

Dedicated to

My Parents

ACKNOWLEDGMENTS

The author is deeply grateful to almighty Allah SWT for enabling him to complete the research in time.

The author would like to express his utmost gratitude to all of his Thesis Committee Members for giving him the opportunity to work in this research area. The author believes that their advices, research proficiencies and personable natures have made working on this research an invaluable experience. The author is especially thankful to his Advisor, Dr. Shamsad Ahmad for his direct support, guidance and encouragement. Moreover, the author is grateful to his Thesis Committee Members Dr. Mohammed Maslehuddin and Dr. Saheed Kolawole Adekunle for their active support and guidance. The author is also thankful to the Civil Engineering Chairman, Dr. Salah U. Al-Duliajan for extending all kinds for supports needed for completing the work on the Thesis.

The author would also like to thank Engr. Mohammed Shameem, Research Engineer, Research Institute, for the necessary support extended by him to carry out the experimental works. The author would also like to express thanks to Engr. Omer Husain, Engr. Syed Imran Ali, and Engr. Syed Khawaja Najamuddin for their supports during the experimental work. Finally, the author would like to express gratitude to his family and the rest of his well-wishers for their continuous support and encouragement.

TABLE OF CONTENTS

LIST OF TABLES

LIST OF FIGURES

LIST OF ABBREVIATIONS

ASTM	:	American Society for Testing and Materials
EDS	:	Energy-Dispersive X-ray Spectrographs
FA	:	Fine Aggregate
ITZ	:	Interfacial transition zone
NA	:	Natural Aggregate
NAC	:	Natural Aggregate Concrete
RA	:	Recycled Aggregate
RAC	:	Recycled Aggregate Concrete
SEM	:	Scanning Electron Micrographs
SP	:	Super Plasticizer
TSMA	:	Two-stage Mixing Approach
w/c	:	water/cement ratio

ABSTRACT

Full Name : Rayhan Md. Faysal

Thesis Title : [Performance Evaluation of Modified-Recycled Aggregate Concrete]

Major Field : [Civil Engineering]

Date of Degree : June 2019

The recent tremendous growth in civil infrastructure has created pressure on the existing sources of natural aggregates as it is the largest ingredient for producing concrete. The scenario becomes more difficult because of the depletion of existing natural sources of aggregates. Consequently, there is a need to utilize recycled coarse aggregates from dismantled concrete structures in the construction of new ones. Few studies have been conducted earlier to utilize recycled aggregates (RA) to produce recycled aggregate concrete (RAC). These studies have reported that the quality of RAC is inferior to that of normal aggregate concrete (NAC) due to the poor quality of RA and the weak interfacial zone between the paste and RA. Therefore, this study was conducted to assess the possibility of improving the quality of RAC using RA treated by adopting different strategies.

Several treatment strategies to overcome the drawbacks of RAC have been reported in the literature. Recently, a trend of using a combination of multiple strategies to improve the properties of RAC has been reported. This study was conducted to develop an optimum strategy for producing RAC of the required quality utilizing locally sourced recycled aggregates. For this purpose, RAC with 40% recycled coarse aggregates was selected since a further increase in the quantity of recycled aggregates has been reported to significantly degrade the properties of RAC. Several trial mixtures were considered to select suitable improvement strategies for RAC. Subsequently, RAC specimens were prepared with the selected improvement strategies and were tested to evaluate their mechanical properties, shrinkage, and durability characteristics.

The workability of the treated RAC mixtures was found to be higher than that of the untreated RAC mixtures. As for hardened properties, three improvement strategies, namely: incorporation of 7% silica fume along with two-stage mixing approach (TSMA), inclusion of 20% GGBFS along with TSMA, and Los Angeles treatment were found useful in improving both the mechanical properties, shrinkage resistance, and durability characteristics of RAC.

ملخص الرسالة

الاسم الكامل: ريحان محمد فيصل

عنوان الرسالة: تقييم الأداء لتعديل--إعادة تدوير الخرسانة الإجمالية

التخصص: الهندسة المدنية

تاريخ الدرجة العلمية حزيران/يونية 2019

لقد أدى النمو الهائل الذي حدث مؤخراً في البنية التحتية المدنية إلى خلق ضغط على المصادر الحالية للركام الطبيعي حيث إنه أكبر مصدر لإنتاج الخرسانة. يصبح السيناريو أكثر صعوبة بسبب استنفاد المصادر الطبيعية الموجودة للركام الطبيعي. وبالتالي هناك حاجة لاستخدام الركام المعاد تدويره من الهياكل الخرسانية المفككة في بناء هياكل جديدة. أجريت دراسات قليلة في وقت سابق لاستخدام الركام المعاد تدويره (RA) لإنتاج خرسانة الركام المعاد تدويره (RAC). أفادت هذه الدراسات أن جودة الـ RAC أدنى من جودة خرسانة الركام العادي (NAC) بسبب رداءة نوعية الـ RA بالإضافة لضعف المنطقة البينية بين عجينة الاسمنت والـ RA. لقد أجريت هذه الدراسة لتقييم إمكانية تحسين جودة الـ RAC.

العديد من الاستراتيجيات أو العلاجات للتغلب على عيوب الـ RAC تم ذكرها في الادبيات. حديثاً، تم ذكر الاتجاه لاستخدام مجموعة من الاستراتيجيات المتعددة لتحسين خصائص الـ RAC. لقد أجريت هذه الدراسة لتطوير استراتيجية مثالية لإنتاج الـ RAC ذي الجودة المطلوبة باستخدام الركام المعاد تدويره من مصادر محلية. لهذا الغرض، تم اختيار RAC بنسبة 40% من الركام المعاد تدويره حيث تم الابلاغ عن تدني جودة الـ RAC مع الزيادة في كمية الركام المعاد تدويره. تم النظر في العديد من المخاليط التجريبية لاختيار استراتيجيات تحسين مناسبة لـ RAC. بالتالي، تم تحضير عينات RAC باستخدام استراتيجيات التحسين المختارة وتم اختبارها لتقييم خواصها الميكانيكية وخصائص ديمومتها.

لقد وجد بأن قابلية تشغيل خلطات RAC المعالجة أعلى من تلك الخاصة بخلطات RAC الغير معالجة. بالنسبة للخصائص الصلبة، فقد تم العثور على ثلاث استراتيجيات للتحسين، وهي: دمج غبار السيليكا بنسبة 7٪ جنباً إلى جنب مع أسلوب الخلط على مرحلتين (TSMA)، وإدراج 20 ٪ من GGBFS الى جانب TSMA، و معالجة لوس انجلوس والتي أدت الى تحسين الخواص الميكانيكية وخصائص الديمومة للـ RAC.

CHAPTER 1

INTRODUCTION

1.1 General

Coarse aggregate is an important component in Portland cement concrete. But, the depleting natural sources of coarse aggregates necessitate the need to find alternative sources [1]. Aggregates retrieved from demolished concrete structures, commonly known as recycled aggregate (RA), can be used as a viable alternative to natural aggregate (NA). Besides, the construction industry in the Arabian Gulf has grown significantly in the past and there is a significant potential for further development. More often, construction of new structures are done after dismantling aged structures while the demolished concrete is not properly disposed causing environmental problems. To address this issue, several studies have been undertaken using crushed concrete obtained from demolished structures to produce new concrete mixtures. Several studies conducted in other parts of the world and few local investigations have indicated that the performance of recycled aggregate concrete (RAC) is marginally inferior to that of natural aggregate concrete (NAC) [2]–[6]. Notwithstanding this trait, efforts have to be made to identify methods that can improve the properties of RAC. A number of studies have been conducted in this direction to develop strategies focusing on improving the performance of RAC. The well-known

strategies and some new ones need to be adopted to enhance the performance of RAC produced by utilizing the local RA.

The focus of this thesis was to assess the performance of a range of strategies to enhance the performance of RAC and identify the most suitable one for the local RA. The development of strategies for enhancing the performance of the local RAC will lead to a useful utilization of the local RA, thus culminating in technical, economic and environmental benefits to the Kingdom. It will also contribute to a sustainable growth of the local construction industry.

1.2 Need for Research

In general, the physical and mechanical properties of RAC are inferior to those of NAC [7]. As shown in Figure 1-1 (a), particles of RAs are made up of old NA particles bound or coated by old mortar.

(a) (b)

Figure 1-1: (a) Untreated and (b) cement-slurry-treated recycled aggregates.

There are several treatment strategies that can be used to improve the properties of RAC. Some treatment strategies focused on improving the quality of the new cement paste or

mortar whereas others concentrated on improving the quality of RA itself either by removing or strengthening the attached mortar on the surface of the RA. Some studies have been conducted on different treatment methods to improve the properties of RA. As an example, Figure 1-1 (b) shows cement-slurry-treated form of the RA in Figure 1-1 (a). Essentially, a comprehensive evaluation of the existing RA improvement strategies, with a view to identifying the most suitable one for the local RA, is necessary.

1.3 Objective

The primary objective of the study was to identify suitable strategies (RA treatment and concrete production methods) for improving the quality of RACs. The specific objectives are as follows:

1. Evaluate the selected strategies for improving the properties of RAC.
2. Assess the workability, mechanical properties, shrinkage, and durability characteristics of the RAC mixtures, developed utilizing the selected strategies.
3. Provide recommendations on the most appropriate RAC improvement strategies.

1.4 Organization of the thesis

The organization of this thesis is outlined in Figure 1-2.

Figure 1-2: Organization of the thesis

CHAPTER 2

LITERATURE REVIEW

The performance of RAC is reported to be inferior to that of NAC in almost all aspects [8]. The inferior quality of the adhered mortar on the RA surface is primarily responsible for the degradation of properties of RAC [7]. Besides, the properties of RA themselves play a major role in shaping the quality of RAC [9]. However, some studies have reported the beneficial properties of RAC. A review of literature on studies conducted both locally and internationally, on the properties of RAC, and strategies adopted to improve the properties of RAC, is presented in the following sub-sections.

2.1 Specific Features of Recycled Aggregate Concrete

The compression or flexural properties of RAC are influenced by the quantity of NA replaced by RA [10] (See Figure 2-1). Katz [2] reported a maximum decrease of 25% for complete use of RA instead of NA. The reduction in the tensile strength of RAC was comparatively less than the reduction in the compressive strength. The maximum reduction was reported to be about 10% [3], [4]. However, it was reported that, in the long term, the tensile strength of RAC may be more than that of NAC [11]. According to Bravo et al. [12], the mechanical properties of RAC are highly dependent on the quality of RA. A reduction of 34% and 43 % in the compressive and tensile strength, respectively, have been reported due to the use of poor-quality RA in producing concrete [11], [12]. The presence

of microcracks and adhered mortar on the RA surface are believed to be responsible for the poor performance of RAC [13].

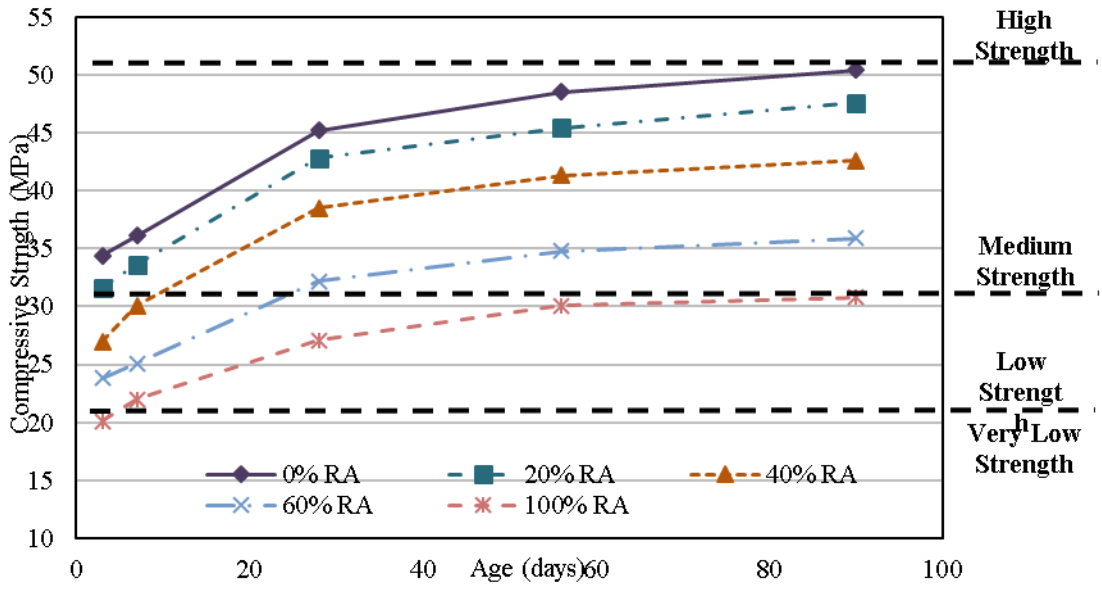

Figure 2-1 : Compressive strength of high strength RAC [7].

In terms of creep and drying shrinkage, it was reported that RAC performed better than NAC [14]. Corinaldesi [15] reported that the drying shrinkage of a particular RAC was 15% lower than that of NAC. But, a contradictory behavior has been reported by Tam et al. [16]. The performance of RAC with 100% RA was reported to be inferior to that of NAC in terms of creep and shrinkage (See Figure 2-2). The modulus of elasticity of RAC was reported to be less than that of NAC. This reduction was significant (20 to 40%) beyond 30% replacement of NA with RA [5]. The bond strength of RAC with reinforcement was reportedly less than that of NAC. According to some researchers [8], [17], it can decrease by up to 19%. Butler et al. [3] reported a strong correlation between split tensile strength of RAC and aggregate crushing value (ACV) of RA. The higher the ACV, lower was the split tensile strength. Further, the workability of RAC was expected

to be less than that of NAC due to the poor quality of RA, its surface texture and high-water absorption. It was suggested that a suitable superplasticizer or rounded RA can be used to overcome this drawback [18].

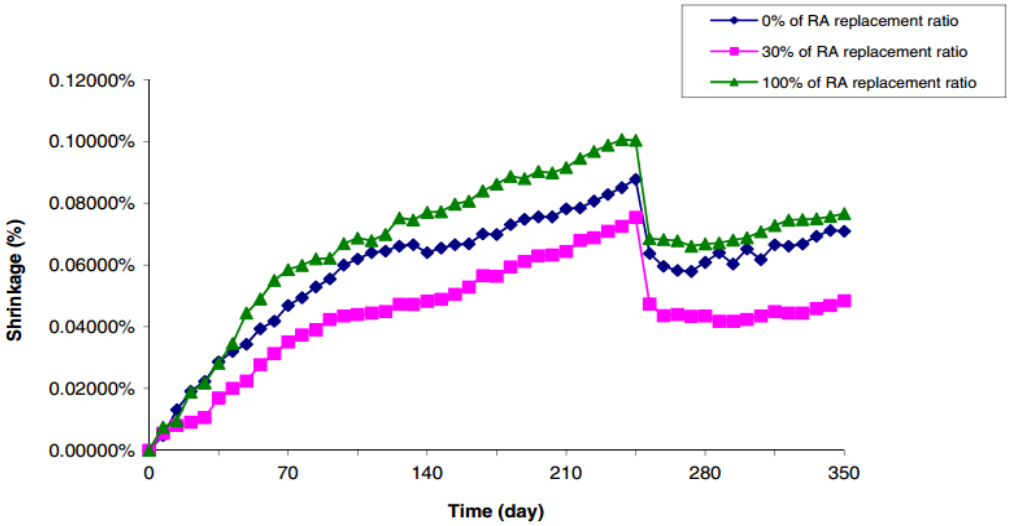

Figure 2-2 : Drying shrinkage of RAC prepared with varying quantity of RA [16].

Ozbakkaloglu et al. [19] investigated the durability and mechanical characteristics of different RACs. It was reported that an increase in the coarse aggregate size from 7 to 12 mm led to an increase in the 28-day elastic modulus (i.e., up to 6%) and a decrease in the 28-day flexural and tensile strength (up to 9 and 11%, respectively). The increase in the elastic modulus was ascribed to the inferior ITZ volume fraction of mixtures prepared with larger coarse aggregates, and the decrease in the tensile strength was explained by the lower mortar strength of mixtures containing larger coarse aggregates produced by their greater effective water-binder ratio. Owing to the higher water absorption of the coarser RA used, mixtures prepared with coarser RA had a higher drying shrinkage (up to 49% at 70 days) and water absorption (up to 30% at 28 days) than those of mixtures prepared with finer RA. RAC with up to 25% RA exhibited close, but slightly inferior, mechanical

properties (up to 5% lower elastic modulus, 8% lower flexural strength, and 8% lower splitting tensile strength) and durability characteristics (up to 4% more water absorption and 12% higher 70-day drying shrinkage) compared to the companion NAC of the same compressive strength. However, the differences between the properties of NAC and RAC containing 100% RA were reported to be significant (up to 14% lower elastic modulus, 27% lower flexural strength, 24% lower splitting tensile strength, 8% higher water absorption and 20% higher 70-day drying shrinkage).

There are several suggestions on the best choice of replacements of NA with RA. According to Corinaldesi [15], 30% replacement of NA with RA will produce concrete having strength of up to 40 MPa. Dilbas et al. [20] also agreed that 30% replacement is an optimum choice. But a detailed investigation by Maslehuddin and Al-Amoudi [7] indicated that 40% NA replacement with RA is optimum considering both mechanical properties and durability characteristics for concrete having medium to high strength. However, for low strength concrete, only 20% RA was suggested. However, considering only the durability aspect, the replacement can be increased up to 60% in medium to high strength concrete. The variation of compressive strength for different replacement levels of RA is depicted in Figure 2-3.

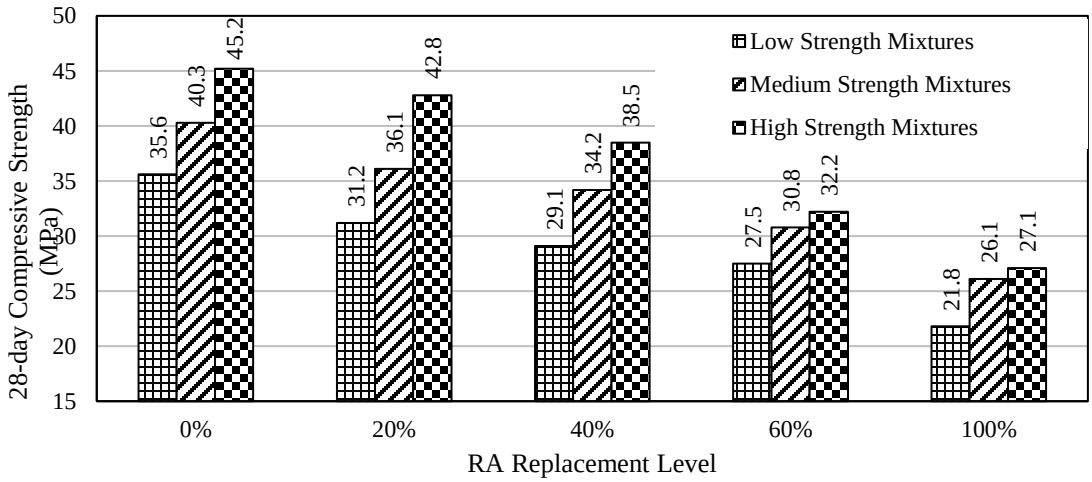

Figure 2-3 : Variation of compressive strength after 28 days of curing for different replacement levels of RA [7].

2.2 Treatments to Improve the Quality of RAC

Various methods or strategies are reported in the literature to improve the quality of RAC (See Figure 2-4). Based on the working principles, they can be broadly categorized as: (i) grading or proportioning strategy, (ii) mixing strategy, (iii) improvement of RA strategy, and (iv) improvement of concrete matrix (mortar) strategy.

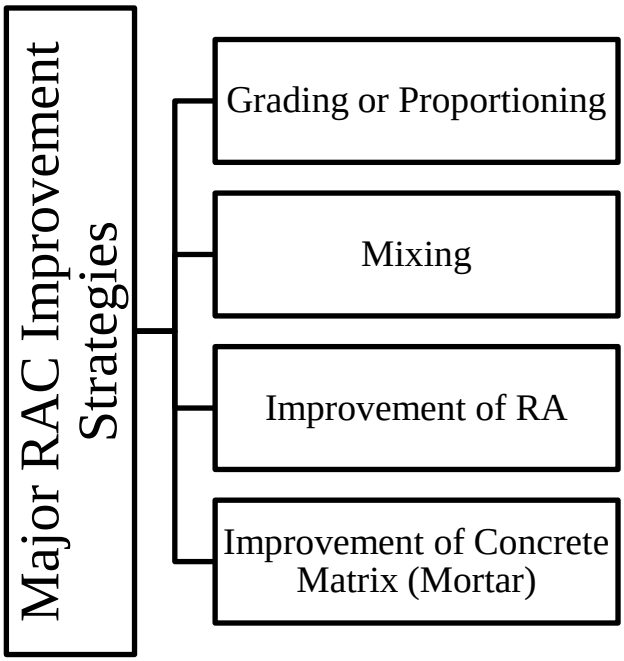

Figure 2-4 : Pictorial representation of major RAC improvement strategies.

Recently, a trend of combining one or more strategies has been reported. A brief review of the recent improvement strategies is presented in the following paragraphs.

Bui et al. [21] improved the mechanical properties of RAC by replacing only larger size particles of RA with NA. With this technique, replacement of NA with RA can be increased to 50% from conventional 30% replacement limit. Pradhan et al. [22] used particle packing concept in their mixture design along with the conventional two-stage mixing approach (TSMA).The resulting RAC for 100% RA showed encouraging results. In the TSMA, coarse aggregates are mixed with cement paste, in a bid to seal cracks on the aggregate surface as well as improving the bond between RA and new cement mortar [23]. A graphical illustration of RA after TSMA is depicted in Figure 2-5. Rajhans et al. [24], [25] upgraded the two-stage mixing approach by adding silica fume and fly ash in the concrete mixture and obtained the desired compressive strength. Adding only silica fume also

improved the strength of RAC [26]–[28]. The inclusion of ground granulated blast furnace slag (GGBFS) in RAC was reported to improve microstructural properties of RAC, hence significant improvement in durability and mechanical properties [29]–[31]. Use of fly ash in RAC also proved to be beneficial in the long run [32], [33].

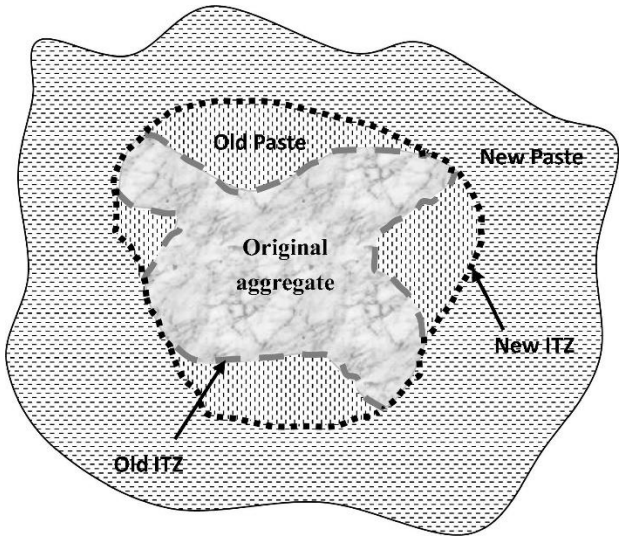

Figure 2-5: Shift in the ITZ due to TSMA [34].

Junak and Sicakova [35] used geopolymer slurry to coat the RA for producing better RAC. They reported that coating during mixing performs better than pre-mix coated RA. Some researchers [36] used nano-slurry to improve the surface of RA. But a combination of normal Portland cement and nano-slurry yielded better performance [37]. Kou et al. [38] used CO_2 treatment to modify the properties of RA. It was reported that the resulting RAC exhibited better durability and mechanical properties. Further, it was stated that the performance can be further enhanced by combining lime water treatment with CO_2 treatment as it will cause inclusion of extra calcium into the mortar pores which leads to an increase in the quality of RA [39]. Sci et al. [40] used three different pozzolana slurries and CO_2 treatment to modify the RA. They reported that silica fume slurry performed better

than other treatments (See Figure 2-6). Akter and Sarmah [41] used silicon-rich char to improve the performance of RAC. Senaratne et al. [42] determined the optimum percentage of steel fiber (0.6%) for 30% NA replacement with RA in producing RAC. Some researchers used crumb rubber [43] or a combination of crumb rubber and silica fume [44] along with steel fibers to improve the properties of RAC. A combination of 10% silica fume and 5% crumb rubber was recommended for steel fiber reinforced RAC [44].

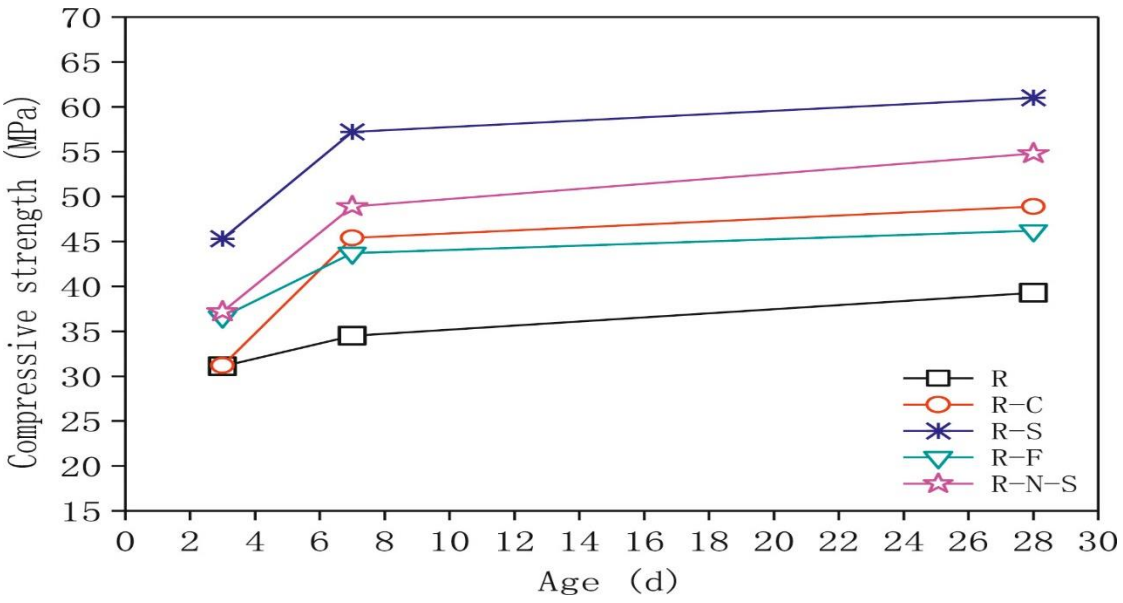

Figure 2-6: Compressive strength of RAC with different treatments [40].

A number of studies reported the use of acid or salt materials to improve the quality of RA by removing the adhering mortar on the surface of RA [45], [46]. Acid treatment (H_2SO_4, HCl, etc.) was found to be better than salt solution (Na_2SO_4) treatment [47]. Kumar and Minocha [48] used acid treatment followed by thermal treatment. They reported that the combined treatment was better than individual treatment. Dimitriou et al. [49] used mechanical action with the help of a rotating machine to increase the removal of adhering mortar on RA from 24% to 9%. They used mechanically treated RA with pozzolana in

producing RAC to improve its performance. A group of researchers used Los angles machine with its charges for the mechanical treatment of the RA [45], [50]. Use of grinder is also reported for the improvement of old mortar removal on RA surfaces[51]. But, the grinding process should be controlled, otherwise there is a possibility of degradation of the quality of RA instead of improvement [52]. Besides, the use of superplasticizer [53], sodium silicate [54], phosphate solution [55], sulfoaluminate cement [56] , slag cement [57] etc. have been reported to improve the properties of RAC. The use of bio materials, such as calcium precipitating bacteria are being investigated recently to enhance the performance of RAC [58], [59]. Although bacterial treatment has shown promising results, further study is needed for its practical application [60].

Although some studies, as summarized in the earlier section, have been conducted to improve the properties of RAC, further investigations are needed to enhance the quality of RAC prepared with RA obtained from the local sources.

CHAPTER 3

RESEARCH METHODOLOGY

This chapter intends to give a short description of the methods used to accomplish the objective of this study. First, a thorough literature review was conducted to identify the existing strategies to improve the quality of RA. The results of literature review were used to select some promising strategies for the preliminary study. The preliminary study was limited to the evaluation of the compressive strength of the treated RAC at 7 and 14 days. The outcome of the preliminary was used as basis for selecting the promising strategies that were finally investigated in detailed. A brief description of the different steps along with the properties of the materials used is presented in the following sections.

3.1 Materials

Following materials were used in the preparation of NAC and RAC mixtures.

1. ASTM Type I cement
2. Natural aggregate (NA)
3. Recycled aggregate (RA)
4. Fine aggregate (Dune sand)
5. Silica fume
6. Fly ash
7. Blast furnace slag
8. Sulfuric acid
9. Hydrochloric acid
10. Sodium sulfate (Na_2SO_4)
11. Sodium silicate (Na_2SiO_3) solution
12. Superplasticizer

3.1.1 ASTM Type I Cement

The ordinary Portland cement used in this study had a specific gravity of 3.15. The chemical composition of the cement is presented in Table 3-1.

Table 3-1: Chemical composition of type I Portland cement

Component	Weight, %
CaO	65.20
SiO_2	19.69
Al_2O_3	5.59
Fe_2O_3	3.85
MgO	2.11
SO_3	2.10
K_2O	0.35
Na_2O	0.20
Equivalent alkalis	0.43
LOI	0.70

3.1.2 Aggregates

The properties of NA and RA and fine aggregates used are shown in Table 3-2 while the gradation of the aggregates is given in Table 3-3. The grading of the fine aggregate is shown in Table 3-4.

Table 3-2: Properties of aggregates

Aggregate	Absorption	Specific gravity
Fine aggregate (FA)	0.6%	2.50
Natural Coarse aggregate (NA)	1.1%	2.60
Recycled Coarse aggregate (RA)	6.1%	2.62

Table 3-3: Grading of both NA and RA

CA Size (mm)	Percentage Passing
19	100
12.5	70
9.5	40
4.75	10
2.36	0

Table 3-4: Grading of FA used in the mixture proportioning

ASTM Sieve No.	Size (mm)	% Passing
4	4.75	100
8	2.36	100
16	1.18	100
30	0.6	76
50	0.3	10
100	0.015	4

3.1.3 Silica Fume

The chemical and physical properties of the used silica fume is given in Table 3-5.

Table 3-5: Chemical and physical properties of used silica fume

Chemical properties	
SiO_2 %	90.68
Al_2O_3 %	0.66
Fe_2O_3 %	0.23
CaO %	0.15
MgO %	0.20
Available alkali as Na_2O %	0.14
Cl %	0.05
C %	5.06
SO_3 %	0.13
H_2O %	0.10
Physical properties	
Relative density	2.08
Volume weight g/l	694

Loss on ignition %	5.23
Activity index %	122
Particles > 0.045mm %	3.20
Surface area m^2/kg	20,200 – 21,200

3.1.4 Fly Ash

The chemical and physical properties of the fly ash used in the RAC mixtures is given in Table 3-6.

Table 3-6: Chemical and physical properties of used fly ash

Chemical composition	
Silica (SiO_2) %	52.8
Alumina (Al_2O_3) %	34.3
Iron (Fe_2O_3) %	3.6
Manganese (Mn_2O_3) %	0.1
Calcium (CaO) %	4.4
Magnesium (MgO) %	1.1
Phosphorus (P_2O_3) %	0.3
Potassium (K_2O) %	0.5
Sodium (Na_2O) %	0.4
Titanium (TiO_2) %	1.6
Sulphur (SO_3) %	0.1
Loss on Ignition (LOI) %	0.8
Physical properties	
Relative density	2.25
Theoretical surface area cm^2/g	3000
pH, in water	11-12
Color	Light Grey
Particle shape	Spherical

3.1.5 Ground Granulated Blast Furnace Slag (GGBFS)

The chemical and physical properties of used GGBFS are given in Table 3-7.

Table 3-7: Chemical and physical properties of used fly GGBFS

Chemical composition	
Loss on Ignition, %	0.6
Insoluble Residue, %	0.2
Silicon Dioxide, (SiO_2), %	33.32
Aluminum Oxide, (Al_2O_3), %	14.09
Ferric Oxide, (Fe_2O_3), %	0.73
Calcium Oxide, (CaO), %	42.4
Magnesium Oxide, (MgO), %	6.98
Manganese Oxide, (Mn_2O_3), %	0.33
Sulphide, (S), %	0.4
Sulphate, (as SO_3), %	0.22
Chloride, (Cl), %	0.012
Sodium Oxide, (Na_2O), %	0.14
Glass Content, %	> 95
Chemical Moduli	
Sum (CaO+MgO+SiO2), %	82.7
Modulus (CaO+MgO)/(SiO2), %	1.48
Modulus (CaO)/(SiO2), %	1.27
Physical properties	
Relative Density	2.9
Moisture, %	0.24
Fineness (Air-permeability Test), m2/kg	458

3.1.6 Acid

Two types of reagent grade acids were used. The key characteristics of the used acids are given in Table 3-8 and Table 3-9.

Table 3-8: Properties of H_2SO_4

Property	Value
Assay (H_2SO_4)	37%
Color (APHA)	< 5
Specific Gravity at 60º/60ºF	1.85
Residue after Ignition	0.0003

Table 3-9: Properties of HCl

Property	Value
Assay (HCL)	Min 37%
Ammonium (NH_4)	Max 0.0001%
Residue after Ignition (as sulfates)	Max 0.0005%
Non-Volatile Matter	Max 0.005%
Specific Gravity at 60º/60ºF	1.19

3.1.7 Sodium Sulfate

The properties of used sodium sulfate are given in Table 3-10.

Table 3-10: Properties of sodium sulfate

Property	Value
Grade	Industrial
Assay (Na_2SO_4)	≥ 99%
Impurities	• Heavy Metal (as Pb): max 0.004% • Free acid (as H_2SO_4): max 0.1% • Free alkali (as NaOH): max 0.2%
Density	2.68 g/ml at 25 ºC

3.1.8 Sodium Silicate

The sodium silicate used in this study was sourced from a local company known as Basic Chemical Industries Ltd (BCI), Saudi Arabia. The basic properties of sodium silicate are given in Table 3-11.

Table 3-11: Properties of sodium silicate

Property	Value
Chemical formula	$Na_2O(SiO_2)x.(H_2O)x$
$Na_2O(SiO_2)$	35-40%
H_2O	60-65%
Appearance	Clear to cloudy, viscous liquid

Odor	odorless
Solubility	Complete (100%)
Specific Gravity	1.3-1.5
pH	11-12.5
Boiling Point	102 ºC (216 ºF)
Vapor pressure (mm Hg)	18 @ 20 ºC (68 ºF)

3.1.9 Superplasticizer

A commercially available superplasticizer known as Conplast SP 430 was used. The physical and chemical properties of the used superplasticizer are given in Table 3-12.

Table 3-12: Properties of Conplast SP430

Property	Value
Recommended doges	0.5 - 2.0 liters /100 kg of cement
Appearance	liquid
Odor	Slight/faint
Solubility	Complete (100%)
Specific Gravity	1.2 @ 20ºC
pH	7-8
Boiling Point and range	>100ºC @ 101 kPa
Vapor pressure (mm Hg)	2.3 kPa @ 20°C

3.2 RAC Treatment Strategies

A brief description of the treatment strategies used in the preliminary and detailed investigations is discussed in the following sub-sections.

3.2.1 Two-Stage Mixing Approach (TSMA)

The two-stage mixing approach (TSMA) has a major advantage: it does not require any extra materials for the improvement in the properties of RAC. Instead of mixing coarse and

fine aggregate together with cement, as done in the conventional 'one-stage' mixing method, TSMA requires mixing coarse aggregates (the mixture of NA and RA) with cement paste prior to the addition of fine aggregate. This causes inclusion of the cement paste into the cracks of RA which in turn acts to fill the cracks and improve the quality of the RA itself. There are a number of variations of TSMA in the literature. In this study, a simple TSMA was used. A schematic presentation of TSMA used in the present study, is presented in Figure 3-1 while the normal mixing (NM) method is presented in Figure 3-2. The acronym "MCA" represents the mixture of NA and RA in Figure 3-1 and Figure 3-2.

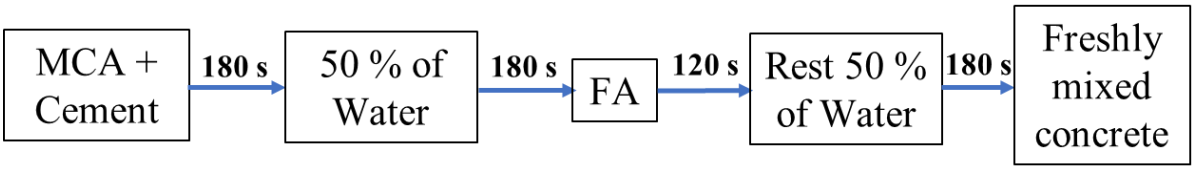

Figure 3-1 : A schematic representation of TSMA

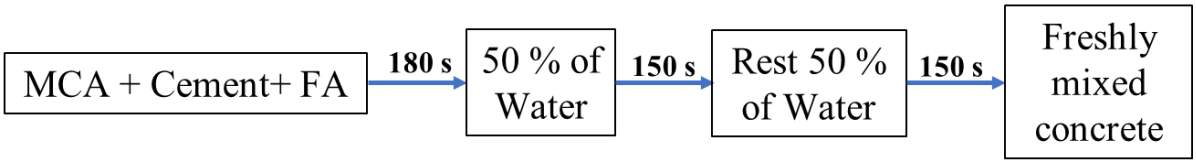

Figure 3-2: A schematic presentation of normal mixing (NM).

3.2.2 Gradation or Proportioning Technique

A simplified proportioning method has been used in this study. Part of the small sized (2.36 and 4.75 mm) natural coarse aggregate was replaced with similar sized RA. The principle of this method is based on the assumption that larger sized coarse aggregate plays a major role in the strength deployment of the concrete, whereas the smaller ones acts

primarily as a filler of the intra particle space [21]. A pictorial presentation of this concept is given in Figure 3-3.

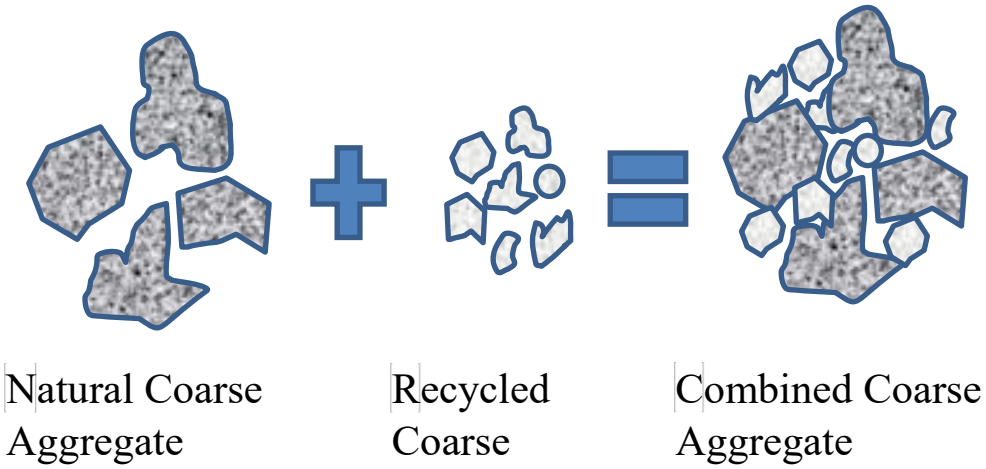

Figure 3-3 : Gradation Technique Proposed by Bui et al. [21]

3.2.3 Los Angeles Treatment (LAT)

This treatment is kind of abrasive treatment. In this method the RA is placed in Los Angeles abrasion machine for 500 revolutions with 12 charges at 30 RPM. For each batch of treatment, 25 kg of RA was used to ensure uniform abrasion level in all the batches (Figure 3.4). The working principle of this treatment is to remove old mortar from RA through abrasion in the Los Angeles machine. However, traces of old mortar still exist on the surface of RA even after sieving the treated aggregate for sufficient duration of time. This residue can be removed through washing by clean water. However, the LAT-treated RA used in this study was not washed considering the added cost due to washing and the

potential contribution of the old mortar powder as a rich source of calcium hydroxide which might contribute to the strength gain of concrete.

Figure 3-4 : Los Angeles abrasion machine (left) and LAT-treated RA aggregates (right).

3.2.4 Improvement of Concrete Matrix (Mortar)

Improvement of concrete matrix is not only responsible for the enhancement of mechanical properties, but also durability of RAC. It is worth mentioning that durability does not mean the material performs indefinitely. Rather, it means to have its required strength and serviceability throughout its service period. Basically, the durability of concrete is largely dependent on its permeability. The lower the permeability the higher the durability of concrete. Permeability itself primarily depends on the microstructure of concrete. The microstructure which reduces porosity, especially the interconnectivity of pores, of concrete is effective in reducing permeability, hence enhancing the durability of concrete. Mineral admixtures are popularly used to ensure less porous microstructure of concrete. There are different types of mineral admixtures, namely, silica fume, natural pozzolans, fly ash, ground granulated blast furnace slag (GGBFS), etc. For this study part of the ASTM

Type I cement was replaced with silica fume, fly ash, and ground granulated blast furnace slag. The replacement percentages were 7% for silica fume, 20% for fly ash and 20% for GGBFS. The improved performance of the resulting RAC is due to the change of microstructure of concrete after adding mineral admixtures. This change of microstructure is basically from two effects. The first effect is filling effect, in which very fine mineral admixtures act as filler materials just as fine aggregates acts for coarse aggregates. The second one is chemical contribution, in which mineral admixtures react with the released calcium hydroxide from on-going hydration of ordinary Portland cement that results in the formation of additional binding materials. This additional binding material is primarily responsible for improved properties of hardened concrete containing mineral admixtures. Figure 3.5 shows samples of cement and the pozzolanic materials used in this study.

(a) ASTM type I Cement

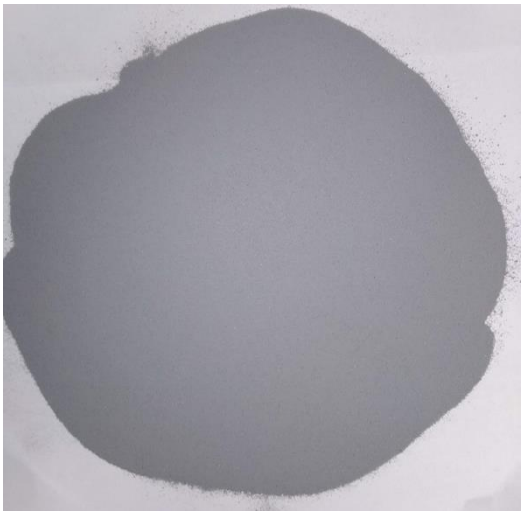

(b) Silica Fume

(c) Fly Ash

(d) GGBFS

Figure 3-5 : Cement and Mineral admixtures used for concrete matrix improvement

3.2.5 Na_2SO_4 Treatment

In this treatment, RA was soaked in the Na_2SO_4 solution (30%). The aggregate:solution ratio was kept at 1:4.5 by weight. The soaking of aggregates in the salt solution causes

partial removal of the adhered mortar on the RA. After 48 hours of soaking, the aggregates were removed and washed with clean water to remove the loose mortar on the surfaces of the treated aggregates. Figure 3.6 shows the Na_2SO_4 treatment stages of RA.

(a) RA soaked in Na_2SO_4 solution

(c) Na_2SO_4 treated RA

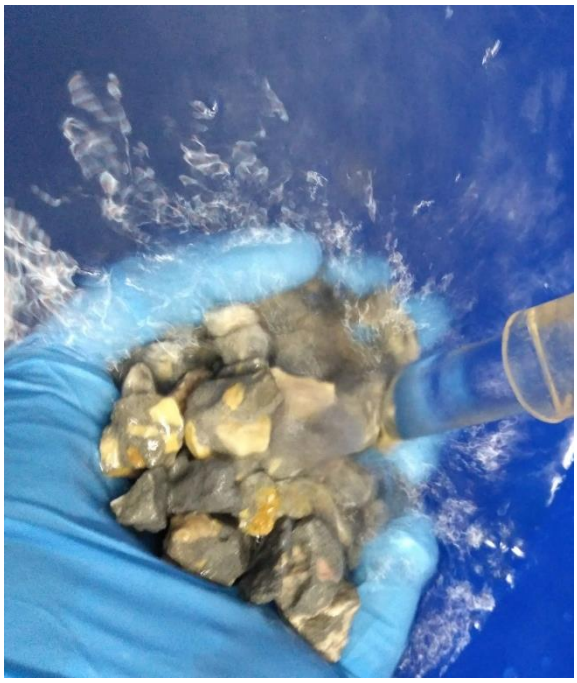

(b) Washing of RA after soaking in Na_2SO_4 solution

Figure 3-6 : Different stages of Na_2SO_4 treatment of RA

3.2.6 Slurry Treatment

Recycled aggregates were submerged in 10% sodium silicate solution for one hour. Then the aggregates were kept in air for air drying. After four hours of air drying, the aggregates were coated with silica fume incorporated cement slurry. The cement consists of 3% silica fume and 97% ASTM Type I cement. The water cement ratio of the slurry was kept 0.4.

The amount of cementitious material for coating was determined on the RA/total aggregate ratio multiplied by the total cement used in the mixture design to produce RAC. The coated aggregates were further dried in air for about four hours before using it in the concrete mixture. Figure 3.7 shows the cement slurry treatment.

(a) Soaking of RA in 10% sodium silicate (SS) solution

(b) Air drying of RA after sodium silicate (SS) treatment

(c) Silica fume induced slurry treatment of RA

(d) Air drying of slurry-treated RA

Figure 3-7 : Different stages of slurry treatment

3.2.7 Acid Treatment

Two acids, namely, H_2SO_4 and HCl, were used for the acid treatments. The acid solutions were prepared by adding 1 part of acid to 10 parts of neutral water, i.e., at a dilution ratio of 1:10. The aggregates were soaked in the acid solution for 48 hours. The soaking of aggregates causes partial removal of adhered mortar on the RA. The aggregates were washed properly after removing from acidic solution. For both acidic treatments, the aggregate to solution ratio was kept at 1:4.5. Figure 3.8 shows the different stages of acid treatment.

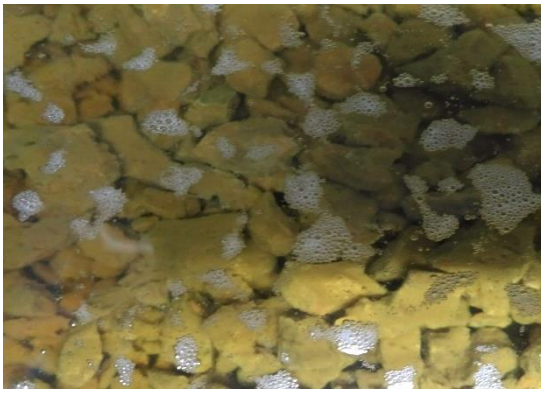

(a) Soaking of RA in acidic solution

(b) Washing of RA after soaking in acidic solution

(c) Close-up view of acid-treated RA after washing

Figure 3-8: Various stages of acid treatment

3.3 Preliminary Investigation

The aim of this task was to investigate the performance of different RACs in small scale. As discussed earlier, trial mixtures were prepared with RA subjected to some selected treatment methods, and RAC specimens were tested to evaluate their compressive strengths after 7 and 14 days of water curing. Based on the compressive strength data, some promising treatment methods were selected for detailed evaluation. The replacement level

of NA with RA was kept 40%, as per the recommendations of previous studies [61], [62]. The outcome of the preliminary study is presented in Table 3-13.

Table 3-13 : Outcome of the preliminary investigation

Treatment	Compressive strength (MPa)		Observation	Remark
	7 days	14 days		
Untreated RAC	37.5	43.6	-	
LAT	40.4	48.5	> Control Mix	Selected
LAT + Na_2SiO_3	39.4	48.2	> Control Mix	Selected
7% silica fume	41.1	46	> Control Mix	Selected
20% fly ash	33.6	39.4	< Control Mix	Selected
TSMA	42.5	45.4	> Control Mix	Selected
Na_2SO_4 solution	39.7	49.1	> Control Mix	Selected
H_2SO_4 solution	35.0	41.9	< Control Mix	Not Selected
20% GGBFS	42.5	45.0	> Control Mix	Selected
Gradation technique	34.5	42.0	< Control Mix	Not Selected
HCl solution	37.6	42.0	<Control Mix	Not Selected
20% fly ash+ TSMA	36.1	41.9	> Control Mix	Selected
20% GGBFS + TSMA	43.4	48.0	> Control Mix	Selected
7% silica fume + TSMA	46.1	51.0	> Control Mix	Selected
3% SF slurry	41.5	46.8	> Control Mix	Selected

The strategies giving compressive strength higher than control mixture were selected for detailed investigations. However, the fly ash mixture which exhibited lower strength than control mixture was also selected for detailed investigations as its low early strength is well known in the literature. The selected treatment strategies are presented below:

i. 0% RA
ii. Untreated RAC
iii. TSMA
iv. 20% fly ash
v. 20% fly ash + TSMA

vi. 20% GGBFS

vii. 20% GGBFS +TSMA

viii. 7% silica fume

ix. 7% silica fume TSMA

x. Na_2SO_4 solution

xi. 3% SF slurry

xii. LAT

xiii. LAT+ sodium silicate (SS)

3.4 Mixture proportions

Concrete mixture proportions were obtained according to the absolute volume method. The weights of constituent materials required to produce 1 m^3 of concrete are shown in Table 3-14.

Table 3-14: Quantities of ingredients in 1 m^3 concrete

Mixture description	Gross Water (kg)	Cementitious Materials (kg)		FA (kg)	CA (kg)	RA (kg)	Total Wt. (kg)
		Cement	Mineral Admixtures				
0% RA	167	375	0	748	1122	0	2412
Untreated RAC	189	375	0	750	675	450	2438
TSMA	189	375	0	750	675	450	2438
20% fly ash	189	300	75	740	666	444	2413
20% fly ash + TSMA	189	300	75	740	666	444	2413
20% GGBFS	189	300	75	748	673	449	2433
20% GGBFS +TSMA	189	300	75	748	673	449	2433
7% silica fume	189	349	26	745	671	447	2427
7% silica fume + TSMA	189	349	26	745	671	447	2427

Na_2SO_4 treated	188	375	0	750	675	450	2437
3% SF slurry treated	189	375	0	750	675	450	2438
LAT	189	375	0	750	675	450	2437
LAT +SS	189	375	0	750	675	450	2437

3.5 Test Details

Several tests related to workability, durability and mechanical characteristics were conducted to evaluate the performance of the selected RAC mixtures. The procedures of the selected tests are described in the following sub-sections.

3.5.1 Workability

The slump cone was used to determine the workability of the freshly mixed concrete. The upper diameter, lower diameter and height of the cone are 100 mm, 200 mm and 305 mm, respectively. The cone was filled with freshly mixed concrete with approximately three equal layers and each layer was tamped by a steel tamping rod. The steel rod was of 16 mm in diameter and 600 mm long. Only the bullet nosed side was used for tamping of the concrete layers. After levelling the freshly mixed concrete at the top of the cone, it was lifted allowing concrete to freely slump. The vertical displacement of the top surface of the cone shaped poured concrete gave the slump value. This procedure satisfied the requirements of ASTM C143. The slump value is an indirect indication of the workability of fresh mixed concrete. Figure 3-9 shows the steps involved in the measurement of the slump.

Figure 3-9 : Slump test set (left) and slump of freshly mixed concrete (right)

3.5.2 Compressive Strength

Compressive strength of concrete was determined according to ASTM C 39. In this process, 100 mm concrete cube specimens were prepared for testing. For each mixture, the strength of concrete cubes was determined at 3, 7, 14, 28 and 90 days of water curing. Each representative value is generally the average of three tested specimens. The allowable loading rate is 0.15 - 0.35 MPa. For this study, the loading rate was maintained at 0.2 MPa (2 kN/s). The dominant failure was found to be aggregate failure during compression. Figure 3-10 shows the preparation and testing of concrete specimens.

(a) Preparation of mould

(b) Casting of concrete into the mould

(c) Testing of the cube specimen

(d) Cube specimen after testing

Figure 3-10 : Various Stages of compressive strength test

3.5.3 Pulse velocity

The ultrasonic pulse velocity (UPV) test was conducted according to ASTM C 597. A UPV tester, manufactured by CNS electronics, was used to determine the pulse velocity. The device consists of a pulse generator and a pulse receiver. The generator and receiver were used to determine the time required (pulse transit time) to pass the generated pulse from one end face of the prepared concrete specimen to the other end face. Pulse velocity can be easily calculated by dividing the specimen length (end to end distance) by the transit time.

The interface of the concrete and the transmitting and receiving transducer were greased to maintain good contacts between them and the concrete end face. The specimens prepared for the compressive strength were used for this test prior to compressive strength test. Figure 3-11 shows the experimental setup.

(a) Calibrating the UPV tester

(b) Determination of the pulse retention time

Figure 3-11 : Different stages of pulse velocity measurements

3.5.4 Splitting Tensile Strength

Three Cylindrical specimens (diameter = 75 mm and height = 150 mm) were cast from each mixture to determine the splitting tensile strength. Concrete specimens were tested at 28 days of water curing, according to ASTM C 496.

(a) Specimen in the testing setup

(b) Specimen after testing

Figure 3-12 : Splitting tensile strength test

3.5.5 Water Absorption

Four cylindrical specimens (diameter = 75 mm and height = 150 mm) were prepared from each mixture to determine the water absorption. After 28 days of water curing, the cylindrical specimens were placed in an oven at 110 ºC for 24 ± 4 hours. Then, they were allowed to cool and subsequently submerged in water for another 48 hours. The weight of the each specimen in dry and saturated surface dry condition were noted and the absorption was determined according to ASTM C642. Figure 3-13 shows the steps involved in determining the water absorption.

(a) Drying of concrete specimens

(b) Submerging of concrete specimens

Figure 3-13 : Water absorption test

3.5.6 Rapid Chloride Permeability (RCP)

Three concrete disks of 50 mm thickness were cut from 100 mm × 200 mm cylindrical specimens. The curved surface of each cut disk specimen was coated with an epoxy resin. The cured coated specimens were then tested according to ASTM C1202. The total charge (in Coulombs) that passed through the concrete disk over a six-hour period was recorded. Figure 3-14 shows the experimental setup for measuring the chloride permeability.

(a) Coating of the curved surface (b) RCP test setup

Figure 3-14 : RCP test specimens and setup.

3.5.7 Corrosion Potentials

Three cylindrical specimens (diameter = 75 mm and height = 150 mm) with steel bar (diameter = 20 mm) inserted into it (see Figure 3-15-top), were prepared to evaluate reinforcement corrosion. These specimens were placed in 5% NaCl solution up to 100 mm. Then, the corrosion potentials were measured using a saturated calomel reference electrode (SCE) and a high impedance voltmeter. The positive terminal of a high impedance digital voltmeter was connected to the electrical lead from the reference electrode while the negative terminal was connected to the steel bar extruding from the concrete specimen. The procedure was in accordance to ASTM C876. The potentials were measured once in a week for a period of 140 days. Figure 3-14 shows the experimental setup for measuring corrosion potentials.

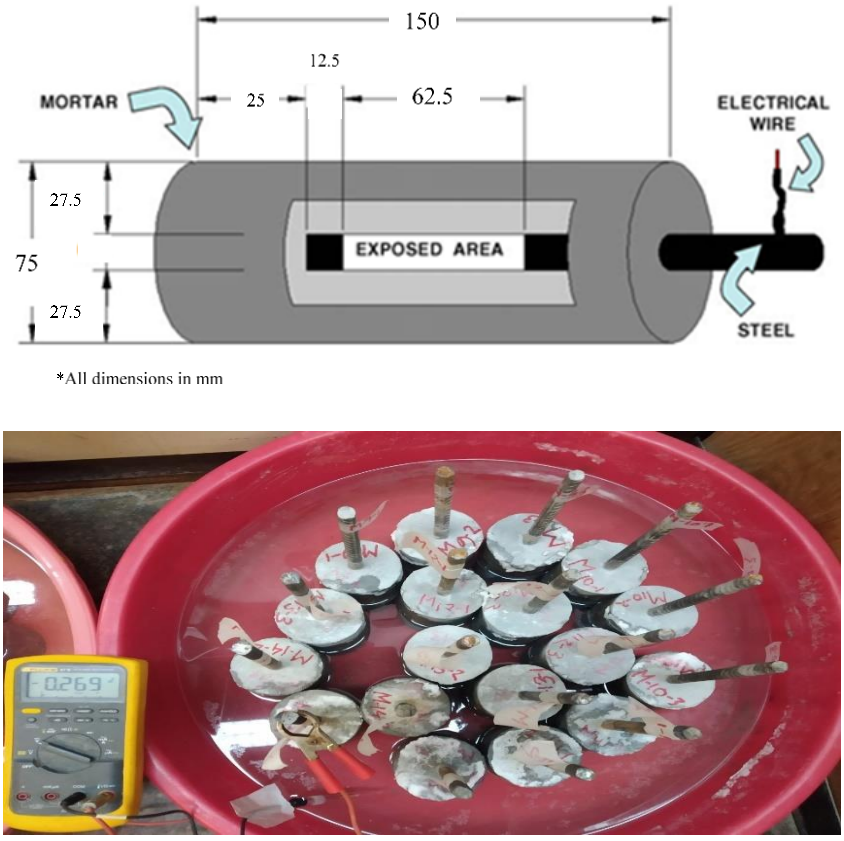

Figure 3-15 : Details of the lollipop specimen (top) and measurement of half-cell potential (bottom).

3.5.8 Sulfate Attack

Six 50 mm concrete cube specimens were prepared from each mixture. At 21 days of water curing, three of them were placed in the into sulfate (5% Na_2SO_4) solution for three months. The reduction in the compressive strength was recorded at 3 months of sulfate exposure. Figure 3-16 shows the experimental setup used to determine the sulfate resistance of RAC.

Figure 3-16 : Concrete cube (50 mm) into palatable water (left) and into 5% Na_2SO_4 solution (right)

3.5.9 Drying Shrinkage

Drying shrinkage was measured on 50 × 50 × 250 mm specimens at 7, 14, 21, 28, 42, 56, 70, 84 and 98 days of air drying starting at 28 days of water curing, according to ASTM C157. Drying shrinkage setup consists basically of an LVDT bearing frame and a data logger to measure the change in length over time. Figure 3-17 shows the experimental setup used to measure the drying shrinkage.

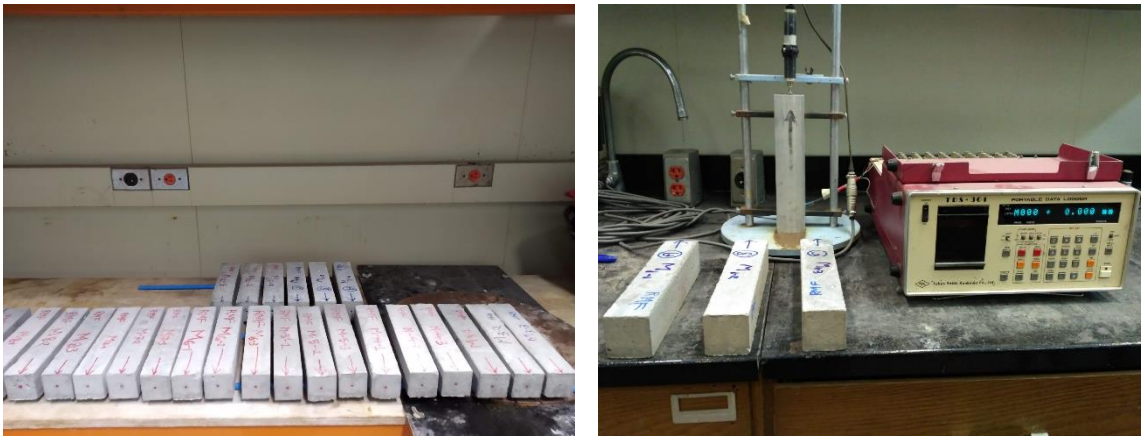

Figure 3-17 : Drying shrinkage prisms (left) and its setup (right)

The details of all the tests conducted are presented in Table 3-15.

Table 3-15: Details of tests conducted.

Property	Test standard	Specimen shape and size	Testing Time
Slump of Hydraulic-Cement Concrete	ASTM C143	Fresh mixed concrete	Immediately after mixing and before initial setting time
Compressive strength	ASTM C39	100 mm cube	3, 7, 14, 28 & 90 days
Pulse velocity	ASTM C 597	100 mm cube	3, 7, 14, 28 & 90 days
Splitting tensile strength	ASTM C496	150 mm × 75 mm cylinder	28 days
Water absorption	ASTM C642	150 mm × 75 mm cylinder	28 days
Chloride permeability	ASTM C1202	150 mm × 75 mm cylinder	28 days
Corrosion Potential	ASTM C876	150 mm × 75 mm cylinder reinforced with Φ12 mm rebar	Up to 140 days
Sulfate resistance	ASTM C 1012	50 mm cube	3 months
Drying shrinkage	ASTM C157	50 × 50 × 250 mm prism	Up to 3 months

CHAPTER 4

RESULTS AND DISCUSSION

This chapter presents the findings of workability, durability and mechanical properties of modified RACS considered in this study. The findings have been primarily depicted with the help of relevant tables, bar charts and graphs. Further, a number of notable trends and key findings have been discussed with logic and information available in the literature.

4.1 Workability

The measured workability (slump) of the studied RACs is presented in Table 4-1.

Table 4-1: Slump of considered RACs

Mixture ID	Description	*Superplasticizer (SP 430) dosages (% of cementitious materials)	Slump (mm)
M0	0% RA	1.4	75
M1	Untreated RAC	1.4	100
M2	TSMA	1.4	88
M3	20% fly ash	1.26	106
M4	20% fly ash + TSMA	1.26	94
M5	20% GGBFS	1.26	125
M6	20% GGBFS +TSMA	1.26	100
M7	7% silica fume	1.26	100
M8	7% silica fume + TSMA	1.26	81
M9	Na_2SO_4 treated	1.01	113
M10	3% SF slurry treated	1.01	100
M11	LAT	1.24	113
M12	LAT +SS	1.05	113

The workability of untreated RAC (M1) was more than that of NAC (M0). This can be attributed to the excess water required to compensate the high absorption of the RA [26]. The addition of mineral admixtures to RAC (Mixtures M3, M5 & M7) increased the workability, even better than the untreated RAC (Mixture M1). This can be attributed to the lubricant affect [63] of the added mineral admixtures. However, the treatments of RAC involving TSMA (Mixtures M2, M4, M6 & M8) slightly decreased the workability of the same treatments without TSMA (Mixtures M1, M3, M5 & M7). This can be attributed to the enhanced mixing time due to TSMA. The extra mixing time causes more loss of water, which is primarily responsible for loss of workability [64]. Although there is reduction in workability due to preparation of the RAC mixtures adopting TSMA, the net effect of the use of mineral admixtures and TSMA on the workability of the RAC mixtures is beneficial. All the RAC mixtures with TSMA had achieved a higher workability at a significantly lower SP dosage as compared to the workability of untreated RAC (M1). Due to larger surface area of silica fume the increase in the workability of mixtures M7 & M8 is slightly less than that of mixtures with fly ash (M3 & M4) and GGBFS (M5 & M6). The other treated RACs (Mixtures M9 through M12) also showed improved workability. The smoothening of the surface of RA due to various treatments is primarily responsible for the improvement in the workability of RACs [49].

4.2 Pulse Velocity

The average pulse retention time and corresponding pulse velocity at different curing ages for the considered RACs are presented in Table 4-2 and Table 4-3, respectively

Table 4-2 : Pulse retention time at different ages of considered RACs

Mixture Id	Description	Pulse retention time (μ sec) for 100 mm length				
		3 days	7 days	14 days	28 days	90 days
M0	0% RA	22.3	21.43	21.23	21	20.95
M1	Untreated RAC	23	22.2	21.93	21.23	21.03
M2	TSMA	22.17	22.03	21.85	21.17	20.97
M3	20% fly ash	22.4	21.97	21.87	21.4	20.8
M4	20% fly ash + TSMA	22.1	21.93	21.75	21.2	20.6
M5	20% GGBFS	22.37	21.9	21.6	21.13	20.87
M6	20% GGBFS +TSMA	22.05	21.87	21.37	20.73	20.6
M7	7% silica fume	22.53	22.2	22.03	21.3	21.27
M8	7% silica fume + TSMA	21.93	21.8	21.4	21.23	21
M9	Na_2SO_4 treated	22.17	21.77	21.6	21.27	21.2
M10	3% SF slurry treated	22.67	22.3	21.7	21.3	21.23
M11	LAT	22.13	22.07	21.5	21.33	20.8
M12	LAT +SS	22.43	21.9	21.7	21.23	21.17

Table 4-3: Pulse velocity at different ages of considered RACs

Mixture Id	Description	Pulse velocity (km/s)				
		3 days	7 days	14 days	28 days	90 days
M0	0% RA	4.48	4.67	4.71	4.76	4.77
M1	Untreated RAC	4.35	4.50	4.56	4.71	4.76
M2	TSMA	4.51	4.54	4.58	4.72	4.77
M3	20% fly ash	4.46	4.55	4.57	4.69	4.81
M4	20% fly ash + TSMA	4.52	4.56	4.60	4.72	4.85
M5	20% GGBFS	4.47	4.57	4.63	4.73	4.79
M6	20% GGBFS +TSMA	4.54	4.57	4.68	4.82	4.85
M7	7% silica fume	4.44	4.50	4.54	4.69	4.70
M8	7% silica fume + TSMA	4.56	4.59	4.67	4.71	4.76
M9	Na_2SO_4 treated	4.51	4.59	4.63	4.70	4.72
M10	3% SF slurry treated	4.41	4.48	4.61	4.69	4.71
M11	LAT	4.52	4.53	4.65	4.69	4.81
M12	LAT +SS	4.46	4.57	4.61	4.71	4.72

There is an opposite relationship between pulse velocity and pulse retention time. The lower the pulse retention time the higher the pulse velocity. Further, the pulse velocity increased with an increase in the curing time of all the prepared RACs. The denser microstructure due to longer curing time is primarily responsible for an increase in the pulse velocity.

4.3 Compressive Strength

The compressive strength of considered RACs at different ages is given in Table 4-4. The effect of the selected treatment strategies on the compressive strength of RACs is discussed in the following sub-sections.

Table 4-4: Compressive strengths of considered RACs at different ages

Mixture Id	Description	Average Compressive Strength (MPa)				
		3 days	7 days	14 days	28 days	90 days
M0	0% RA	40	50	51	56	63
M1	Untreated RAC	34	38	44	46	50
M2	TSMA	34	43	46	47	53
M3	20% fly ash	32	34	39	46	55
M4	20% fly ash + TSMA	34	37	41	48	57
M5	20% GGBFS	39	42	44	50	57
M6	20% GGBFS +TSMA	38	45	49	55	58
M7	7% silica fume	39	43	46	55	58
M8	7% silica fume + TSMA	40	46	50	56	59
M9	Na_2SO_4 treated	39	43	48	49	53
M10	3% SF slurry treated	37	42	44	50	55
M11	LAT	35	40	47	53	55
M12	LAT +SS	38	41	47	54	57

4.3.1 TSMA and Mineral Admixture Based Strategies

The compressive strength development in RACs with TSMA and fly ash is depicted in Figure 4-1. The mere use of TSMA caused significant improvement in the compressive strength at all curing ages. The initial strength development due to fly ash treatment is notably lower compared to the control specimens. The reason for a lower early strength of concrete in the presence of fly ash is due its very low lime content and a high silica content. The silica in fly ash takes time to react with the calcium hydroxide (liberated from the primary hydration of the OPC) giving additional calcium-silicate-hydrate gel that contribute to the strength gaining in the later stage of hydration [65], as evident from the higher strength of RAC mixture containing FLA after 90 days of curing. The addition of TSMA with fly ash improved the compressive strength further. The percentage increase in the compressive strength, due to fly ash and TSMA treatment, at 90 days curing with respect to untreated RAC are presented in Figure 4-2.

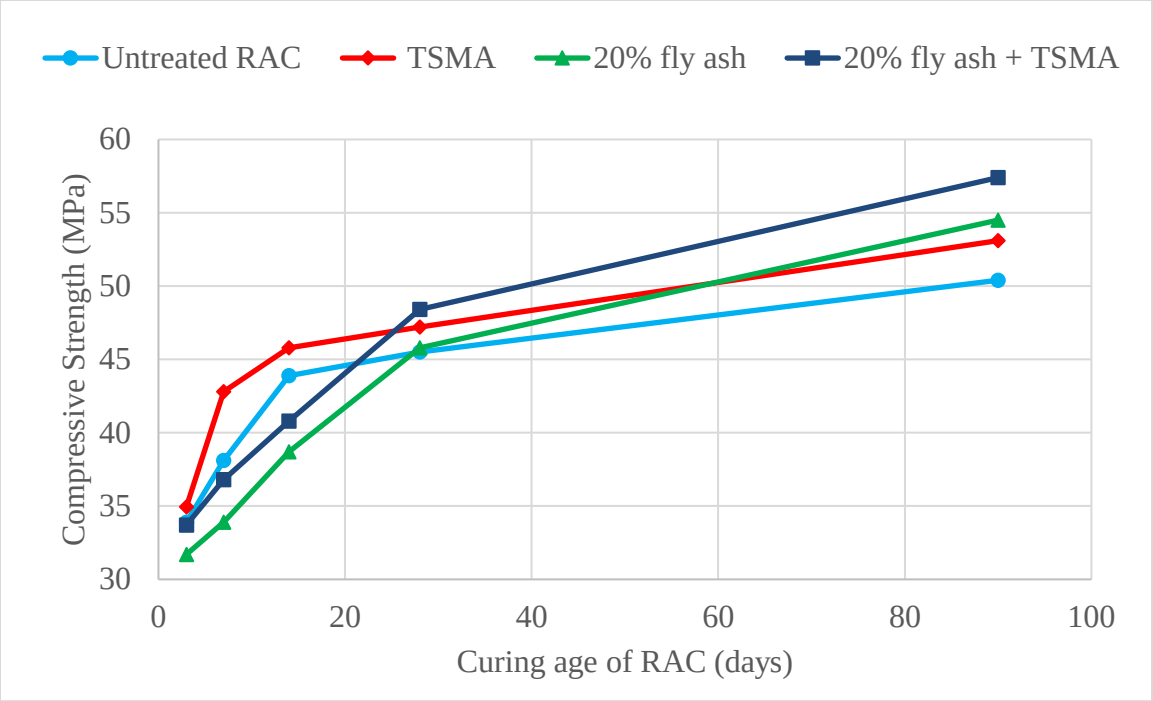

Figure 4-1: Development of compressive strength of RACs modified with TSMA and fly ash.

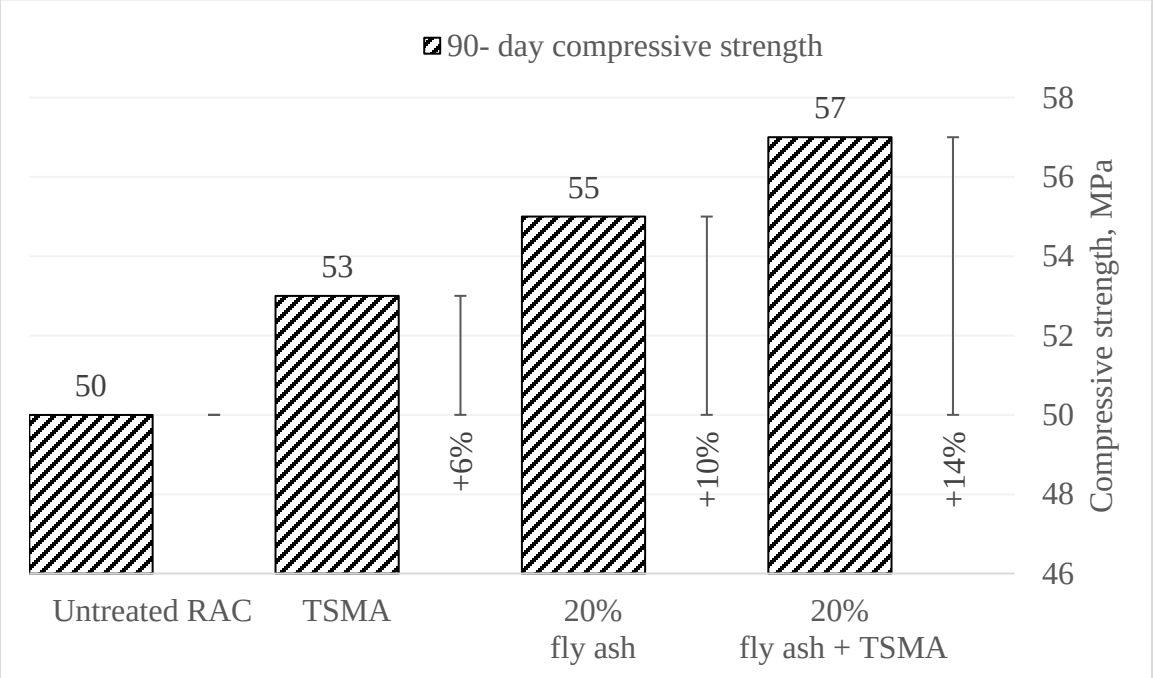

Figure 4-2: Change (%) in compressive strength of RACs modified with TSMA and fly ash at 90 days curing.

The compressive strength development in RACs with the use of GGBFS, silica fume and TSMA is depicted in Figure 4-3 and Figure 4-4. The compressive strength of treated RACs was more than that of control RAC at all ages. However, the performance of RAC with silica fume was better than that of RAC with GGBFS. The application of TSMA with silica fume or GGBFS, separately, caused further improvement in the compressive strength in both cases compared to that with TSMA only. The percent increase in the compressive strength, due to GGBFS, silica fume and TSMA, at 90 days curing, with respect to untreated RAC is presented in Figure 4-5 and Figure 4-6, respectively.

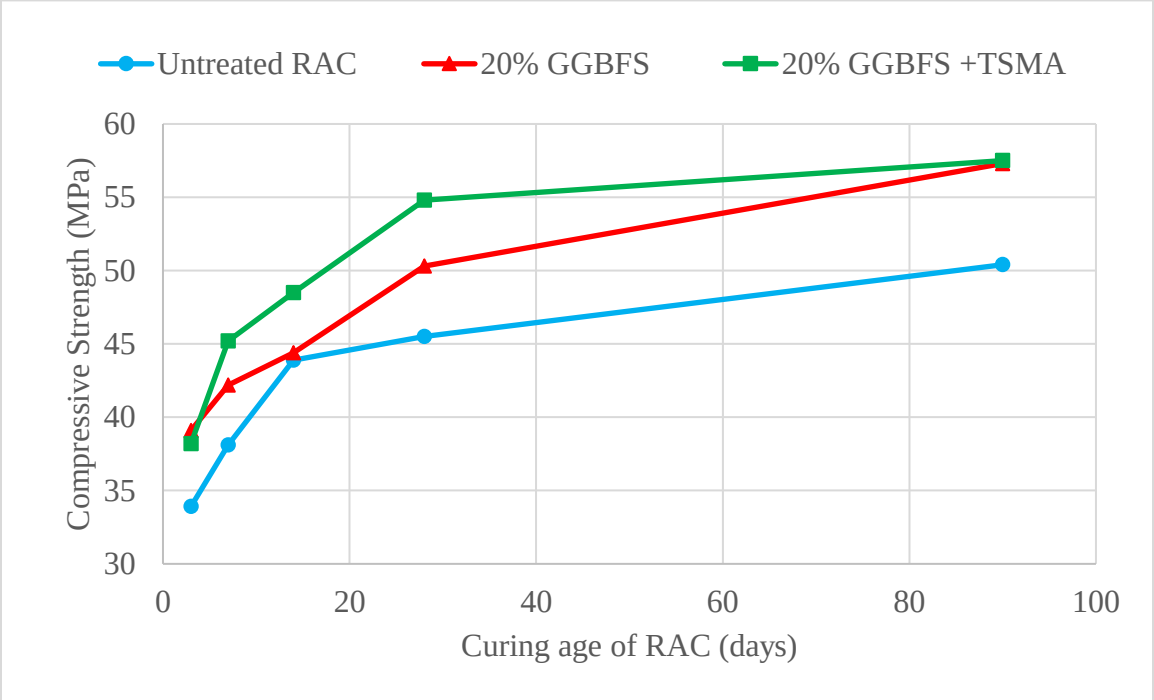

Figure 4-3 : Compressive strength development of RACs modified with GGBFS and TSMA.

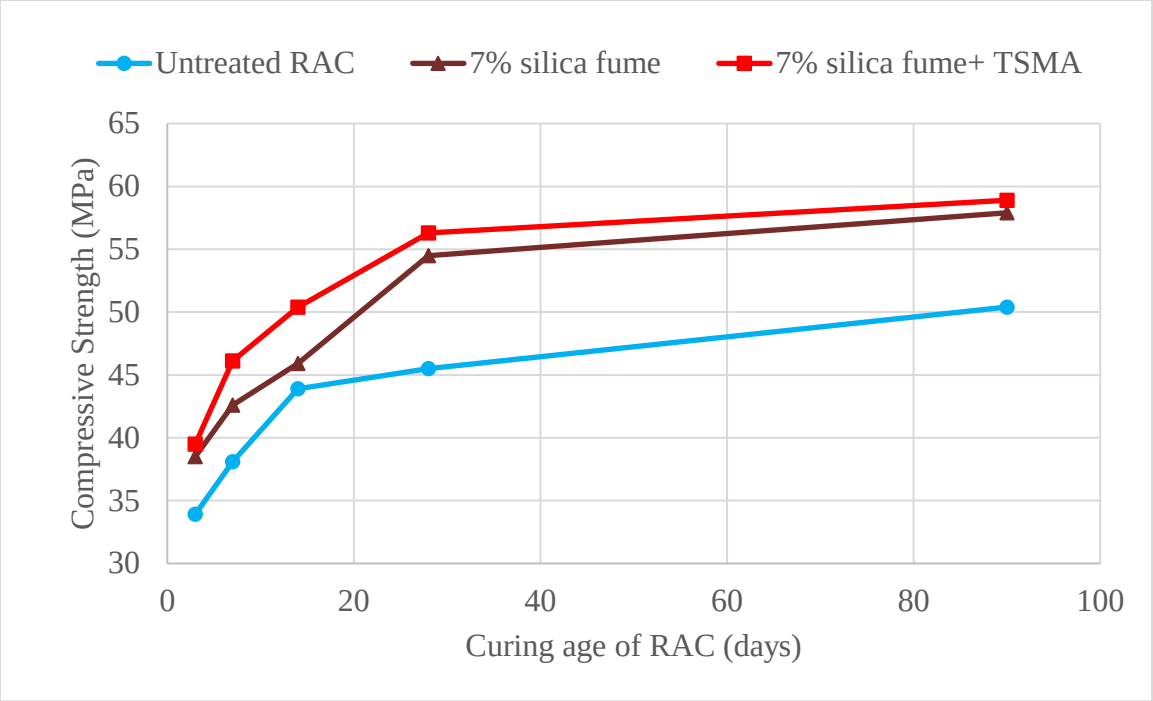

Figure 4-4: Compressive strength development of RACs modified with silica fume and TSMA.

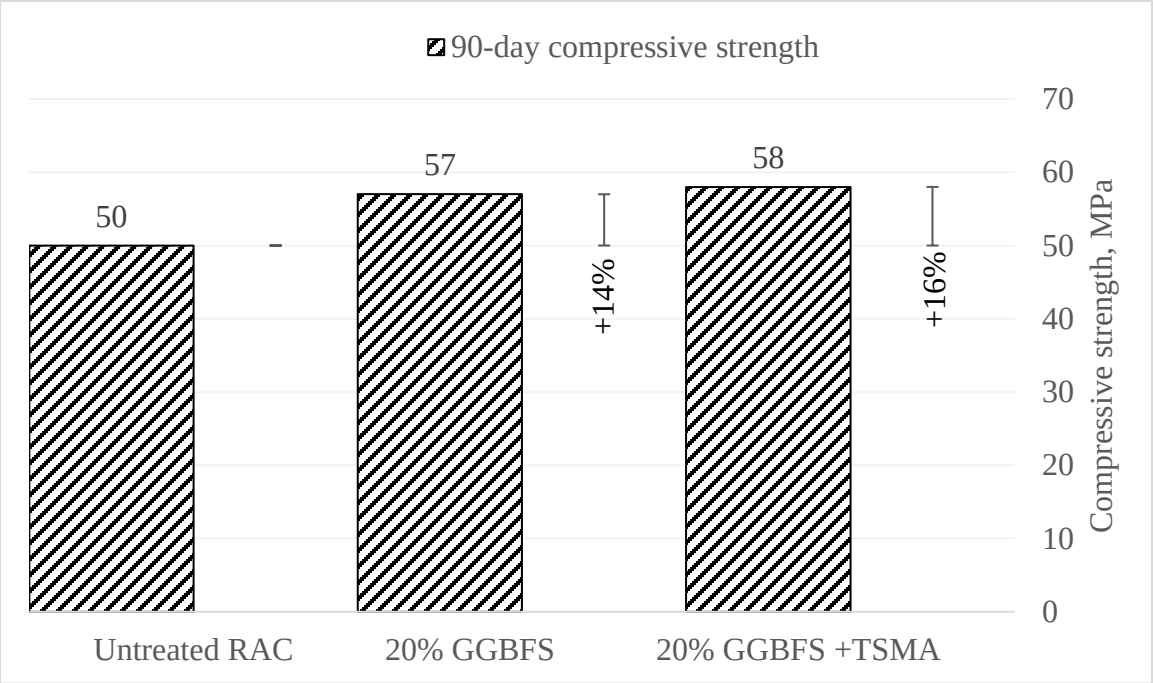

Figure 4-5: Change (%) in the compressive strength of RACs modified with GGBFS and TSMA.

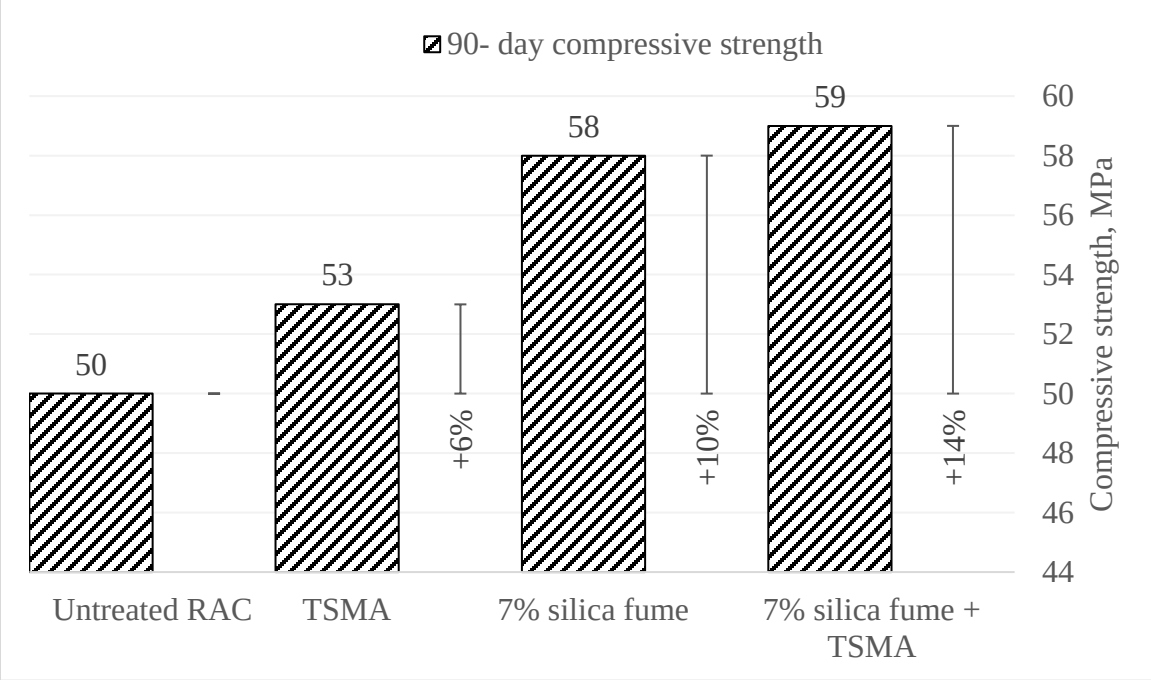

Figure 4-6: Change (%) in the compressive strength of RACs modified with silica fume and TSMA.

4.3.2 Na_2SO_4 and Silica Fume Slurry Based Strategies

The compressive strength development of RACs due to Na_2SO_4 and silica fume slurry is depicted in Figure 4-7. The compressive strength of treated RACs was more than that of control RAC at all ages. However, the initial strength gain of RAC with Na_2SO_4 treatment was more than that of RAC with silica fume slurry treatment. However, the 28 days compressive strength of RAC treated with silica fume slurry was more than that of RAC treated with Na_2SO_4. The percent increase in the compressive strength, due to Na_2SO_4 and silica fume slurry treatment, at 90 days curing with respect to untreated RAC is presented in Figure 4-8.

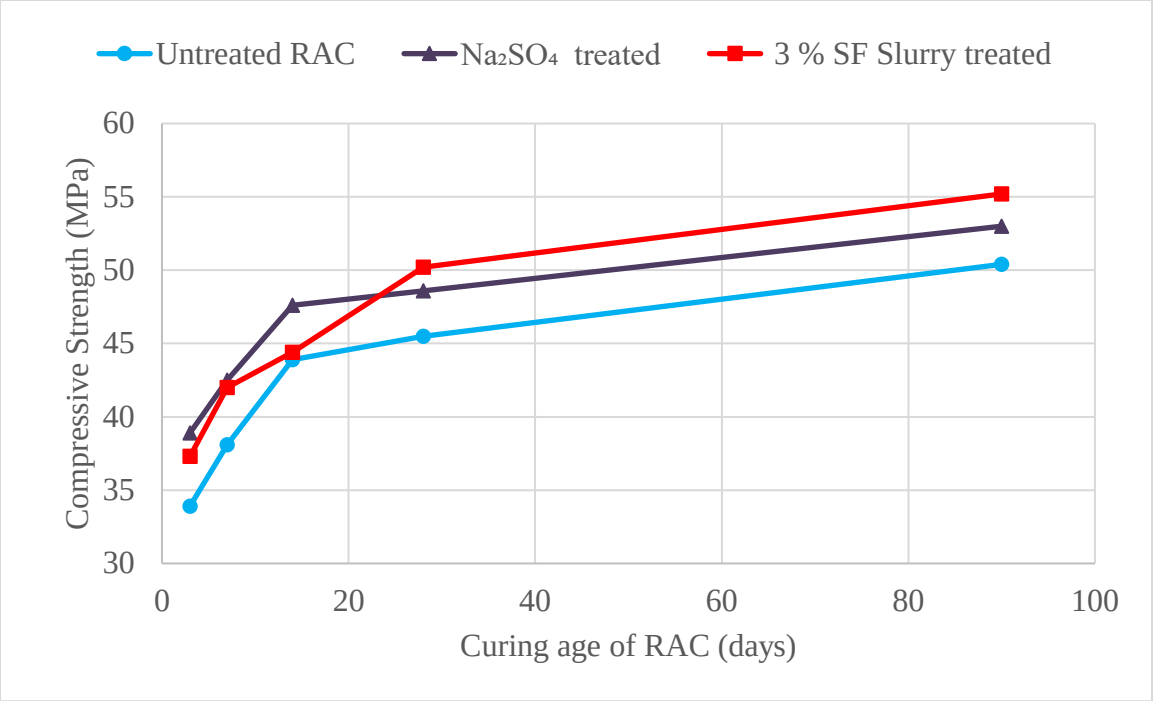

Figure 4-7: Compressive strength development of RACs treated with Na_2SO_4 and silica fume slurry.

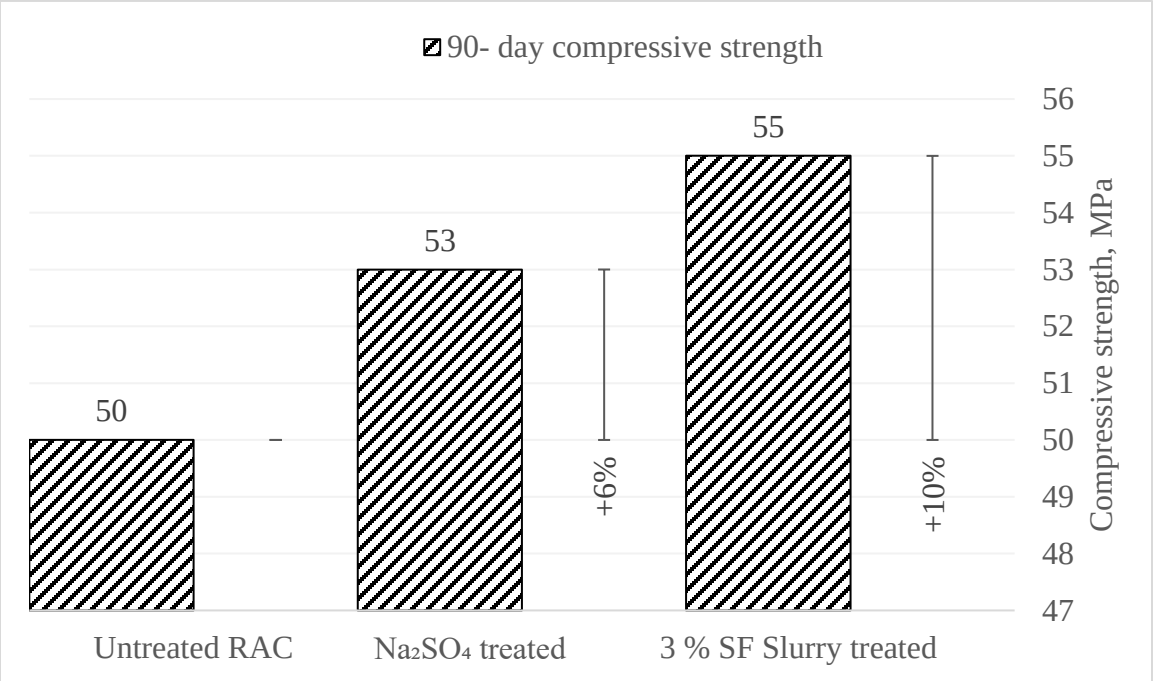

Figure 4-8: Change (%) in the compressive strength of RACs treated with Na_2SO_4 and silica fume Slurry.

4.3.3 Los Angeles Treatment-Based strategies

The compressive strength development of RACs with three different combinations of Los Angeles treatment (LAT) are depicted in Figure 4-9. The LAT treatment of RACs with and without sodium silicate yielded identical compressive strength. However, both LAT treatments gave higher compressive strength than control RAC at almost all ages. The percent increase in the compressive strength, due to two different combinations of LAT, at 90 days curing with respect to untreated RAC are presented in Figure 4-10.

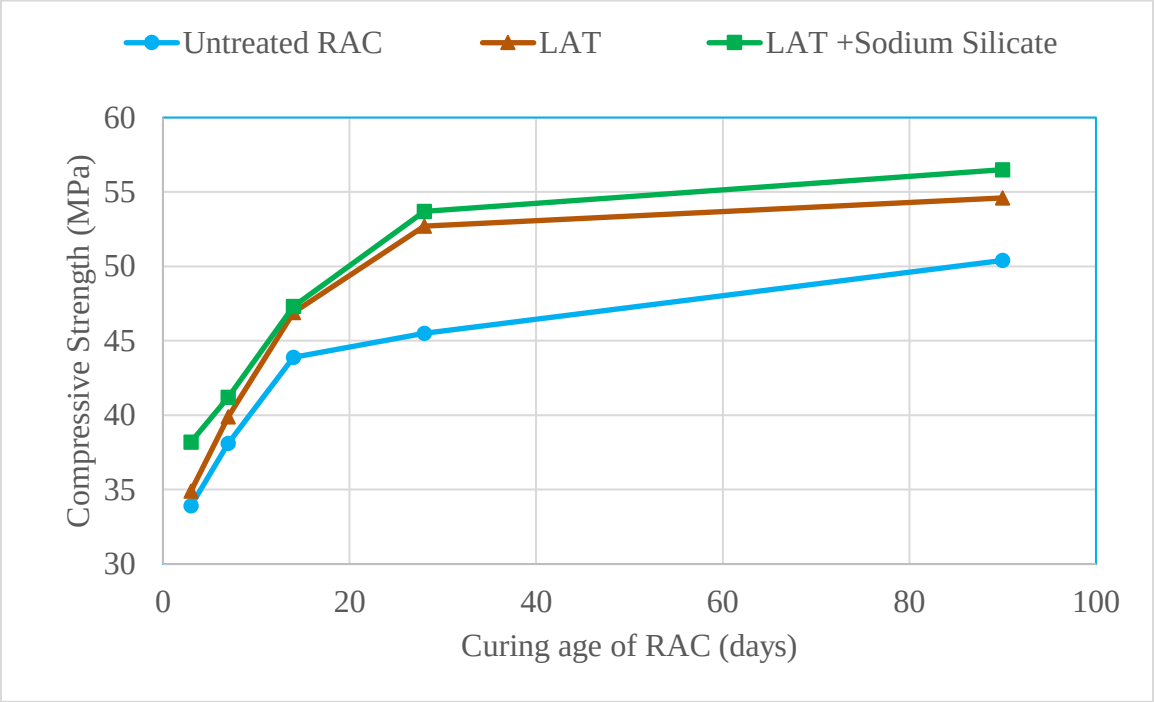

Figure 4-9: Compressive strength development of RACs modified with two different combinations of Los Angeles treatments.

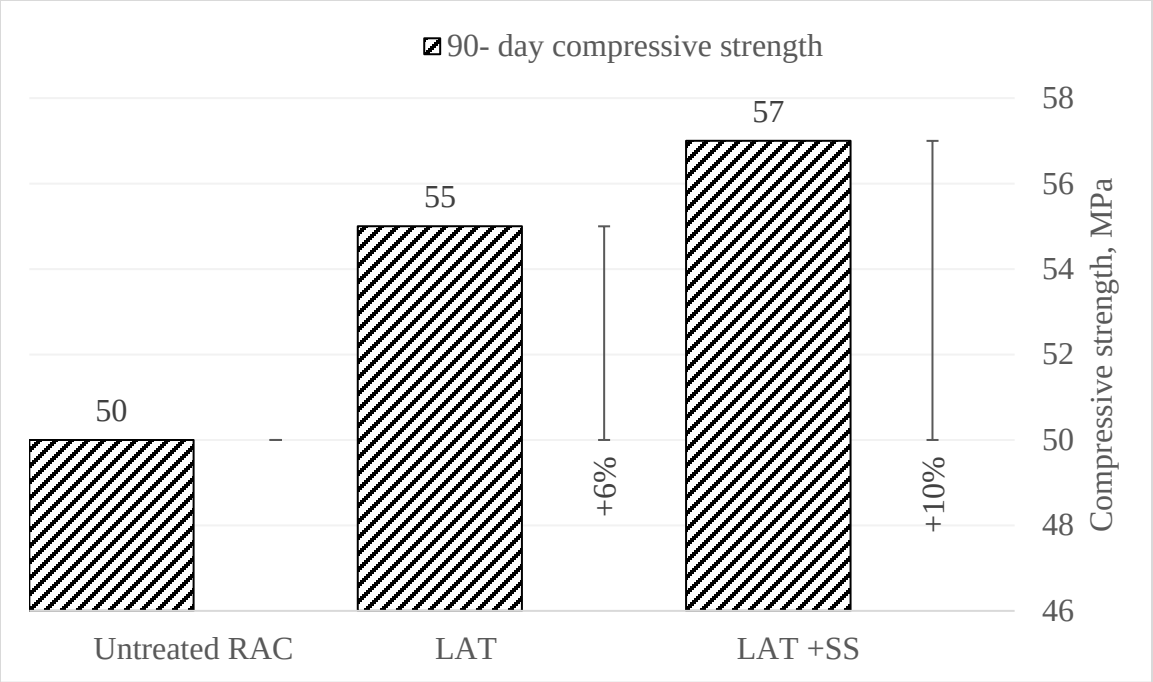

Figure 4-10: Change (%) in the compressive strength of RACs modified with two different combinations of Los Angeles treatments.

4.3.4 Discussion of Results

The RACs modified with different mineral admixtures caused an improvement in the compressive strength ranging from 10% to 16% compared to control specimens at 90 days. The pozzolanic actions and packing effect of mineral admixtures might have played a significant role in the strength enhancement of RAC with these treatments. The TSMA along with mineral admixtures resulted in further strength enhancement ranging from 14% to 18%. The positive effect of TSMA is due to the improvement in the bond between the fresh mortar and the RA. The RA particles bear partial/full coating of the old mortar. The old mortar on the surface of the RA particles consists of pores and cracks that weaken the bond between the RA and fresh mortar, i.e., a weak interfacial zone (ITZ) in the RAC mixture. The TSMA helps in improving the quality of the ITZ by sealing the cracks and

pores on the surface of the RA particles. This is also termed as ‘shifting of ITZ’ that provides a better bond between the fresh mortar and RA thereby resulting into a densified microstructure of the RAC prepared using TSMA. The RAC mixture with denser microstructure helps in achieving better mechanical properties and the durability characteristics [66], [67]. The Na_2SO_4 and silica fume slurry treatments brought moderate (6% to 10%) enhancement in the compressive strength. The Los Angeles treatments without sodium silicate treatment, showed promising improvements (10% and 14%) in the compressive strength. These improvements can be attributed to the improved surfaces of RA due to the removal of old mortar from the surfaces of RA by abrasive action using Los Angeles machine. However, inclusion of sodium silicate in LAT showed further positive effect on the compressive strength of the resultant RAC. Sodium silicate reacts with portlandite of RA which produces calcium silicate hydrate [54]. These extra calcium silicate hydrate contributed to the enhanced compressive strength of the RAC treated with LAT and sodium silicate together.

4.4 Splitting Tensile Strength

The 28 days splitting tensile strength of the developed RACs is presented in Table 4-5. The effect of each treatment on the splitting tensile strength is further discussed in the following sub-sections.

Table 4-5: Splitting tensile strength of considered RACs at 28 days

Mixture Id	Description	Average Splitting Tensile Strength (MPa)
M0	0% RA	3.1
M1	Untreated RAC	2.4
M2	TSMA	2.7
M3	20% fly ash	2.4
M4	20% fly ash + TSMA	2.6
M5	20% GGBFS	2.6
M6	20% GGBFS +TSMA	2.8
M7	7% silica fume	2.7
M8	7% silica fume + TSMA	3.1
M9	Na_2SO_4 treated	2.5
M10	3% SF slurry treated	2.9
M11	LAT	3.2
M12	LAT +SS	3.3

4.4.1 TSMA and Mineral Admixture-based Strategies

The change (%) in the splitting tensile strength of RACs modified with TSMA and fly ash compared to untreated RAC after 28 days of curing is depicted in Figure 4-11. The TSMA caused around 13% increase in the splitting tensile strength. The RAC with only 20% fly ash yielded similar splitting tensile strength as untreated RAC. However, the fly ash treatment along with TSMA caused a significant (8%) improvement in the splitting tensile strength.

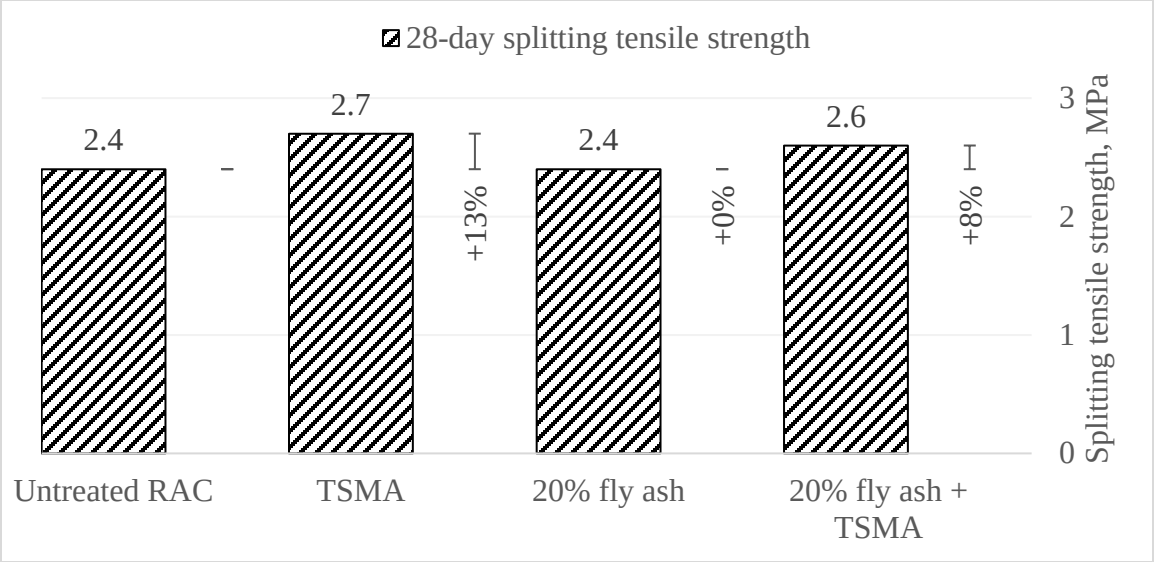

Figure 4-11 : Change (%) in the splitting tensile strength of RACs modified with TSMA and fly ash after 28 days of curing.

The change (%) in the splitting tensile strength of RACs modified with GGBFS or silica fume and TSMA with respect to untreated RAC after 28 days of curing is depicted in Figure 4-12 and Figure 4-13. The RAC with only 20% GGBFS yielded 8% higher splitting tensile strength compared to untreated RAC. However, the GGBFS treatment along with TSMA caused a substantial (17%) increase in the splitting tensile strength. The silica fume treatment was superior to the GGBFS treatment. The increase in the splitting tensile strength due to silica fume treatment with or without TSMA is 13% and 29%, respectively.

Figure 4-12 : Change (%) in the splitting tensile strength of RACs modified with GGBFS and TSMA after 28 days of curing.

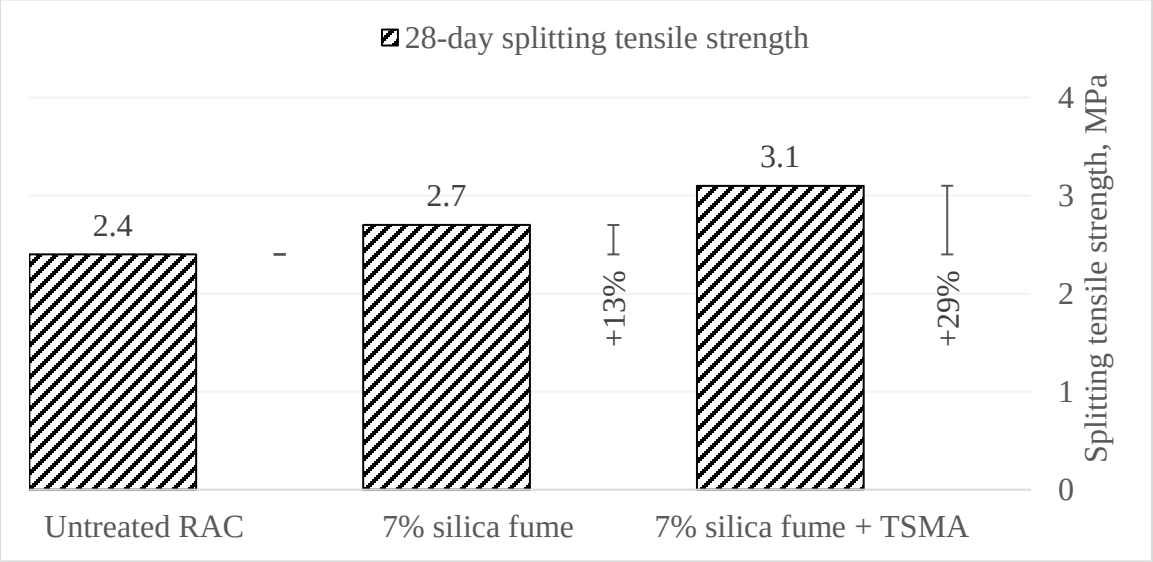

Figure 4-13: Change (%) in the splitting tensile strength of RACs modified with silica fume and TSMA after 28 days of curing.

4.4.2 Na_2SO_4 and Silica Fume Slurry Based Strategies

The change (%) in the splitting tensile strength of RACs modified with Na_2SO_4 and silica fume slurry with respect to untreated RAC after 28 days curing is depicted in Figure 4-14.

The strength increase of RAC modified with Na_2SO_4 treatment is minimal (4%). However, silica fume slurry treatment alone caused a substantial (21%) improvement in the splitting tensile strength. This enhanced performance can be attributed to improved surface of RAC due to silica fume slurry treatment.

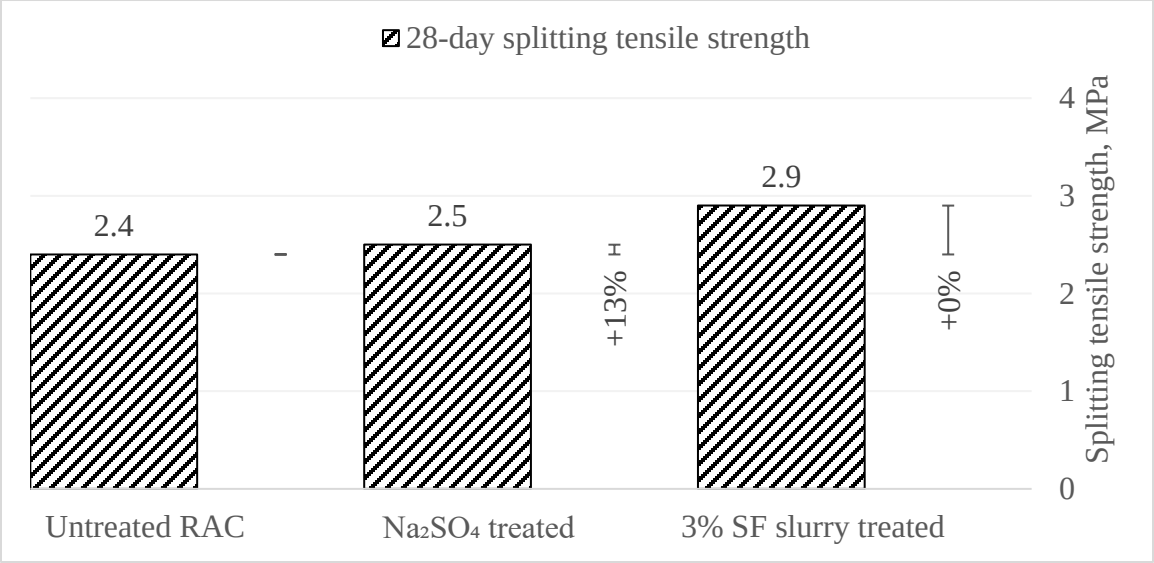

Figure 4-14: Change (%) in the splitting tensile strength of RACs modified with Na_2SO_4 and silica fume slurry after 28 days of curing.

4.4.3 Los Angeles Treatment-based strategies

The change (%) in the splitting tensile strength of RACs modified with three different combinations of Los angeles treatments (LAT), with respect to untreated RAC after 28 days curing, is depicted in Figure 4-15. The RAC modified with LAT alone showed notable increase (33%) in the splitting tensile strength. However, the combined effect of LAT and sodium silicate treatment lead to an increase of 38% splitting tensile strength.

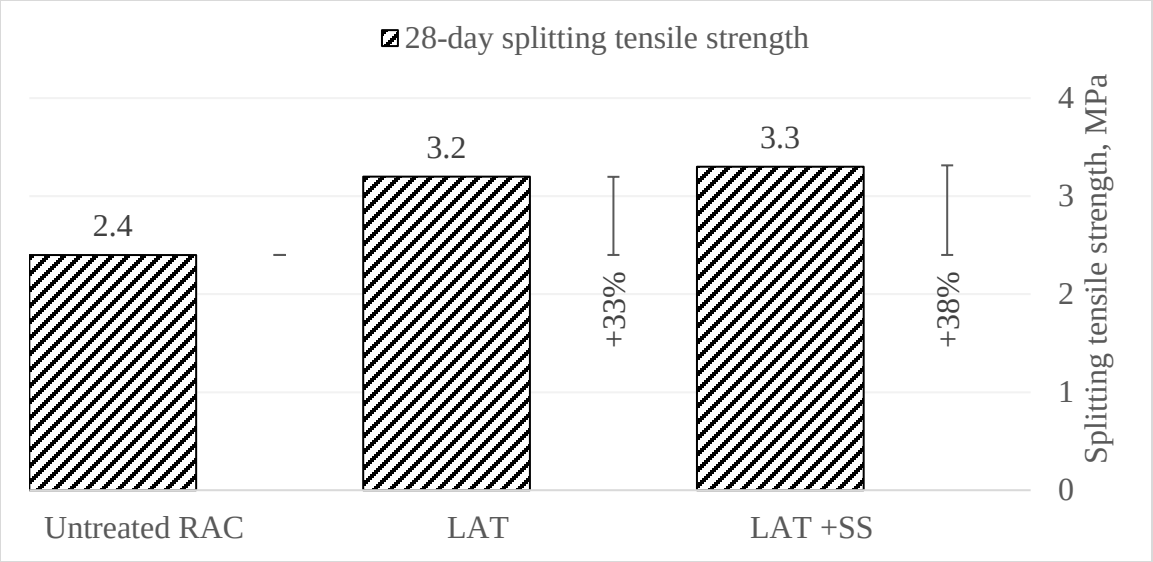

Figure 4-15: Change (%) in the splitting tensile strength of RACs modified with two different combinations of Los Angeles treatments.

4.4.4 Discussion of results

The splitting tensile strength of RACs modified with silica fume increased by around 13% compared to control specimens at 28 days. The stronger concrete matrix (mortar) might have played a significant role in the strength enhancement in the treated RACs. The splitting tensile strength of fly ash and GGBFS treated RACs was 8% more compared to the untreated RAC. However, the splitting tensile strength of RACs treat with all mineral admixtures and TSMA increased by 8% to 29%. The improved interfacial transition zone due to TSMA is responsible for the increase in the strength. The mechanism of enhancement of splitting tensile strength due to TSMA is explained in Figure 4-16. There was a moderate (4%) increase in the splitting tensile strength of RACs treated with Na_2SO_4 treatments brought moderate (4%) enhancement in the splitting tensile strength. However, silica fume slurry and Los Angeles treatments with or without sodium silicate treatments,

showed remarkable increase (21%, 33% and 38%) in the splitting tensile strength. The improvements in Los Angeles treated RACs can be attributed to improved surfaces of RA due to the removal of old mortar from the surfaces of RA by abrasive action. For slurry treatments the improved surfaces of RA resulted due to the formation of a layer of slurry on the old mortar.

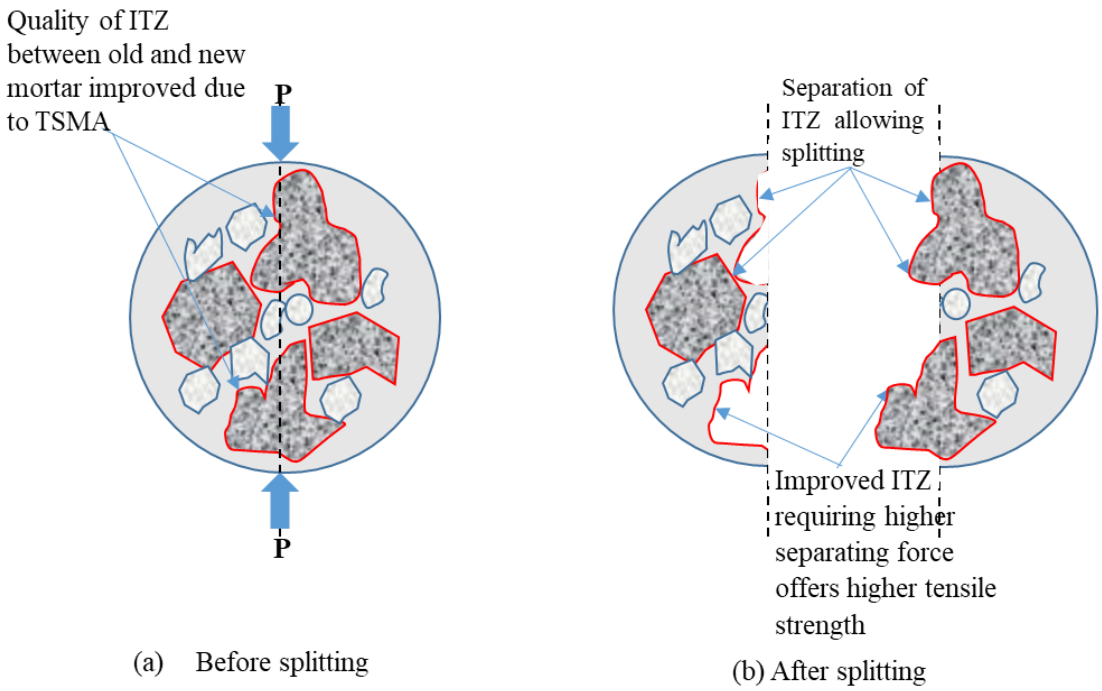

Figure 4-16: Mechanism of enhancement of splitting tensile strength due to TSMA

4.5 Water Absorption

The water absorption of the prepared RACs after 28 days of curing is presented in Table 4-6. The effect of the selected treatment methods on the water absorption of the developed RACs is discussed in the following sub-sections.

Table 4-6: Absorption of the prepared RACs

Mixture ID	Description	Average water absorption (%)
M0	0% RA	3.8
M1	Untreated RAC	5.1
M2	TSMA	5.0
M3	20% fly ash	5.0
M4	20% fly ash + TSMA	4.7
M5	20% GGBFS	4.7
M6	20% GGBFS +TSMA	4.6
M7	7% silica fume	4.7
M8	7% silica fume + TSMA	4.7
M9	Na_2SO_4 treated	5.1
M10	3% SF slurry treated	5.1
M11	LAT	4.9
M12	LAT +SS	4.7

4.5.1 TSMA and Mineral Admixture Based Strategies

The change (%) in the absorption of RACs modified with TSMA and fly ash treatment with respect to untreated RAC after 28 days curing is depicted in Figure 4-17. The TSMA caused around 2% decrease in the absorption. However, the fly ash treatment along with TSMA decreased the water absorption of RAC by 8%.

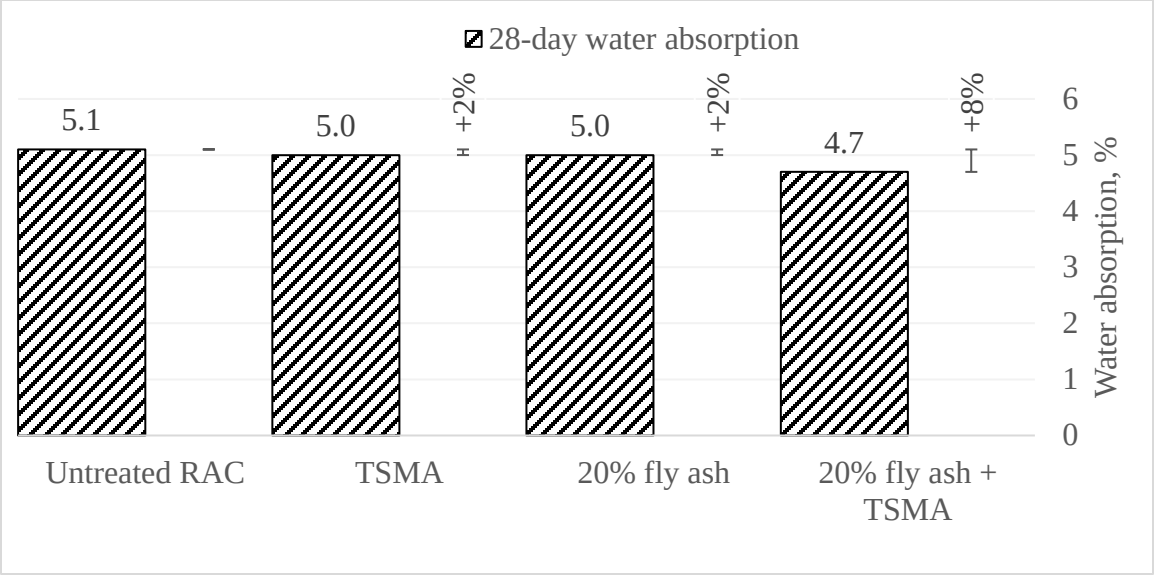

Figure 4-17: Change (%) in the absorption of RACs modified with TSMA and fly ash after 28 days of curing.

The change (%) in the absorption of RACs modified with GGBFS, silica fume and TSMA with respect to untreated RAC after 28 days of curing is depicted in Figure 4-18 and Figure 4-19, respectively. The decrease in the absorption due to treatment with silica fume and GGBFS slurry is similar (8%). However, the GGBFS treatment along with TSMA caused a substantial decrease (15%) in the absorption. This improvement is not significantly better for RAC modified with both silica fume and TSMA than with only silica fume.

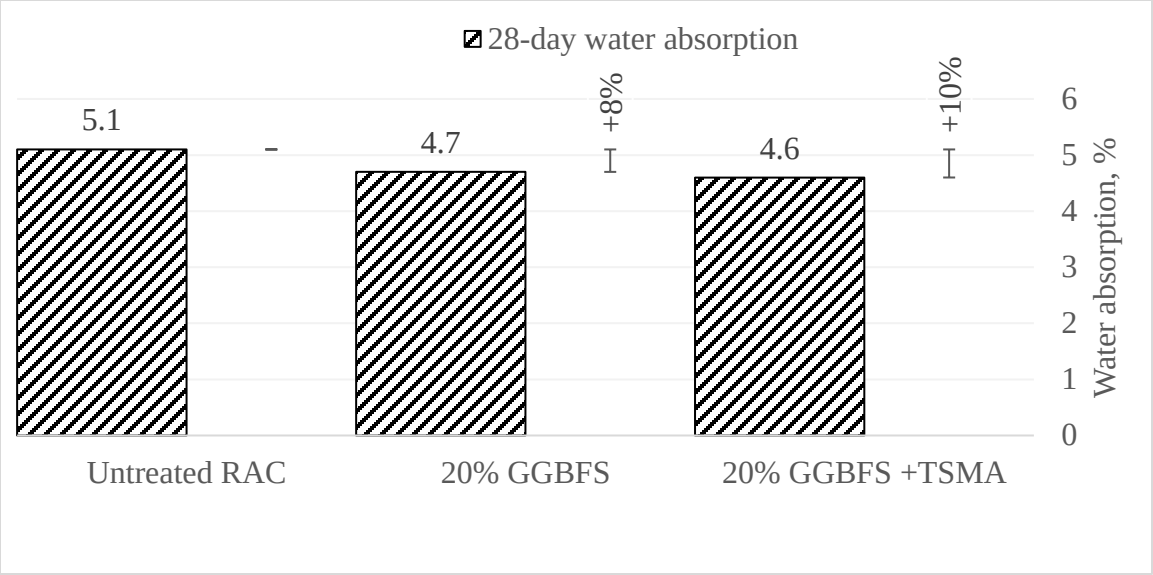

Figure 4-18: Change (%) in the absorption of RACs modified with GGBFS and TSMA after 28 days of curing.

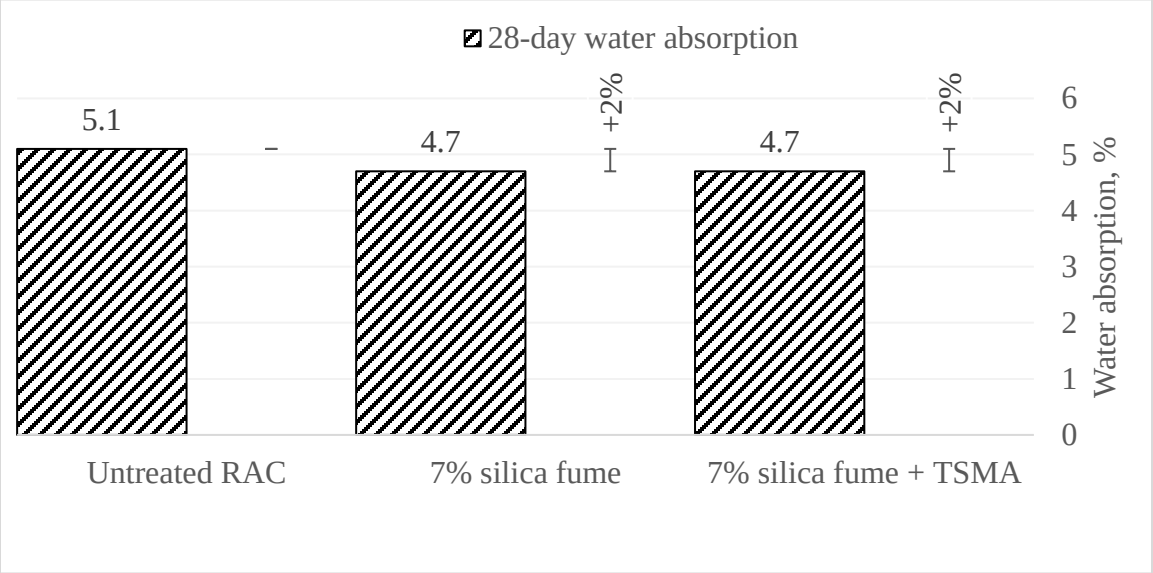

Figure 4-19: Change (%) in the absorption of RACs modified with silica fume and TSMA after 28 days of curing.

4.5.2 Na_2SO_4 and Silica Fume Slurry-Based Strategies

The change (%) in the absorption of RACs modified with Na_2SO_4 and silica fume slurry, with respect to untreated RAC, after 28 days of curing is depicted in Figure 4-20. There

was no significant change in the absorption due to these two treatments. In fact, the RAC treated with Na_2SO_4 resulted in slightly higher water absorption. However, the slurry treated RAC showed similar absorption compared to the untreated RAC.

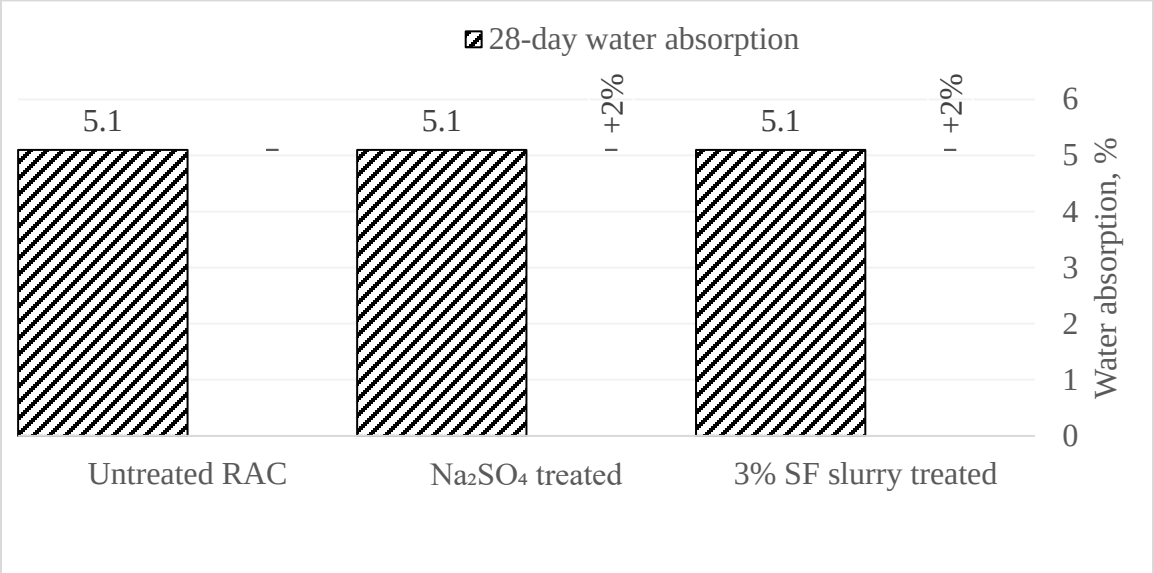

Figure 4-20: Change (%) in the absorption of RACs modified with Na_2SO_4 and silica fume Slurry.

4.5.3 Los Angeles Treatment-based Strategies

The change (%) in the absorption of RACs modified with two different combinations of Los Angeles treatments (LATs), with respect to untreated RAC after 28 days curing, is depicted in Figure 4-21. The RAC modified with LAT alone showed slight decrease (4%) in absorption. However, the combined effect of LAT and sodium silicate treatment showed a significantly better performance (8%).

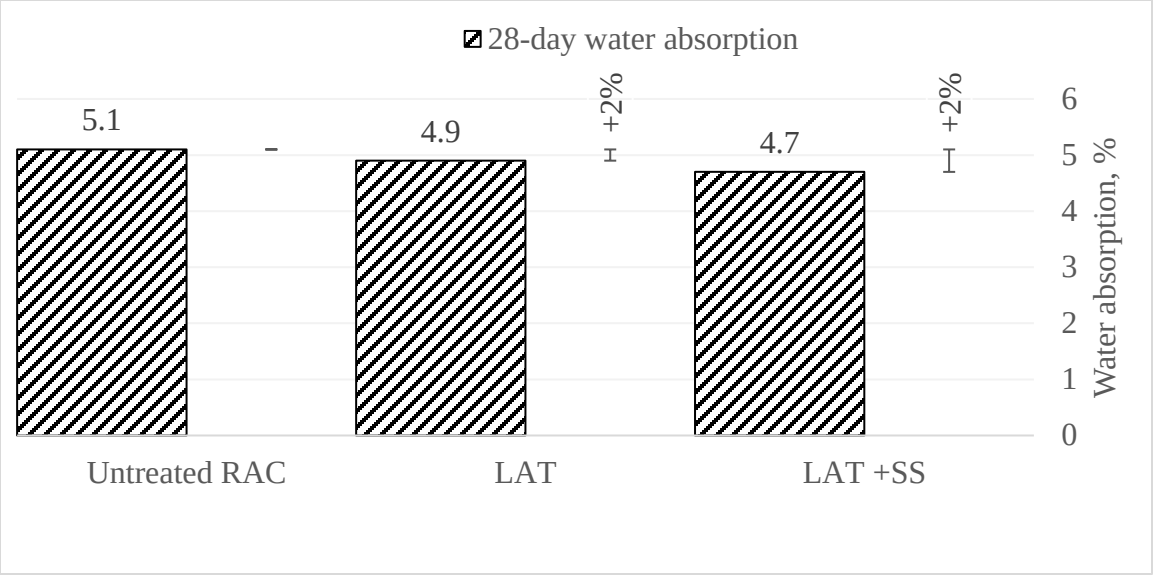

Figure 4-21: Change (%) in the absorption of RACs modified with different combinations of Los Angeles treatments.

4.5.4 Discussion of results

The RACs treated with mineral admixtures caused improvement in decreasing the water absorption, which was in the range of 2% to 8%, compared to control specimens at 28 days. The denser microstructure formed due to the pozzolanic reaction might have played a significant role in decreasing the water absorption. However, all mineral admixtures with TSMA resulted in further improvements in decreasing the water absorption, which was in the range of 8% to 14%. The sealing of cracks due to TSMA might have contributed to a decrease in the porosity of RACs, hence reducing the water absorption. However, treatment of RA with silica fume slurry or Na_2SO_4 treatments resulted in an insignificant change in the water absorption compared to control specimen. The Los Angeles treatment without sodium silicate treatment, exhibited moderate improvements (4%) in decreasing the water absorption. The fact that RAC with Los Angeles treated RA has lower water absorption

than RAC with untreated RA. However, Los Angeles treatment in addition to sodium silicate treatment resulted in considerably better performance (8%) than without sodium silicate treatment. This can be attributed to the crack sealing property of sodium silicate as well as its densification process due to reaction with calcium hydroxide available in concrete [54].

4.6 Rapid Chloride Permeability

The rapid chloride permeability of the prepared RACs is depicted in the Table 4-7 and it is discussed in the following sub-sections.

Table 4-7: Rapid chloride permeability of the developed RACs

Mix ID	Description	Average charge passed (Coulombs)	Permeability Class
M0	0% RA	1816	Low
M1	Untreated RAC	2833	Moderate
M2	TSMA	2585	Moderate
M3	20% fly ash	2012	Moderate
M4	20% fly ash + TSMA	1582	Low
M5	20% GGBFS	2457	Moderate
M6	20% GGBFS +TSMA	2298	Moderate
M7	7% silica fume	1335	Low
M8	7% silica fume + TSMA	1159	Low
M9	Na_2SO_4 treated	3681	Moderate
M10	3% SF slurry treated	2803	Moderate
M11	LAT	2154	Moderate
M12	LAT +SS	1486	Low

4.6.1 TSMA and Mineral Admixture-based Strategies

The change (%) in the total charge passed in RACs modified with TSMA and fly ash, with respect to untreated RAC, after 28 days curing, is depicted in Figure 4-22. The TSMA caused around 9% decrease in the chloride permeability. A significant decrease in the

chloride permeability (20%) in the RAC with 20% fly ash treatment compared to untreated RAC. However, the fly ash treatment along with TSMA resulted in further decrease in the chloride permeability (44%).

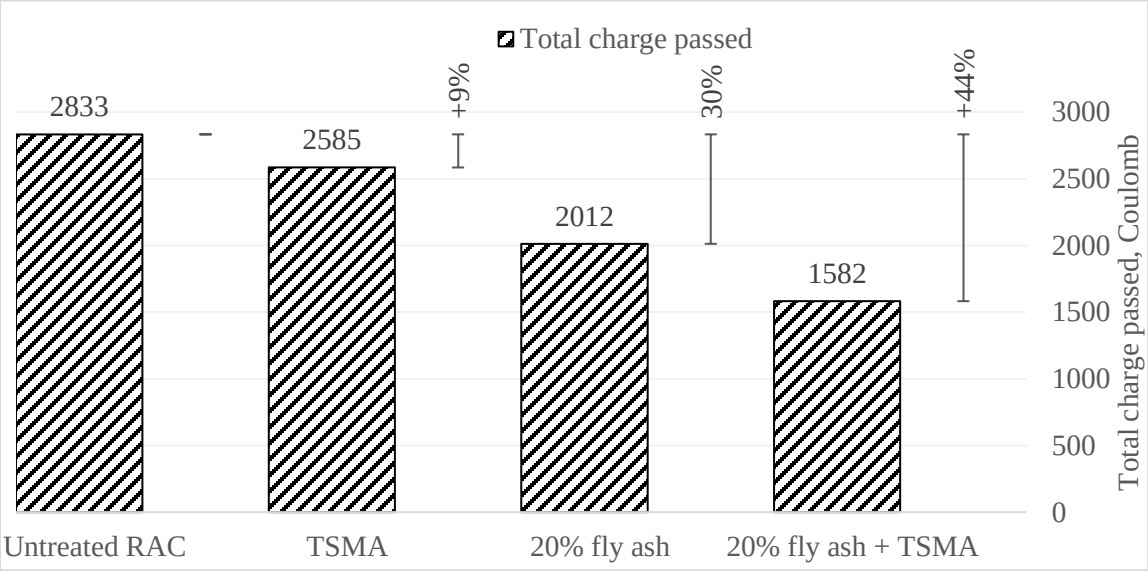

Figure 4-22: Change (%) in the chloride permeability of RACs modified with TSMA and fly ash after 28 days of curing.

The change (%) in the chloride permeability of RACs treated with silica fume or GGBFS and TSMA with respect to untreated RAC after 28 days of curing is depicted in Figure 4-23 and Figure 4-24, respectively. The chloride permeability of RAC with 20 % GGBFS and 7% silica fume decreased by 13% and 53%, respectively, compared to the untreated RAC. However, both treatments along with TSMA caused further decrease (19% and 59%, respectively) in the chloride permeability.

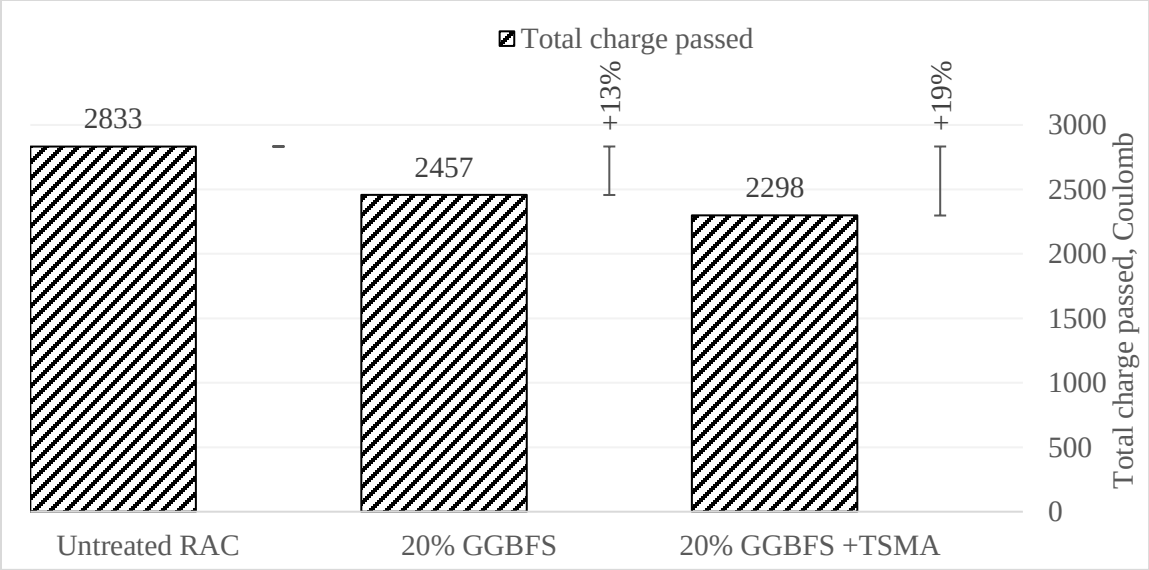

Figure 4-23: Change (%) in the chloride permeability of RACs modified with GGBFS and TSMA after 28 days of curing.

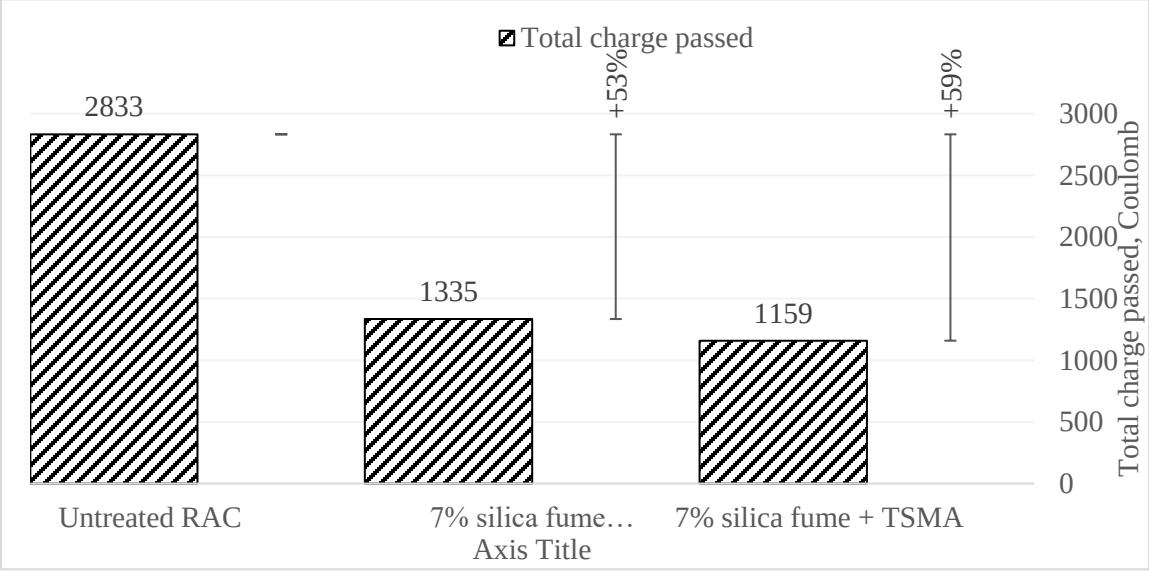

Figure 4-24: Change (%) in total coulomb of RACs modified with silica fume and TSMA after 28 days of curing.

4.6.2 Na_2SO_4 and Silica Fume Slurry-based Strategies

The change (%) in the chloride permeability of RACs treated with Na_2SO_4 and silica fume slurry, with respect to untreated RAC, after 28 days curing, is depicted in Figure 4-25.

There was no improvement in the chloride permeability due to the Na_2SO_4 treatment of RACs. The corresponding decrease in the chloride permeability of the Na_2SO_4 treated RACs was 30%. However, it was only 1% in the RAC with silica fume slurry treatment.

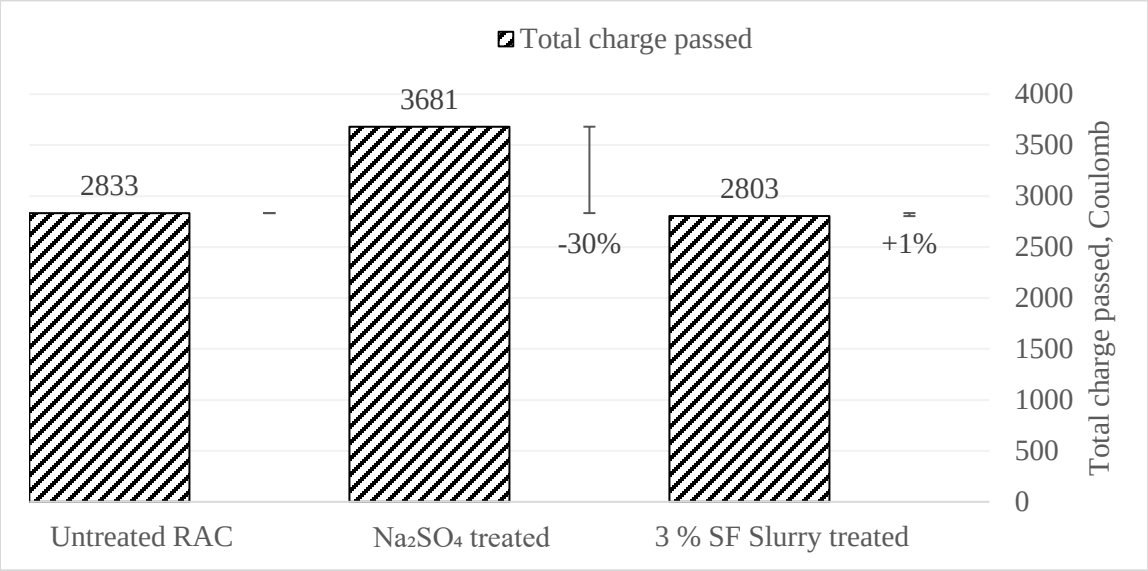

Figure 4-25: Change (%) in the chloride permeability of RACs modified with Na_2SO_4 and silica fume slurry.

4.6.3 Los Angeles Treatment-based Strategies

The change (%) in the chloride permeability of RACs modified with two different combinations of Los Angeles treatments (LATs), with respect to untreated RAC, after 28 days curing, is depicted in Figure 4-26. The RAC modified with LAT alone showed significant improvement (24%) in the chloride permeability. However, the combined effect of LAT and sodium silicate treatment decreased the chloride permeability by 48%.

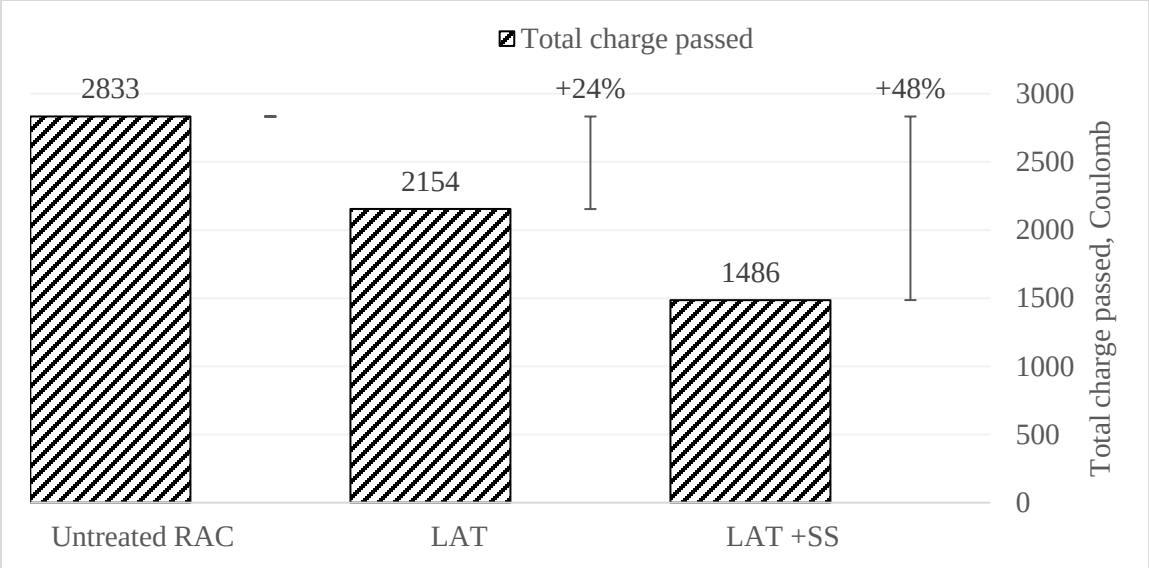

Figure 4-26: Change (%) in the chloride permeability of RACs modified with different combinations of Los Angeles treatments.

4.6.4 Discussion of Results

The RACs modified with mineral admixtures caused a significant decrease in the chloride permeability (as total charge passed), ranging from 13% to 53%, compared to control specimen at 28 days. The dense microstructure due to the pozzolanic reaction might have played a significant role in decreasing the chloride permeability. However, treatment with all mineral admixtures and TSMA further decreased the chloride permeability, which ranged from 19% to 59%. The sealing of cracks due to TSMA might have contributed to decrease the porosity of the RACs, hence reducing the chloride permeability. However, Na_2SO_4 treatment resulted in a chloride permeability (30%) in the chloride permeability compared to the control specimen. There was no significant decrease in the chloride permeability of RAC with silica fume treatment. Los Angeles treatments without sodium silicate treatments, significantly decreased the chloride permeability (24%). The fact that

the Los Angeles treated RA has lower water absorption than untreated RA, might have contributed to produce RCA with less permeable concrete, hence lower chloride permeability. However, RAC with Los Angeles and sodium silicate treatments showed considerably better performance (48%) than without sodium silicate in decreasing the chloride permeability. This can be attributed to the crack sealing property of sodium silicate as well as its densification process due to the reaction with calcium hydroxide available in concrete [54].

4.7 Drying Shrinkage

The drying shrinkage of considered RACs at different ages of air-drying are presented in Table 4-8.

Table 4-8: Drying shrinkage of considered RACs at different ages of air drying

Mix ID	Description	Average Shrinkage (microns) at different ages (days)								
		7	14	21	28	42	56	70	84	98
M0	0% RA	110	273	433	464	585	650	739	776	818
M1	Untreated RAC	424	529	593	757	894	952	1014	1030	1012
M2	TSMA	346	508	618	686	733	770	786	828	859
M3	20% fly ash	271	342	486	533	570	627	672	732	732
M4	20% fly ash + TSMA	209	316	420	536	568	594	659	719	735
M5	20% GGBFS	537	663	773	851	907	964	1024	992	1000
M6	20% GGBFS +TSMA	311	516	602	678	840	958	1013	1034	1054
M7	7% silica fume	440	550	566	699	825	849	856	864	899
M8	7% silica fume + TSMA	401	531	649	676	712	736	780	804	816
M9	Na_2SO_4 treated	141	323	420	548	594	634	717	720	730
M10	3% SF slurry treated	232	387	441	571	639	683	751	814	826
M11	LAT	337	528	651	758	810	896	996	1024	1036
M12	LAT +SS	418	540	723	760	893	911	937	974	988

4.7.1 TSMA and Mineral Admixture-based Strategies

The drying shrinkage of RACs with TSMA and fly ash treatment is depicted in Figure 4-27. The TSMA treatment alone caused significant increase in the dying shrinkage. The performance of RAC due to fly ash treatment is notably better compared to that of untreated RAC. The combination of fly ash and TSMA treatment showed further improvement in the drying shrinkage. However, the drying shrinkage of all the treated RACs was leas than 500 microns at 7 days. The drying shrinkage decreased by 15%, 26% and 27% (with respect to

untreated RAC) for TSMA, fly ash and a combination of both, respectively, after 98 days of drying.

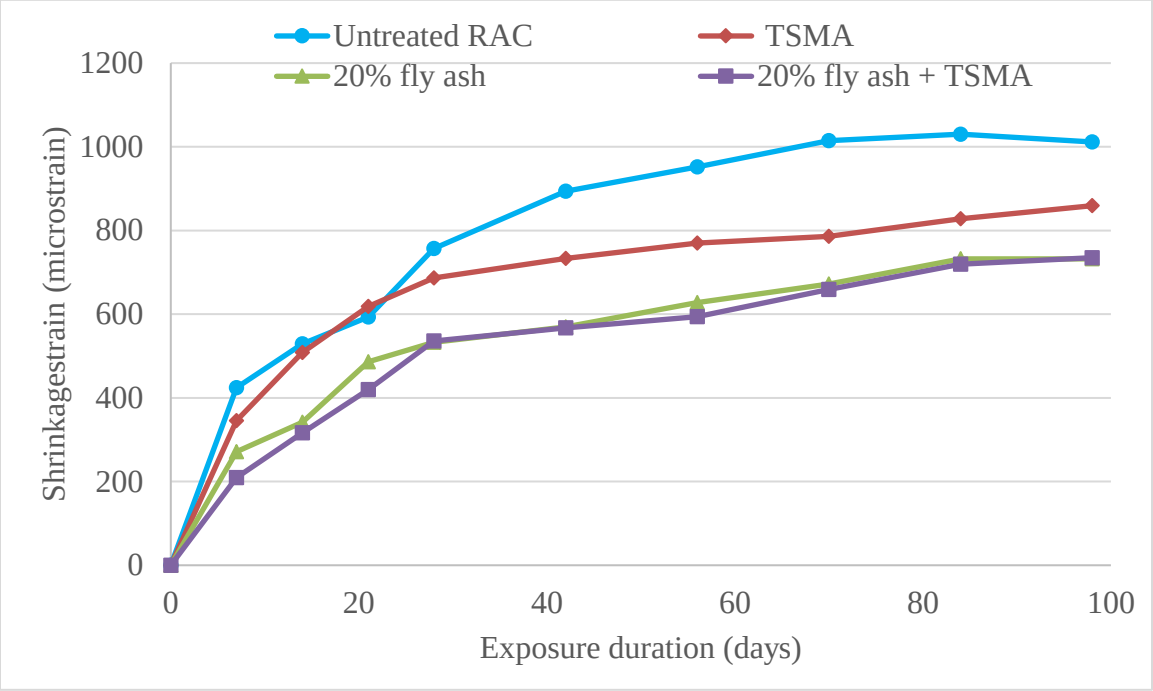

Figure 4-27: Drying shrinkage of RACs modified with TSMA and fly ash.

The drying shrinkage of RACs with GGBFS, silica fume and TSMA treatments is depicted in Figure 4-28 and Figure 4-29, respectively. The silica fume with and without TSMA caused significant decrease in the drying shrinkage. The performance of RAC due to GGBFS and TSMA together, is similar to that of untreated RAC. However, the drying shrinkage of RAC with only GGBFS treatment was more than the threshold value at 7 days. Beside this, all the treated RAC discussed here, fulfilled the threshold value at 7 days which is 500 microns. The drying shrinkage increased by 13% and 19% (with respect to untreated RAC) in the RAC with silica fume treatment with and without TSMA, respectively after 98 days of drying.

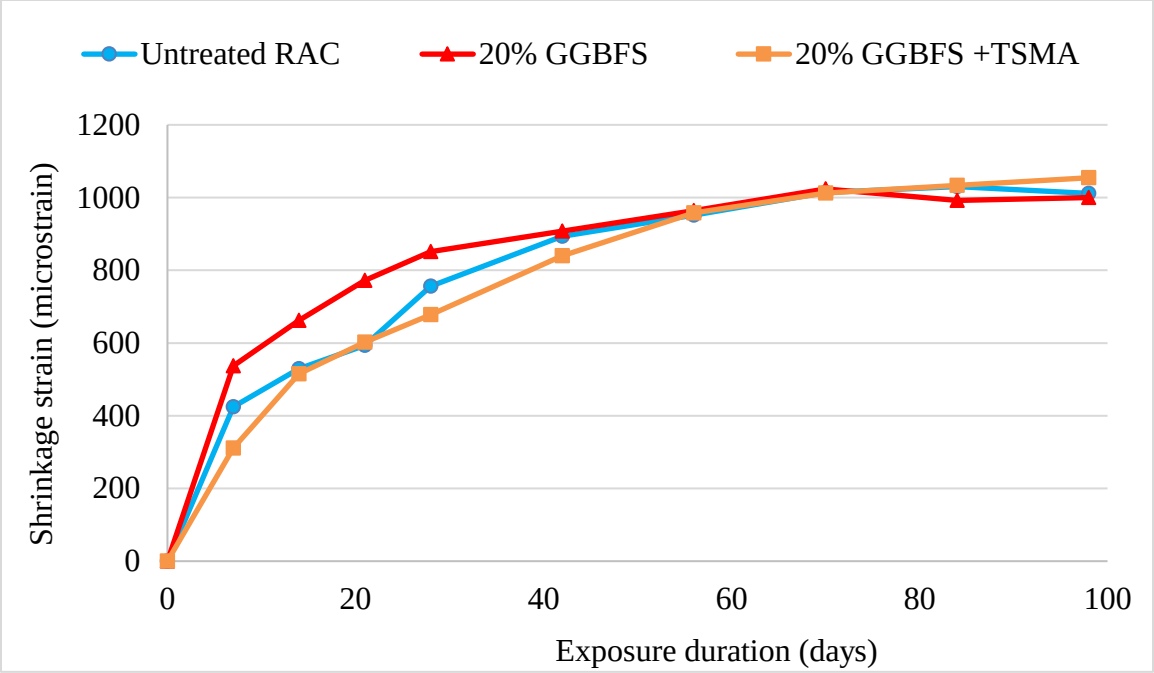

Figure 4-28: Drying shrinkage of RACs treated with GGBFS and TSMA.

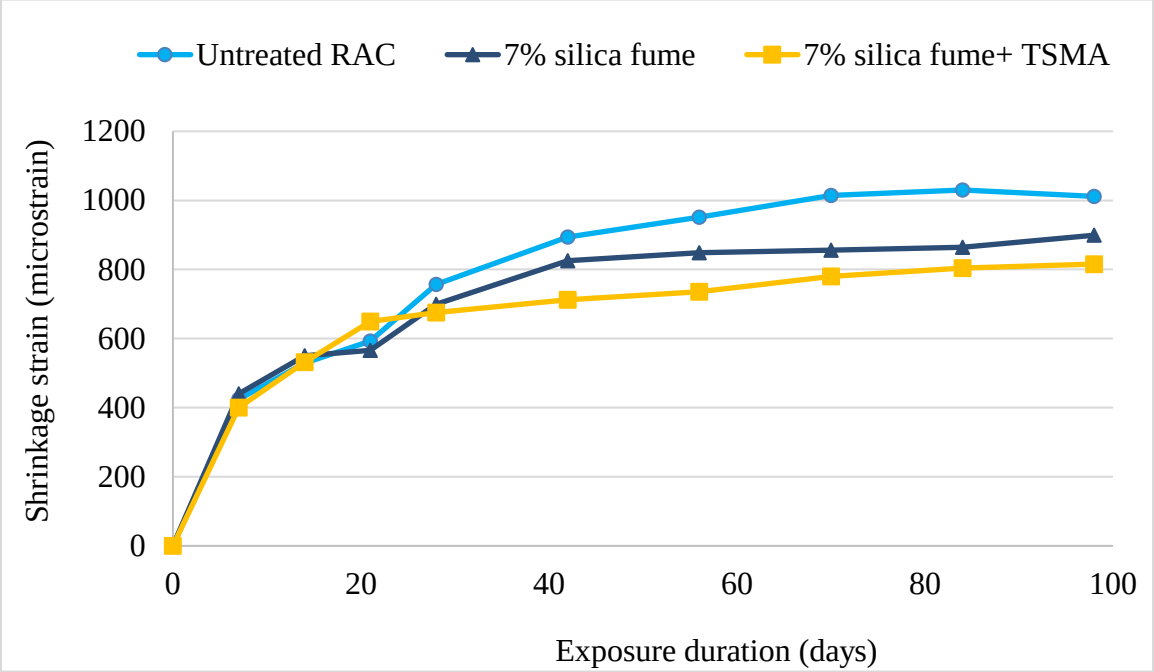

Figure 4-29: Drying shrinkage of RACs treated with silica fume and TSMA.

4.7.2 Na_2SO_4 and Silica Fume Slurry-based Strategies

The drying shrinkage of RACs treated with Na_2SO_4 and silica fume slurry are depicted in Figure 4-30. Both treated RAC discussed here, fulfilled the threshold value at 7 days which is 500 microns. The overall increase in the dying shrinkage of RAC with both the treatments is quite significant. The drying shrinkage decreased by 30% and 24% (with respect to untreated RAC) for Na_2SO_4 and silica fume slurry-based treatment, respectively, at 98 days drying.

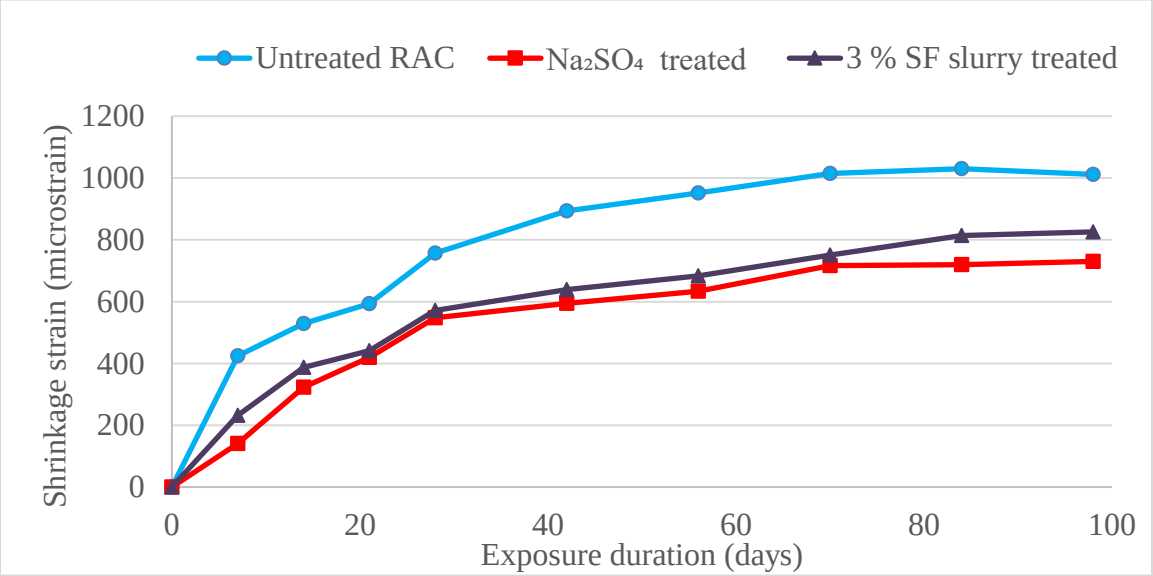

Figure 4-30: Drying shrinkage of RACs treated with Na_2SO_4 and silica fume Slurry.

4.7.3 Los Angeles Treatment-based strategies

The drying shrinkage of RACs with two different combinations of Los Angeles treatments (LATs) is depicted in Figure 4-31. Both the LAT-based RAC discussed here, fulfilled the

threshold value of 500 microns at 7 days. The dying shrinkage both LAT-based RACs was almost similar to that of untreated RAC.

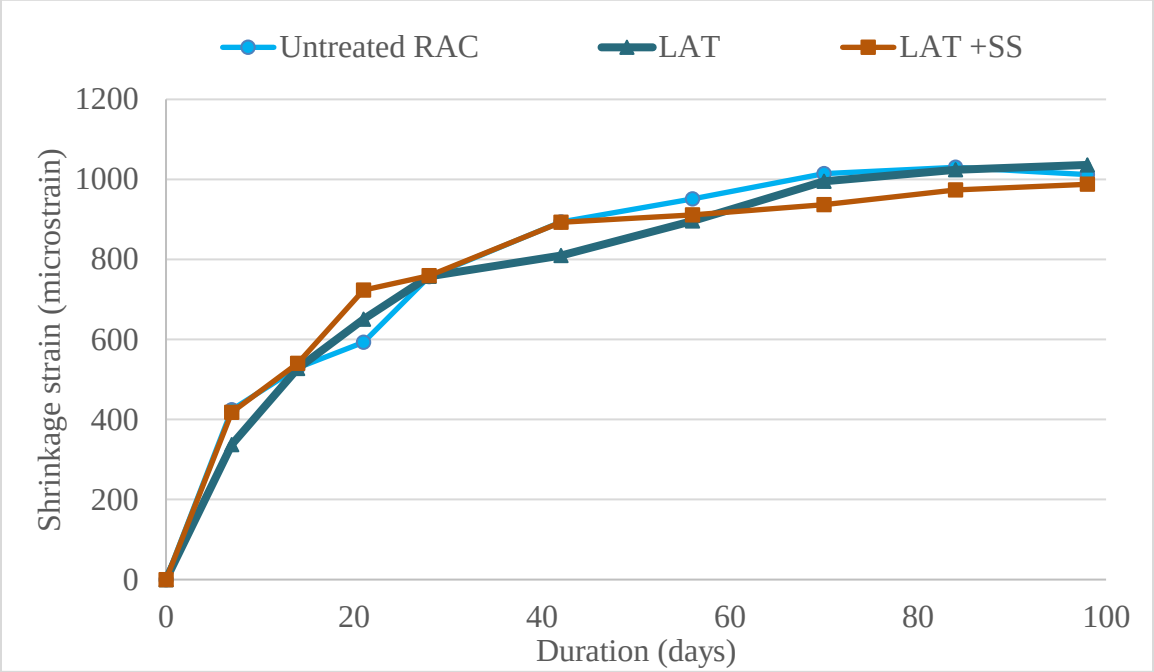

Figure 4-31: Drying shrinkage of RACs modified with two different combinations of Los Angeles treatments.

4.7.4 Discussion of results

The effect of TSMA on drying shrinkage of RAC mixture with and without mineral admixture indicate that the mixing of RAC ingredients using TSMA caused significant reduction in the dying shrinkage. The positive effect of the TSMA may be attributed to the sealing of cracks and pores on the surface of RA by using TSMA leading to refinement of the pores at ITZ. Individual effect of the mineral admixtures in reducing drying shrinkage was also notable. Fly ash has caused a very significant reduction in the drying shrinkage, particularly after 28 days of exposure to the air. The addition of other pozzolanic mineral

admixture (silica fume) also has caused reduction in the drying shrinkage after 28 days exposure to air, but not to the extent to which the FLA has reduced. Unlike the pozzolanic mineral admixtures (fly ash and silica fume), the addition of GGBFS has not caused any noticeable reduction in the drying shrinkage, rather the shrinkage is higher in the early stages of the exposure to air. The reduction in the drying shrinkage due to addition of pozzolanic mineral admixtures (fly ash and silica fume) is due the fact that the chemical shrinkage is lower in presence of the pozzolanic admixtures because of the formation of the extra amount of C-S-H gel that enables refinement of the pores [68]–[75]. Although both pozzolanic admixtures reduced the drying shrinkage significantly, fly ash showed more pronounced reduction in the drying shrinkage as compared to the silica fume. This is because of the fact that the addition of silica fume causes autogenous shrinkage due to its very fine size, particularly at a low water to cementitious materials ratio. This additional shrinkage in presence of SF causes reduction in the ability of the SF to offer resistance against shrinkage as compared to that of the fly ash [68]. Further, the inability of the GGBFS to resist the drying shrinkage [76], [77] is due to its hydration almost similar to that of the OPC resulting into the formation of almost same amount of C-S-H gel causing pore refinement at almost similar level. Unlike the effect of addition of the mineral admixtures on reduction of the drying shrinkage, adoption of TSMA did not show significant improvement, except in case of RAC with silica fume.

The overall reduction of dying shrinkage properties of both Na_2SO_4 and silica fume slurry treatment is quite significant. The drying shrinkages were reduced by 30 % and 24 % (with respect to untreated RAC) for Na_2SO_4 and silica fume slurry-based treatment, respectively at 98 days air drying. The positive effect of the slurry treatment may be attributed to the

sealing of cracks and pores on the surface of RA by using slurry leading to refinement of the pores at ITZ. Besides, the pozzolanic action of silica fume in the slurry also contribute to pore refinement [70], [78]. These eventually contributed to show better performance of drying shrinkage of slurry treated RAC compared to untreated RAC. The possible pore size refinement due to Na_2SO_4 treatment of RA may be contributing in the reduced shrinkage of the resultant RAC. The development of dying shrinkage properties for both LAT based RACs were found like untreated RAC for all ages of drying. Drying shrinkage largely depends on the loss of adsorbed water from concrete. The pore radius of in concrete plays an important role in the extent of loss of water from concrete [69]. Apparently, Los angles treatments (LAT) with and without sodium silicate do not affect to the pore radius of resultant RAC, which might be a possible reason for which their drying shrinkage patterns are similar to the untreated RAC.

4.8 Corrosion Potentials

The corrosion potential of the considered RACs at different ages is summarized in Table 4-9 and Table 4-10. They are discussed in the following sub-sections.

Table 4-9: Corrosion potential of considered RACs at different ages.

	0% RA	Untreated RAC	TSMA	20% fly ash	20% fly ash + TSMA	20% GGBFS	20% GGBFS +TSMA
Days	Corrosion Potential, mV (SCE)						
0	-121	-295	-185	-341	-350	-236	-214
7	-140	-197	-151	-256	-231	-192	-196
14	-143	-178	-141	-260	-226	-158	-176
21	-133	-169	-124	-241	-206	-137	-162
28	-122	-160	-111	-230	-193	-126	-154
35	-105	-139	-111	-230	-193	-102	-128
42	-86	-109	-71	-195	-157	-94	-120
49	-78	-114	-63	-193	-155	-79	-101
56	-55	-122	-54	-184	-145	-82	-105
63	-67	-100	-58	-192	-157	-71	-91
70	-51	-83	-45	-181	-154	-67	-84
77	-51	-220	-38	-247	-149	-60	-78
84	-38	-239	-38	-221	-138	-41	-61
91	-18	-244	-19	-219	-126	-25	-44
98	-18	-287	-7	-193	-177	-22	-38
105	-7	-327	-2	-204	-169	-20	-39
112	-7	-349	-15	-286	-171	-57	-37
119	-95	-360	-24	-317	-170	-50	-38
126	-106	-362	-240	-319	-219	-33	-29
133	-158	-374	-365	-366	-182	-24	-27
140	-100	-378	-401	-366	-167	-18	-23

Table 4-10 (contd.): Corrosion potential of considered RACs at different ages

	7% silica sume	7% silica fume + TSMA	Na_2SO_4 treated	3% SF Slurry treated	LAT	LAT +SS
Days	Corrosion Potential, mV (SCE)					
0	-174	-148	-176	-155	-226	-313
7	-119	-143	-171	-107	-187	-179
14	-94	-136	-164	-180	-181	-160
21	-82	-128	-164	-161	-173	-143
28	-76	-118	-158	-112	-163	-138
35	-55	-165	-154	-123	-157	-124
42	-50	-178	-144	-142	-144	-126
49	-39	-181	-135	-201	-138	-110
56	-45	-151	-139	-205	-249	-99
63	-33	-143	-148	-204	-242	-91
70	-33	-165	-135	-236	-223	-66
77	-30	-107	-130	-250	-220	-30
84	-11	-62	-159	-264	-260	-44
91	-7	-54	-158	-266	-276	-42
98	4	-58	-168	-314	-297	-50
105	3	-87	-345	-322	-342	-37
112	7	-116	-371	-351	-357	-32
119	-34	-73	-381	-427	-358	-29
126	3	-60	-371	-444	-362	-29
133	3	-78	-382	-458	-391	-29
140	7	-71	-386	-461	-400	-23

4.8.1 TSMA and Mineral Admixture-based Strategies

The corrosion potentials on steel in RACs modified by TSMA and fly ash are depicted in Figure 4-32. Because of the presence of moisture, the corrosion potential values were higher (more negative) initially [79]. However, the values decreased with the period of exposure to the chloride solution. The corrosion potentials on steel in the untreated RAC increased after 70 days of exposure and reached the threshold value of -270 mV SCE after 100 days. From the trend of corrosion potentials in other RACs treated by TSMA and fly ash, it is evident that their performance was better than that of the untreated RAC. The

corrosion potential on steel in the fly ash treated RAC crossed the threshold value after about 112 days of exposure, whereas the corrosion potential in the RAC with only TSMA treatment crossed the threshold value after 126 days of exposure. The corrosion potential in RAC treated with both fly ash and TSMA indicated passive condition on the steel state even after 140 days of exposure. Similar results were noted in RACs treated with silica fume or GGBFS plus TSMA (See Figure 4-33 and Figure 4-34). The superior corrosion resistance performance of silica fume treated RAC can be attributed to the dense structure of silica fume concrete that mitigates the diffusion of chloride ions to the steel surface [6], [80].

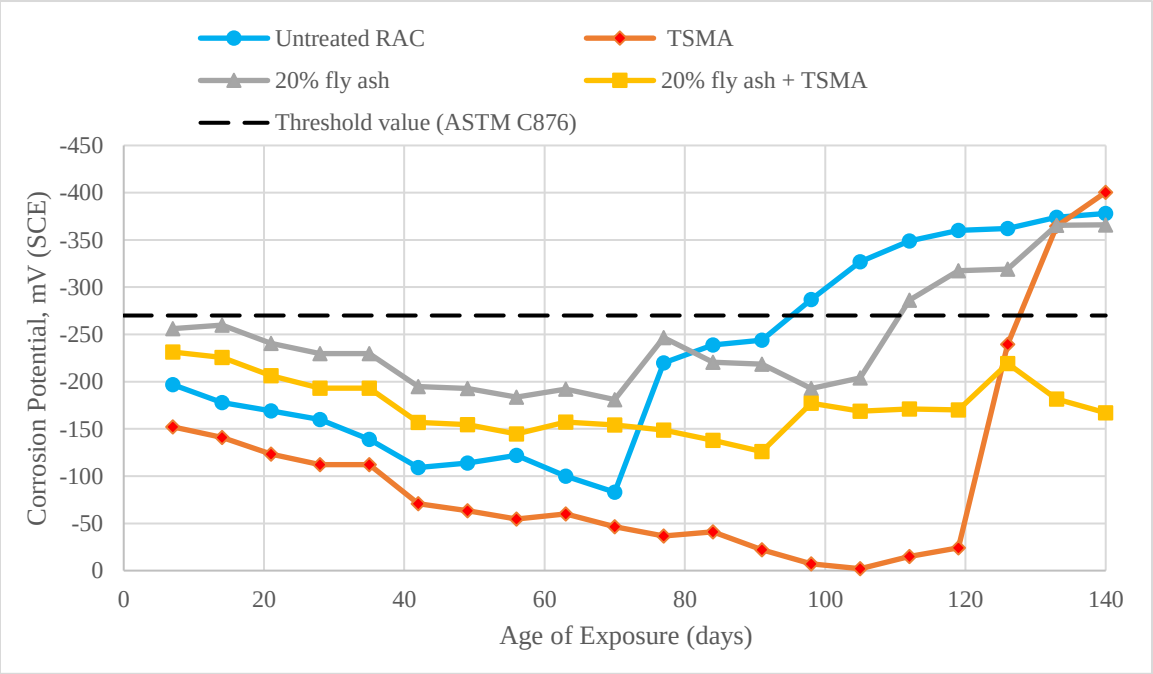

Figure 4-32: Corrosion potential on steel in RACs modified with TSMA and fly ash.

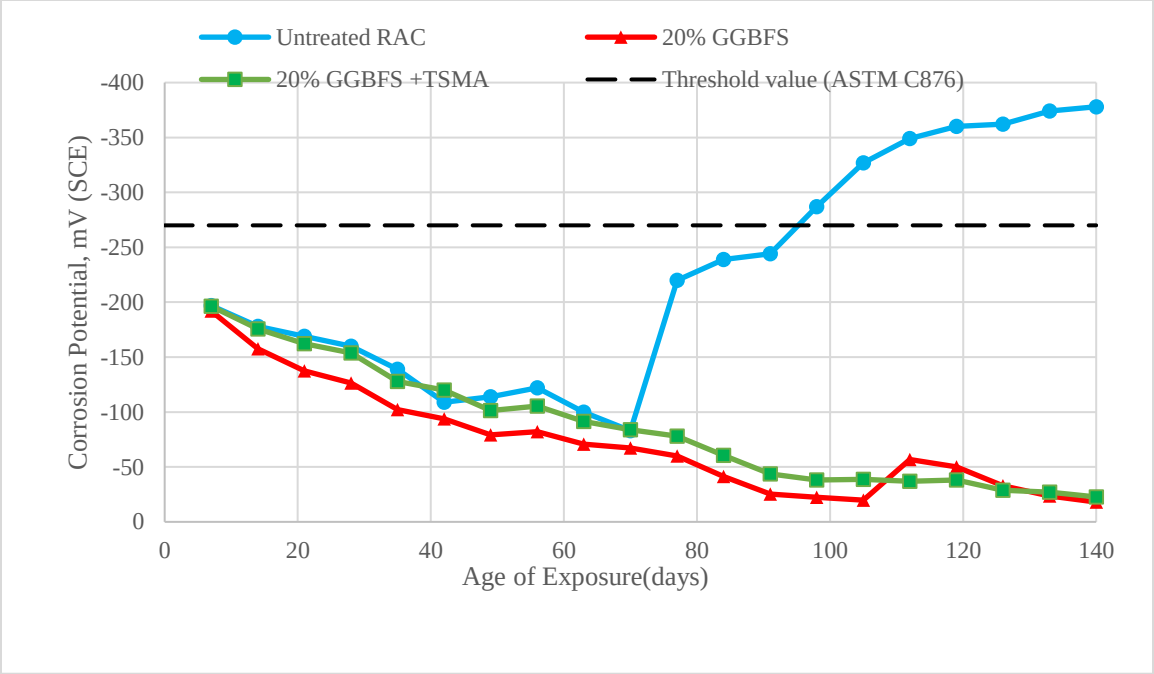

Figure 4-33: Corrosion potential on steel in RACs modified with GGBFS and TSMA.

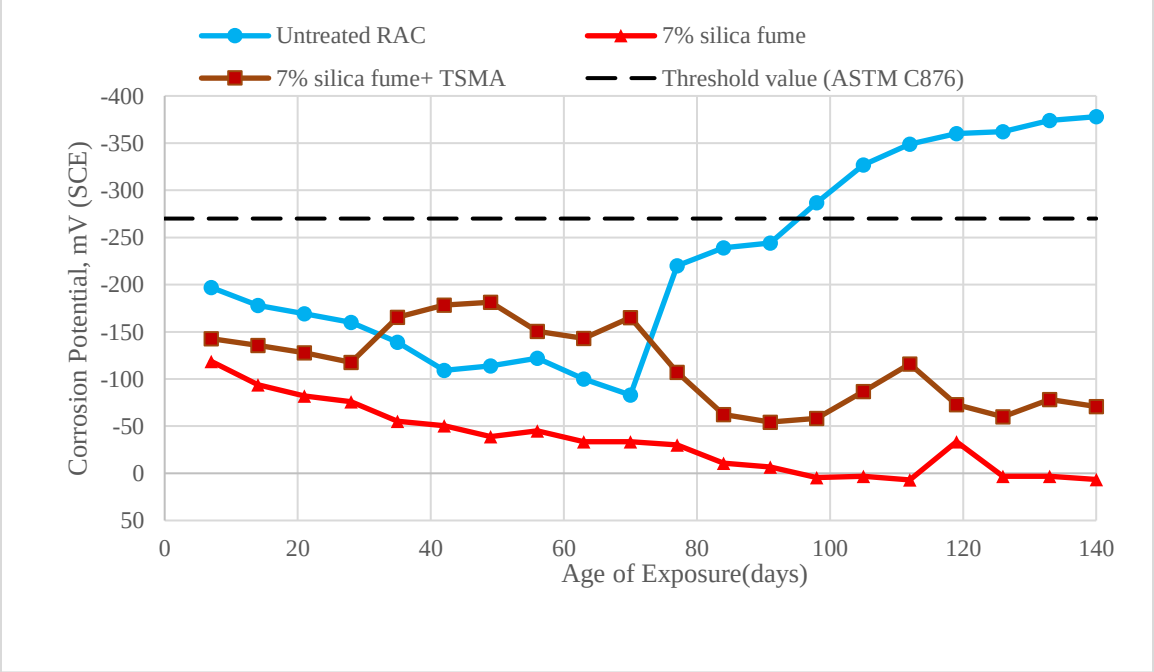

Figure 4-34: Corrosion potential on steel in RACs modified with silica fume and TSMA.

4.8.2 Na_2SO_4 and Silica Fume Slurry-based Strategies

The corrosion potentials on steel in RACs modified by Na_2SO_4 and silica fume slurry are depicted in Figure 4-35. As stated earlier, because of the presence of moisture, the corrosion potentials were high initially. However, they decreased with the period of exposure. The corrosion potentials on steel in the RAC with slurry treated RA increased after 28 days of exposure and almost reached the threshold value after 91 days. The corrosion potentials on steel in the Na_2SO_4 treated RAC were similar to those on the untreated RAC.

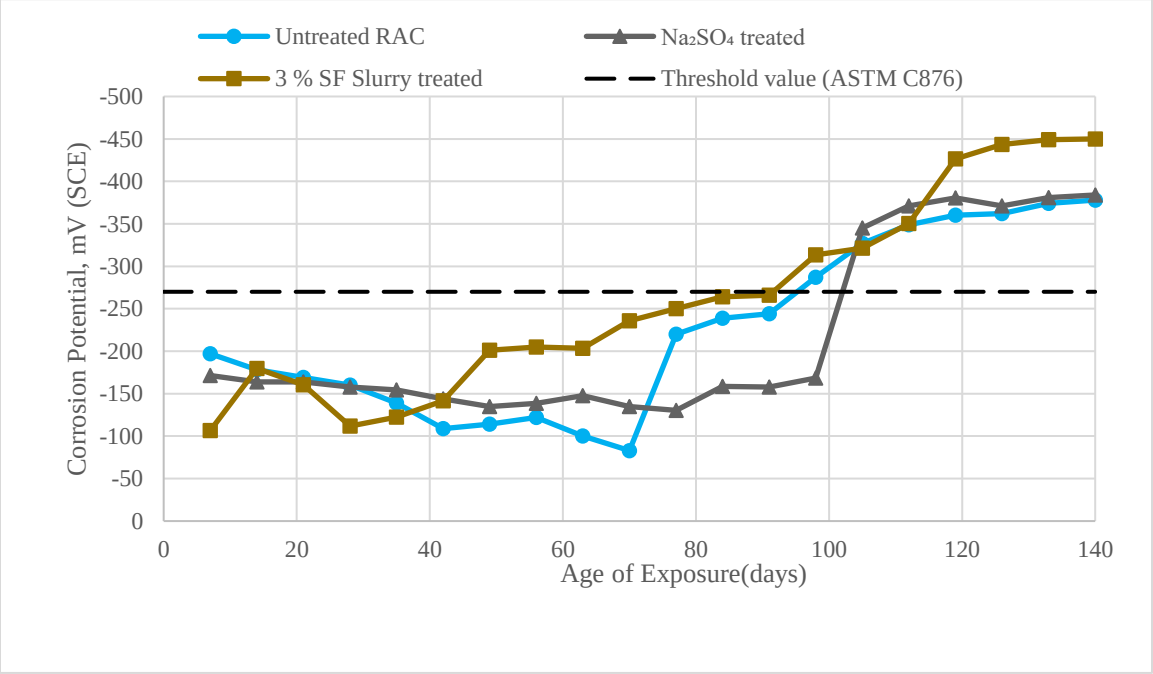

Figure 4-35: Corrosion potential on steel in RACs treated with Na_2SO_4 and silica fume slurry.

4.8.3 Los Angeles Treatment-based strategies

The corrosion potentials on steel in RACs modified by two different combinations of Los Angeles treatments (LATs) are depicted in Figure 4-36. The corrosion potentials on steel

in RACs with LATs were higher potential values initially due to the presence of moisture. But with time they decreased. The corrosion potentials on steel in RAC with only LAT increased after 77 days of exposure and crossed the threshold value after around 84 days of exposure. However, RAC with LAT plus sodium silicate treatment exhibited superior resistance against corrosion and remained in the passive state till the last days (140 days) of measurement. The silicate compound is responsible to increase the bound chloride, which is chemically more stable and does not cause corrosion of the embedded reinforcement. Besides, the surface impregnation of RA with sodium silicate decreased the pore volume leading to slow chloride diffusion and consequent reduction in the corrosion of steel [81].

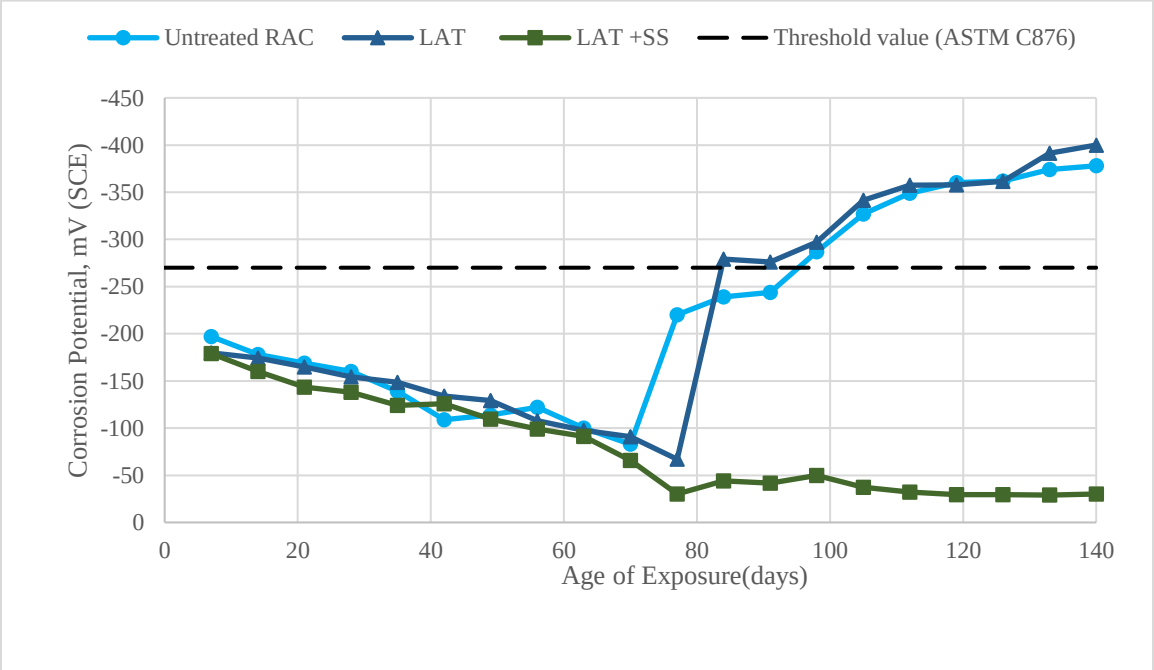

Figure 4-36: Corrosion potential on steel in RACs modified with different combinations of Los Angeles treatments.

4.8.4 Discussion of results

The corrosion potential on steel in the untreated RAC crossed the threshold value after about 100 days of exposure to the chloride solution. However, the potentials on steel in RACs modified by GGBFS or silica fume and with or without TSMA remained in passive state up to 140 days of exposure to the chloride solution. The corrosion potentials on steel in RACs modified with fly ash crossed the threshold value after about 110 days of exposure to the chloride solution. However, the corrosion potentials on steel in RACs modified by fly ash along with TSMA remained in passive state up to 140 days of exposure. The improved microstructure and reduced permeability and water absorption might have contributed to the better performance of this RAC. The corrosion potential on steel in RAC with Los Angeles treatment crossed the corrosion threshold values (-270 mV SCE) after about 90 days of exposure. However, the LAT with sodium silicate showed superior resistance against corrosion and remained in passive state till the last days (140 days) of measurement. The silicate compound is responsible to increase the bound chloride, which is chemically more stable and do not cause corrosion of embedded reinforcement into the concrete. Besides the surface impregnation of RA with sodium silicate is responsible to reduce concrete pore structure, hence the reduction of chloride diffusion and consecutively reduction of corrosion [81].

4.9 Sulfate Resistance

The compressive strength of RAC and control specimens exposed to the sulfate solution for three months is shown in Table 4-11 and discussed in the following sub-sections.

Table 4-11: Compressive strength of the exposed (Na_2SO_4 exposure) specimen and control specimen of considered RACs at three months

Mix Id.	Description	Compressive Strength (MPa)	
		Control Specimen	Na_2SO_4 exposed specimen (3 Months)
M0	0% RA	76	66
M1	Untreated RAC	56	45
M2	TSMA	60	49
M3	20% fly ash	60	57
M4	20% fly ash + TSMA	63	63
M5	20% GGBFS	63	55
M6	20% GGBFS +TSMA	63	57
M7	7% silica fume	60	53
M8	7% silica fume + TSMA	62	56
M9	Na_2SO_4 treated	58	57
M10	3% SF Slurry treated	59	58
M11	Los Angeles treated	63	55
M12	Los Angeles treated +SS	60	59

4.9.1 TSMA and Mineral Admixture-based Strategies

The change (%) in the compressive strength of RACs modified by TSMA and fly ash after three months of Na_2SO_4 exposure is depicted in Figure 4-37. The untreated RAC showed major strength loss (20%) because of sulfate exposure. The mere application of TSMA slightly improved the strength loss. However, the application of fly ash resulted in lower loss of compressive strength (5%) due to sulfate attack. The combined use of fly ash and TSMA resulted in no strength loss due to sulfate attack. The same trend is also applicable for RACs treated with silica fume, GGBFS and TSMA. The strength loss of RACs modified by silica fume and GGBFS with and without TSMA was 13%, 10%, 12% and 10%, respectively (see Figure 4-38 and Figure 4-39).

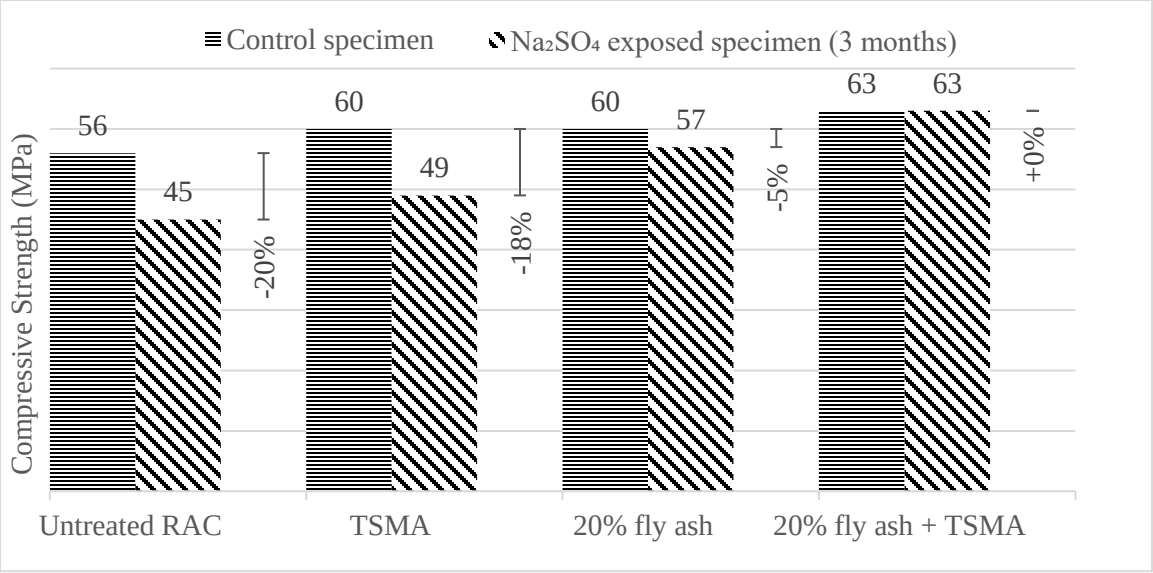

Figure 4-37: Change (%) in the compressive strength of RACs modified with TSMA and fly ash after three months of Na_2SO_4 exposure

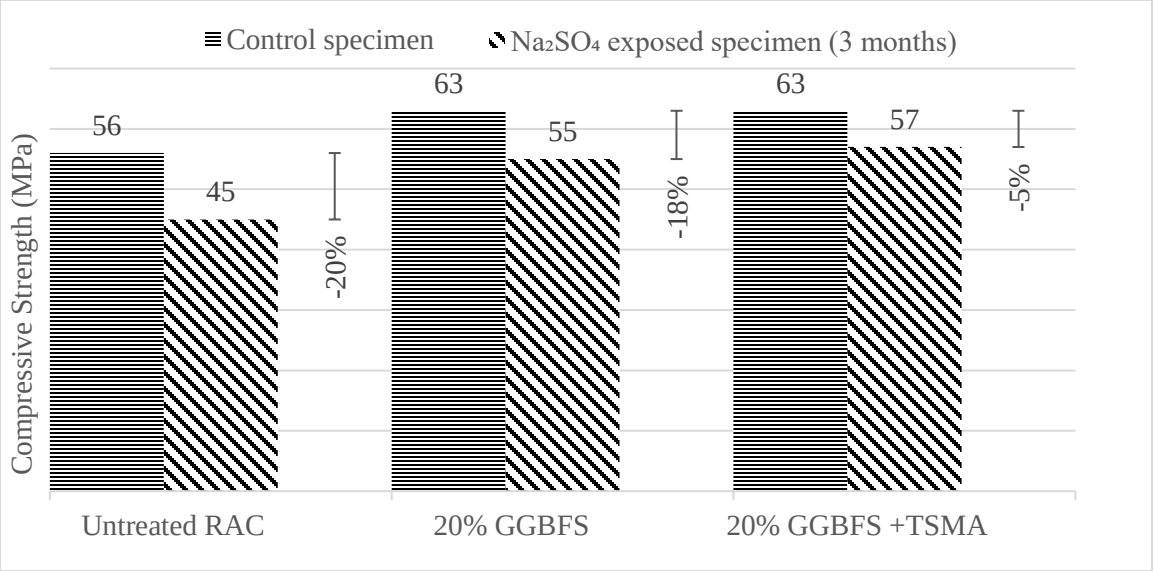

Figure 4-38: Change (%) in the compressive strength of RACs modified with TSMA and GGBFS after three months of Na_2SO_4 exposure

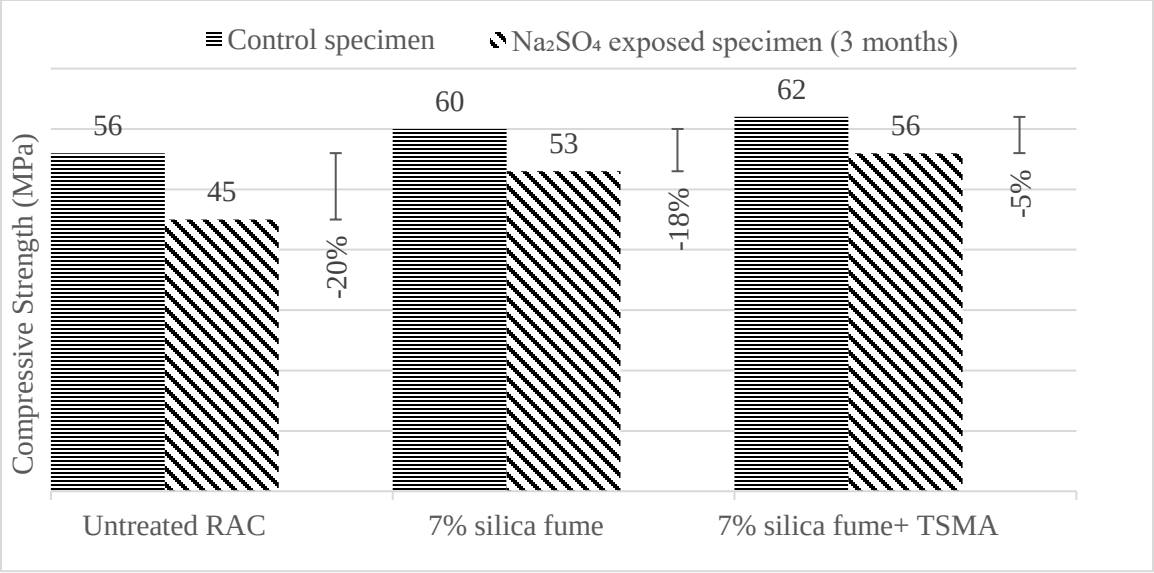

Figure 4-39: Change (%) in the compressive strength of RACs modified with TSMA and silica fume after three months of Na_2SO_4 exposure

4.9.2 Na_2SO_4 and Silica Fume Slurry-based Strategies

The change (%) in the compressive strength of RACs modified by Na_2SO_4 and silica fume slurry after three months of Na_2SO_4 exposure is depicted in Figure 4-40. Both treatments showed higher resistance against the sulfate attack. The strength loss of Na_2SO_4 and silica fume slurry treated RAC due to sulfate attack was 2%.

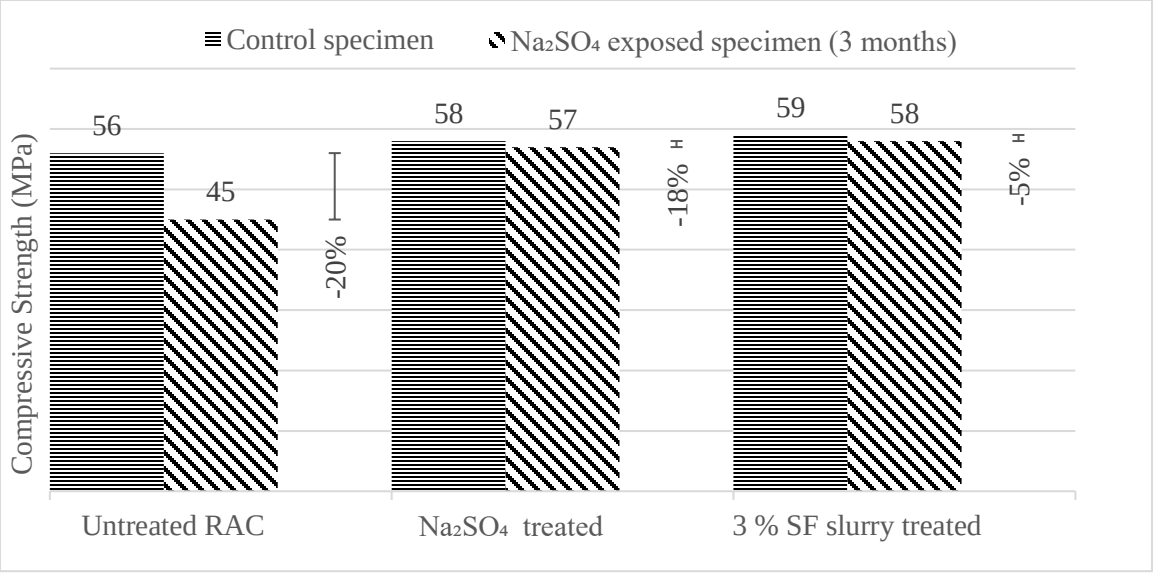

Figure 4-40: Change (%) in the compressive strength of RACs modified with Na_2SO_4 and silica fume slurry after three months of Na_2SO_4 exposure

4.9.3 Los Angeles Treatment-based strategies

The change (%) in the compressive strength of RACs modified by two different Los Angeles treatments after three months of Na_2SO_4 exposure is depicted in Figure 4-41. The mere application of Los Angeles treatments significantly improved the sulfate resistance of RAC (13% strength loss). However, the application of sodium silicate and Los Angeles treatment resulted in low loss in compressive strength (2%) due to sulfate attack.

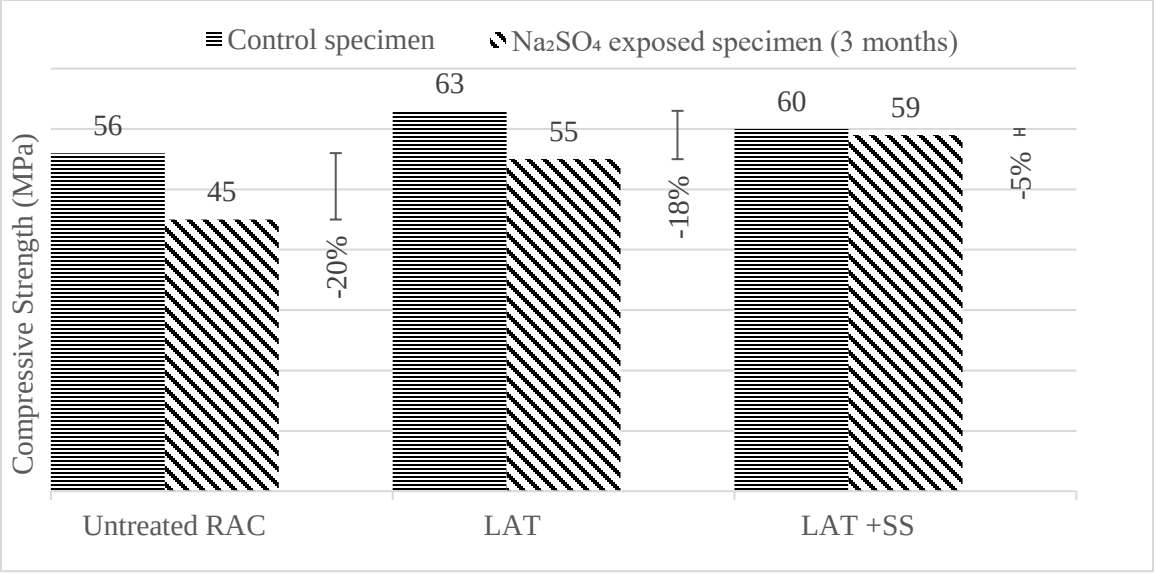

Figure 4-41: Change (%) in the compressive strength of RACs modified with two different combinations of Los Angeles treatments after three months of Na_2SO_4 exposure

4.9.4 Discussion of results

There was only 5% strength loss due to sulfate attack in RAC treated by fly ash. For, GGBFS and silica fume treatments the strength loss was 13% and 12%, respectively. However, the addition of TSMA with mineral admixture treatments improved the sulfate resistance of RAC. The improved microstructure and reduced permeability and water absorption due to the mentioned treatments might have contributed to a better sulfate-resistance. The superior sulfate resistance of fly ash added RAC can be attributed to stabilization mechanism of calcium aluminate hydrates due to fly ash [82].The strength loss of Los Angeles treated RAC was only 13%. The improved RA surface and resulting less permeable RAC might be responsible for improvements. However, the Los Angeles treatments with sodium silicate and the slurry treatments showed remarkable resistance against sulfate attack. This improved sulfate-resistance can be attributed to the crack

sealing property of sodium silicate as well as its densification process due to its reaction with calcium hydroxide available in concrete [54]. The Na_2SO_4 treated RAC also showed high sulfate-resistance. The treatment itself required a dense solution of Na_2SO_4 solution which increased the sulfate content of treated RAC. This might be reason that its performance in the normal and the sulfur exposure was almost the same.

4.10 Microscopic Study

Small pieces of the untreated RAC and several treated RACs were collected in a manner where old aggregate, old mortar and new mortar were present. The pieces were coated with gold before placing them in a scanning electron microscope. The SEM images and the elemental composition at selected spectrum generated in the EDS are discussed in following sub-sections.

4.10.1 Untreated RAC

Figure 4-42 shows the morphology of the untreated RAC. A weak interfacial zone between the aggregate and the old mortar and between the old and new mortar is clearly evident in this micrograph.

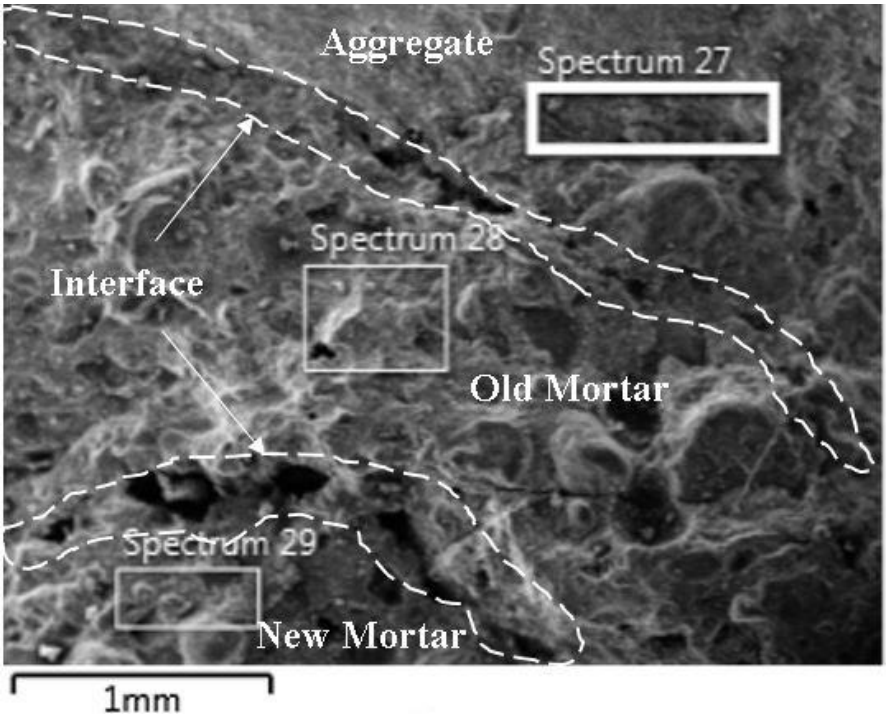

Figure 4-42: SEM of untreated RAC

Table 4-12: Elemental composition of untreated RAC at selected spectrum through EDS

Element	% Weight		
	Spectrum 27 (Aggregate)	Spectrum 28 (Old mortar)	Spectrum 29 (New mortar)
O	44.3	42.9	39.8
Ca	28.7	30.2	22.5
C	12.3	17.6	20.8
Si	9.7	5.4	12.3
K	1.4	0.6	0.9
Al	1.1	1.4	1.5
Mg	0.6	0.6	1

4.10.2 Treated RAC

Three treated RACs were considered for SEM and EDS at selected points. They are-

(a) TSMA

(b) 7% silica fume + TSMA

(c) LAT +7% SF+TSMA

4.10.2.1 TSMA

The morphology of RAC with TSMA treated RA is shown in Figure 4-43. While the interface between the old mortar and aggregate is weak while a strong bond between the old mortar and new mortar can be noted. This indicates that TSMA treatment has led to the formation of a strong bond between the old and the new mortar. This strong bond has probably contributed to the improved properties of RAC with TSMA treatment.

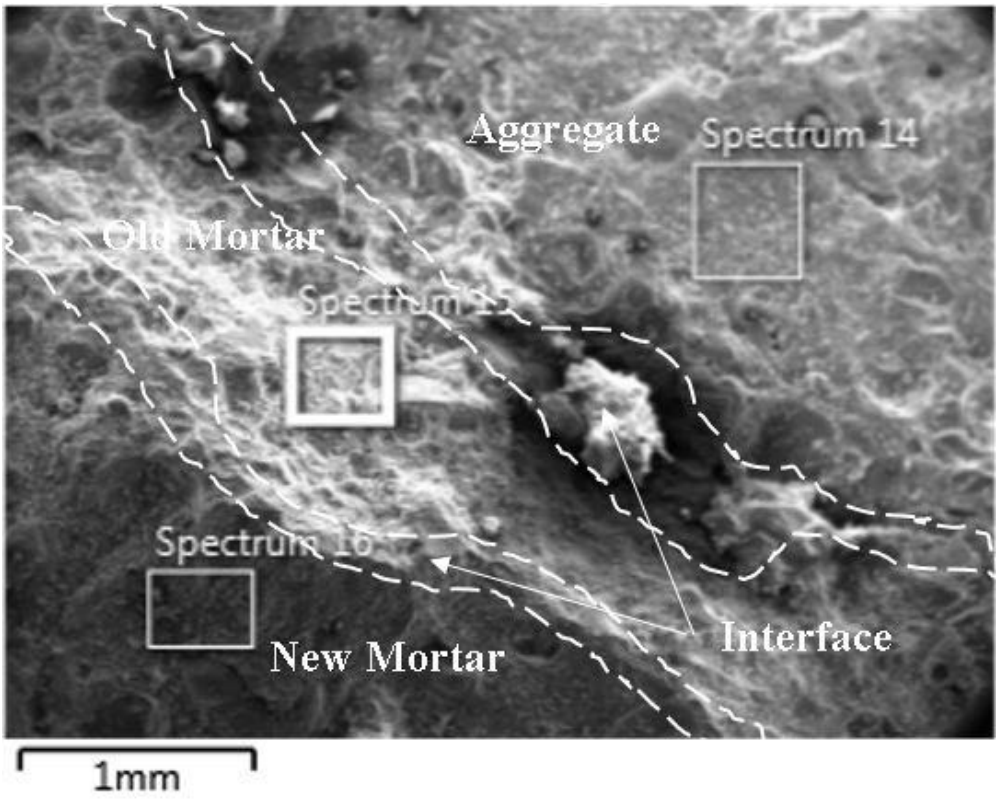

Figure 4-43: SEM of treated RAC (TSMA)

Table 4-13: Elemental composition of treated RAC (TSMA) at selected spectrum through EDS

Element	% Weight		
	Spectrum 14 (Aggregate)	Spectrum 15 (Old mortar)	Spectrum 16 (New mortar)
O	44.7	42.6	48
Ca	32.7	29.8	22
C	12.5	13.9	14.8
Si	6.9	9.5	10.8
Al	1.3	1.1	1.2
K	-	1.0	0.6
Mg	0.5	0.5	-

4.10.2.2 7% silica fume + TSMA

The morphology of RAC treated with silica fume plus TSMA is shown in Figure 4-44. A distinct interface failure between the old mortar and the aggregate can be noted while the interface between the old mortar and new mortar is dense and impermeable. The dense and impermeable interface between the old mortar and the new mortar has contributed to the improvement in the properties of the RAC with this treatment.

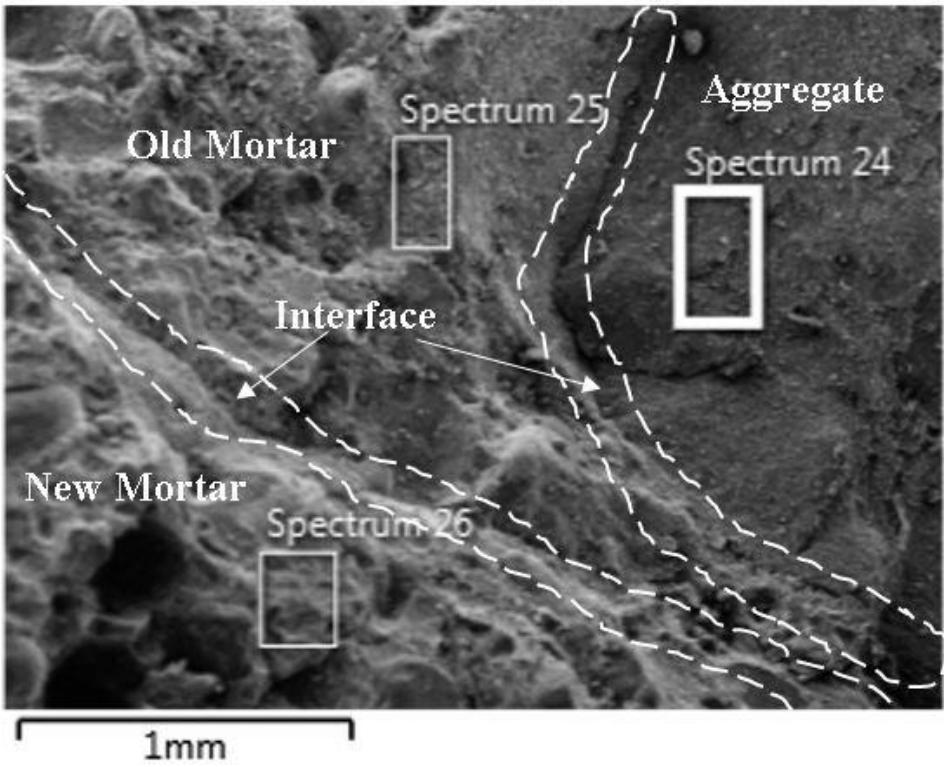

Figure 4-44: SEM of treated RAC (7% SF + TSMA)

Table 4-14: Elemental composition of treated RAC (7% SF + TSMA) at selected spectrum through EDS

Element	% Weight		
	Spectrum 24 (Aggregate)	Spectrum 25 (Old mortar)	Spectrum 26 (New mortar)
O	41.3	38.5	34.1
Ca	46.9	32.4	43.5
C	10.5	13.7	11.7
Si	0.8	8.6	8.9
Al	0.5	1.5	1.7
K	-	1.0	-
Mg	-	1.1	-

4.10.2.3 LAT +7% SF+TSMA

Figure 4-45 shows the morphology of RAC with LAT plus silica fume and TSMA treatment of RA. A weak bond between the old mortar and aggregate was noted. However,

the bond between the new mortar and the old mortar was not that dense as in the other treatments.

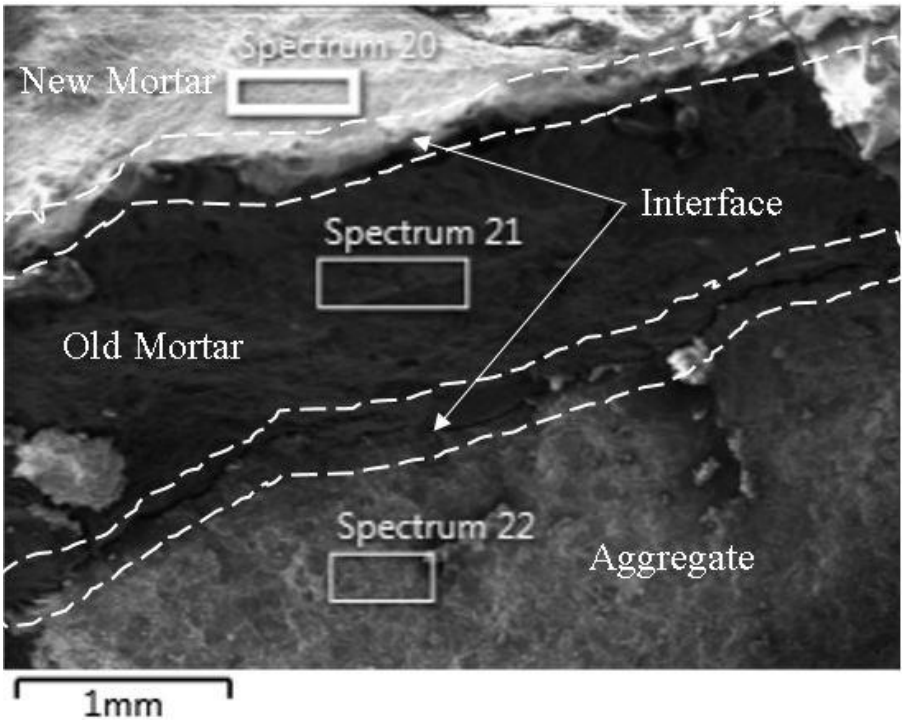

Figure 4-45: SEM of treated RAC (LAT+7% SF + TSMA)

Table 4-15: Elemental composition of treated RAC (LAT+7% SF + TSMA) at selected spectrum through EDS

Element	% Weight		
	Spectrum 20 (New mortar)	Spectrum 21 (Old mortar)	Spectrum 22 (Aggregate)
O	51.1	37.1	45.7
Ca	20.9	49.1	40.2
C	18.8	9.8	12.4
Si	5.1	2.3	0.8
Al	1.0	0.5	0.4
K	0.9	0.9	-
Mg	0.6	0.4	0.4

4.10.3 Discussion

The scanning electron micrographs of RAC with untreated and treated aggregates indicated a clear difference in the interfacial bond between the new mortar and the RA. A weak interfacial zone between the old aggregate and the old mortar was noted in RAC with bth treated and untreated RA. Similarly, the interfacial bond between the aggregate and the new mortar was weak in the RAC without any treatment. However, a good bond was noted between the aggregate and new mortar was noted in the treated RAC. Thus, the treatment of RAC, in most cases, has improved the bond between the new mortar and the RA. This improvement in the interfacial has improved the properties of RAC with treated RA. The improvement in the properties is reflected more in the durability rather than the mechanical properties.

CHAPTER 5

CONCLUSIONS AND RECOMMENDATIONS

5.1 Conclusions

The following conclusions can be made based on the analysis of the experimental data generated through the present study:

1 The workability of untreated RAC was more than that of NAC. This can be attributed to the excess water required in producing RAC to compensate the high absorption of the RA. The excess water in RAC mixture remains available on the surface of the aggregate for some time before being absorbed that enables in reducing friction and therefore in increasing the workability.

2 The workability of treated RAC was more than the untreated RAC. This can be attributed to the lubricating effect of the added mineral admixtures and the smoothening of the RA surface by various treatments, particularly Los Angeles treatment.

3 The pulse velocity increased with the increase in the period of curing in all the RACs. The dense microstructure formed due to longer curing time is primarily responsible for the increase in the pulse velocity.

4 Significant improvement in the properties of RAC was achieved due to TSMA treatment. The addition of 7% silica fume along with TSMA further enhanced both the durability and mechanical properties of RAC (see Table 5-1).

Table 5-1: Improvement in properties of RAC due to TSMA and silica fume addition.

Property	Test age (Days)	Control mixture	7% silica fume + TSMA	% improvement with respect to Control mixture
Compressive strength, MPa	90	50	59	18
Splitting tensile strength, MPa	28	2.4	3.1	29
Shrinkage, micro strain	98	1012	816	19
Pulse Velocity, km/s	90	4.76	4.76	0
Absorption, %	28	5.1	4.7	8
RCP, Coulombs	28	2833	1159	59
Corrosion potential, mV SCE	140	-378	-71	-
Sulfate resistance (strength loss)	90	20	10	50

5 The addition of 20% GGBFS along with TSMA produced further major enhancement in both the durability and mechanical properties of RAC (see Table 5-2).

Table 5-2: Improvement of RAC properties due TSMA and GGBFS.

Property	Test age (Days)	Control mixture	20% GGBFS +TSMA	% improvement with respect to Control mixture
Compressive strength, MPa	90	50	58	16
Splitting tensile strength, MPa	28	2.4	2.8	17
Shrinkage, micro strain	98	1012	1000	1
Pulse velocity, km/s	90	4.76	4.85	2
Absorption, %	28	5.1	4.4	14
RCP, Coulomb	28	2833	2298	19
Corrosion potential, mV SCE	140	-378	-23	-
Sulfate resistance (strength loss)	90	20	10	50

6 The abrasive treatment (Los Angeles Treatment) also showed promising results (see Table 5-3). However, the corrosion potentials in these specimens crossed the corrosion threshold values at early age (84 days) compared to RAC with other strategies.

Table 5-3: Improvement of RAC properties due Los Angeles treatment (LAT).

Property	Test age (Days)	Control mixture	LAT	% improvement with respect to Control mixture
Compressive strength, MPa	90	50	57	14
Splitting tensile strength, MPa	28	2.4	3.2	33
Shrinkage, micro strain	98	1012	1036	similar
Pulse Velocity, km/s	90	4.76	4.81	1
Absorption, %	28	5.1	4.9	4
RCP, Coulomb	28	2833	2154	24
Corrosion potential, mV SCE	140	-378	-400	similar
Sulfate resistance (strength loss)	90	20	13	35

7 The durability problem of the LAT treated RAC was overcome significantly when this treatment was combined with sodium silicate. However, the mechanical properties were found slightly improved (see Table 5-4).

Table 5-4: Comparison properties of RAC with of LAT treated RAC with and without sodium silicate

Property	Test ages (days)	LAT	LAT +SS
Compressive strength, MPa	90	55	57
Splitting tensile strength, MPa	28	3.2	3.3
Shrinkage, micro strain	98	1036	988
Pulse Velocity, km/s	90	4.81	4.72
Absorption, %	28	4.9	4.7
RCP, Coulomb	28	2154	1486
Corrosion potential, mV SCE	140	-378	-23
Sulfate resistance (strength loss)	90	13	2

8 From the SEM images of untreated and treated RACs it is evident that the interfaces at recycled aggregate, old mortar and new mortar become less cracked and dense after treatment of the RA. These improved interfaces contributed to the enhanced properties of the treated RAC.

5.2 Recommendations

The recommended strategies for improving the properties of RAC are presented in Table 5-5.

Table 5-5: Recommended strategies for improving the properties of RAC

Recommended strategies for improving the mechanical properties	Recommended strategies for improving the durability
• 7% silica fume + TSMA • 20% fly ash + TSMA • 20%GGBFS +TSMA • Los Angeles treatment	• 7% silica fume + TSMA • 20% fly ash + TSMA • 20% GGBFS +TSMA • Los Angeles treatment+ Sodium silicate

5.3 Suggestions for Future Work

1. The recommended strategies can be explored for RAC with more than 40% RA.
2. Other mechanical properties, such as modulus of elasticity, creep of treated RAC should be evaluated.

3. Further study can be carried out to identify the effect of grading of the treated RA on the properties of RAC.

References

[1] S. Ismail, K. W. Hoe, and M. Ramli, "Sustainable Aggregates: The Potential and Challenge for Natural Resources Conservation," *Procedia - Soc. Behav. Sci.*, vol. 101, pp. 100–109, Nov. 2013.

[2] A. Katz, "Properties of concrete made with recycled aggregate from partially hydrated old concrete," *Cem. Concr. Res.*, vol. 33, no. 5, pp. 703–711, May 2003.

[3] L. Butler, J. S. West, and S. L. Tighe, "The effect of recycled concrete aggregate properties on the bond strength between RCA concrete and steel reinforcement," *Cem. Concr. Res.*, vol. 41, no. 10, pp. 1037–1049, Oct. 2011.

[4] C. ; Yang, C. Hs, and A. F. Ashour, "Influence of Type and Replacement Level of Recycled Aggregates on Concrete Properties," *ACI Mater. J.*, vol. 105, no. 3, pp. 289–296, 2008.

[5] R. V. Silva, J. de Brito, and R. K. Dhir, "Establishing a relationship between modulus of elasticity and compressive strength of recycled aggregate concrete," *J. Clean. Prod.*, vol. 112, pp. 2171–2186, Jan. 2016.

[6] C. Medina, W. Zhu, T. Howind, M. I. Sánchez de Rojas, and M. Frías, "Influence of mixed recycled aggregate on the physical – mechanical properties of recycled concrete," *J. Clean. Prod.*, vol. 68, pp. 216–225, Apr. 2014.

[7] M. Maslehuddin and O. S. B. Al-Amoudi, "Sustainable Green Recycled Aggregate Concrete for Rigid Pavements," Dahran, 2018.

[8] S.-W. Kim and H.-D. Yun, "Influence of recycled coarse aggregates on the bond behavior of deformed bars in concrete," *Eng. Struct.*, vol. 48, pp. 133–143, Mar. 2013.

[9] M. Malesev, V. Radonjanin, and S. Marinkovic, "Recycled concrete as aggregate for producing structural concrete," in *Sustainability of Constructions – Integrated Approach to Life-time Structural Engineering. COST Action C25*, 2007, p. 2.61.

[10] L. H. Sneed, T. D'Antino, C. Carloni, and C. Pellegrino, "A comparison of the bond behavior of PBO-FRCM composites determined by double-lap and single-lap shear

tests," *Cem. Concr. Compos.*, vol. 64, pp. 37–48, Nov. 2015.

[11] R. V. Silva, J. de Brito, and R. K. Dhir, "Tensile strength behaviour of recycled aggregate concrete," *Constr. Build. Mater.*, vol. 83, pp. 108–118, May 2015.

[12] M. Bravo, J. de Brito, J. Pontes, and L. Evangelista, "Mechanical performance of concrete made with aggregates from construction and demolition waste recycling plants," *J. Clean. Prod.*, vol. 99, pp. 59–74, Jul. 2015.

[13] J. Qiu, D. Q. S. Tng, and E.-H. Yang, "Surface treatment of recycled concrete aggregates through microbial carbonate precipitation," *Constr. Build. Mater.*, vol. 57, pp. 144–150, Apr. 2014.

[14] G. Fathifazl, A. Ghani Razaqpur, O. Burkan Isgor, A. Abbas, B. Fournier, and S. Foo, "Creep and drying shrinkage characteristics of concrete produced with coarse recycled concrete aggregate," *Cem. Concr. Compos.*, vol. 33, no. 10, pp. 1026–1037, Nov. 2011.

[15] V. Corinaldesi, "Mechanical and elastic behaviour of concretes made of recycled-concrete coarse aggregates," *Constr. Build. Mater.*, vol. 24, no. 9, pp. 1616–1620, Sep. 2010.

[16] V. W. Y. Tam, D. Kotrayothar, and J. Xiao, "Long-term deformation behaviour of recycled aggregate concrete," *Constr. Build. Mater.*, vol. 100, pp. 262–272, Dec. 2015.

[17] A. M. Wagih, H. Z. El-Karmoty, M. Ebid, and S. H. Okba, "Recycled construction and demolition concrete waste as aggregate for structural concrete," *HBRC J.*, vol. 9, no. 3, pp. 193–200, Dec. 2013.

[18] H. Qasrawi, I. Marie, and H. Tantawi, "Use of Recycled Concrete Rubbles as Coarse Aggregate in Concrete," in *Proc. 5th Jordanian Int. Civ. Eng. Conf.*, 2012.

[19] T. Ozbakkaloglu, A. Gholampour, and T. Xie, "Mechanical and Durability Properties of Recycled Aggregate Concrete: Effect of Recycled Aggregate Properties and Content," *J. Mater. Civ. Eng.*, vol. 30, no. 2, p. 04017275, Feb. 2018.

[20] H. Dilbas, M. Şimşek, and Ö. Çakır, "An investigation on mechanical and physical properties of recycled aggregate concrete (RAC) with and without silica fume,"

Constr. Build. Mater., vol. 61, pp. 50–59, Jun. 2014.

[21] N. K. Bui, T. Satomi, and H. Takahashi, “Improvement of mechanical properties of recycled aggregate concrete basing on a new combination method between recycled aggregate and natural aggregate,” *Constr. Build. Mater.*, vol. 148, pp. 376–385, Sep. 2017.

[22] S. Pradhan, S. Kumar, and S. V. Barai, “Recycled aggregate concrete: Particle Packing Method (PPM) of mix design approach,” *Constr. Build. Mater.*, vol. 152, pp. 269–284, Oct. 2017.

[23] W. Li, J. Xiao, Z. Sun, S. Kawashima, and S. P. Shah, “Interfacial transition zones in recycled aggregate concrete with different mixing approaches,” *Constr. Build. Mater.*, vol. 35, pp. 1045–1055, Oct. 2012.

[24] P. Rajhans, S. K. Panda, and S. Nayak, “Sustainable self compacting concrete from C&D waste by improving the microstructures of concrete ITZ,” *Constr. Build. Mater.*, vol. 163, pp. 557–570, Feb. 2018.

[25] P. Rajhans, S. K. Panda, and S. Nayak, “Sustainability on durability of self compacting concrete from C&D waste by improving porosity and hydrated compounds: A microstructural investigation,” *Constr. Build. Mater.*, vol. 174, pp. 559–575, Jun. 2018.

[26] S. Kou, C. Poon, and F. Agrela, “Comparisons of natural and recycled aggregate concretes prepared with the addition of different mineral admixtures,” *Cem. Concr. Compos.*, vol. 33, no. 8, pp. 788–795, Sep. 2011.

[27] D. Pedro, J. de Brito, and L. Evangelista, “Mechanical characterization of high performance concrete prepared with recycled aggregates and silica fume from precast industry,” *J. Clean. Prod.*, vol. 164, pp. 939–949, Oct. 2017.

[28] Ö. Çakır, “Experimental analysis of properties of recycled coarse aggregate (RCA) concrete with mineral additives,” *Constr. Build. Mater.*, vol. 68, pp. 17–25, Oct. 2014.

[29] P. L. Maier and S. A. Durham, “Beneficial use of recycled materials in concrete mixtures,” *Constr. Build. Mater.*, vol. 29, pp. 428–437, Apr. 2012.

[30] R. K. Majhi and A. N. Nayak, “Bond, durability and microstructural characteristics of ground granulated blast furnace slag based recycled aggregate concrete,” *Constr. Build. Mater.*, vol. 212, pp. 578–595, Jul. 2019.

[31] K. Y. Ann, H. Y. Moon, Y. B. Kim, and J. Ryou, “Durability of recycled aggregate concrete using pozzolanic materials,” *Waste Manag.*, vol. 28, no. 6, pp. 993–999, 2008.

[32] S.-C. Kou and C.-S. Poon, “Long-term mechanical and durability properties of recycled aggregate concrete prepared with the incorporation of fly ash,” *Cem. Concr. Compos.*, vol. 37, pp. 12–19, Mar. 2013.

[33] M. L. Berndt, “Properties of sustainable concrete containing fly ash, slag and recycled concrete aggregate,” *Constr. Build. Mater.*, vol. 23, no. 7, pp. 2606–2613, Jul. 2009.

[34] N. Kisku, H. Joshi, M. Ansari, S. K. Panda, S. Nayak, and S. C. Dutta, “A critical review and assessment for usage of recycled aggregate as sustainable construction material,” *Constr. Build. Mater.*, vol. 131, pp. 721–740, Jan. 2017.

[35] J. Junak and A. Sicakova, “Effect of Surface Modifications of Recycled Concrete Aggregate on Concrete Properties,” *Buildings*, vol. 8, no. 1, p. 2, Dec. 2017.

[36] P. Nuaklong, V. Sata, A. Wongsa, K. Srinavin, and P. Chindaprasirt, “Recycled aggregate high calcium fly ash geopolymer concrete with inclusion of OPC and nano-SiO2,” *Constr. Build. Mater.*, vol. 174, pp. 244–252, Jun. 2018.

[37] H. Zhang, Y. Zhao, T. Meng, and S. P. Shah, “Surface Treatment on Recycled Coarse Aggregates with Nanomaterials,” *J. Mater. Civ. Eng.*, vol. 28, no. 2, p. 04015094, Feb. 2016.

[38] S.-C. Kou, B. Zhan, and C.-S. Poon, “Use of a CO2 curing step to improve the properties of concrete prepared with recycled aggregates,” *Cem. Concr. Compos.*, vol. 45, pp. 22–28, Jan. 2014.

[39] B. J. Zhan, D. X. Xuan, and C. S. Poon, “Enhancement of recycled aggregate properties by accelerated CO2 curing coupled with limewater soaking process,” *Cem. Concr. Compos.*, vol. 89, pp. 230–237, May 2018.

[40] C. Shi, Z. Wu, Z. Cao, T. C. Ling, and J. Zheng, “Performance of mortar prepared with recycled concrete aggregate enhanced by CO2 and pozzolan slurry,” *Cem. Concr. Compos.*, vol. 86, pp. 130–138, Feb. 2018.

[41] A. Akhtar and A. K. Sarmah, “Strength improvement of recycled aggregate concrete through silicon rich char derived from organic waste,” *J. Clean. Prod.*, vol. 196, pp. 411–423, Sep. 2018.

[42] S. Senaratne, D. Gerace, O. Mirza, V. W. Y. Tam, and W.-H. Kang, “The costs and benefits of combining recycled aggregate with steel fibres as a sustainable, structural material,” *J. Clean. Prod.*, vol. 112, pp. 2318–2327, Jan. 2016.

[43] J. Xie, Y. Guo, L. Liu, and Z. Xie, “Compressive and flexural behaviours of a new steel-fibre-reinforced recycled aggregate concrete with crumb rubber,” *Constr. Build. Mater.*, vol. 79, pp. 263–272, Mar. 2015.

[44] J. Xie, C. Fang, Z. Lu, Z. Li, and L. Li, “Effects of the addition of silica fume and rubber particles on the compressive behaviour of recycled aggregate concrete with steel fibres,” *J. Clean. Prod.*, vol. 197, pp. 656–667, Oct. 2018.

[45] K. Pandurangan, A. Dayanithy, and S. Om Prakash, “Influence of treatment methods on the bond strength of recycled aggregate concrete,” *Constr. Build. Mater.*, vol. 120, pp. 212–221, Sep. 2016.

[46] Y. Kim, A. Hanif, S. M. S. Kazmi, M. J. Munir, and C. Park, “Properties enhancement of recycled aggregate concrete through pretreatment of coarse aggregates – Comparative assessment of assorted techniques,” *J. Clean. Prod.*, vol. 191, pp. 339–349, 2018.

[47] H.-S. Kim, B. Kim, K.-S. Kim, and J.-M. Kim, “Quality improvement of recycled aggregates using the acid treatment method and the strength characteristics of the resulting mortar,” *J. Mater. Cycles Waste Manag.*, vol. 19, no. 2, pp. 968–976, Apr. 2017.

[48] S. G. Kumar and A. K. Minocha, “Studies on thermo-chemical treatment of recycled concrete fine aggregates for use in concrete,” *J. Mater. Cycles Waste Manag.*, vol. 20, no. 1, pp. 469–480, Jan. 2018.

[49] G. Dimitriou, P. Savva, and M. F. Petrou, “Enhancing mechanical and durability properties of recycled aggregate concrete,” *Constr. Build. Mater.*, vol. 158, pp. 228–

235, Jan. 2018.

[50] V. S. Babu, A. K. Mullick, K. K. Jain, and P. K. Singh, “Mechanical properties of high strength concrete with recycled aggregate-influence of processing,” *Indian Concr. J.*, vol. 88, no. 5, pp. 10–26, 2014.

[51] A. Hanif, Y. Kim, Z. Lu, and C. Park, “Early-age behavior of recycled aggregate concrete under steam curing regime,” *J. Clean. Prod.*, vol. 152, pp. 103–114, May 2017.

[52] Despotović and Iva, “The improvement of recycled concrete aggregate- A review paper,” in *4 th international conference contemporary achievements in civil engineering*, 2016, pp. 443–454.

[53] D. Matias, J. de Brito, A. Rosa, and D. Pedro, “Mechanical properties of concrete produced with recycled coarse aggregates – Influence of the use of superplasticizers,” *Constr. Build. Mater.*, vol. 44, pp. 101–109, Jul. 2013.

[54] N. K. Bui, T. Satomi, and H. Takahashi, “Mechanical properties of concrete containing 100% treated coarse recycled concrete aggregate,” *Constr. Build. Mater.*, vol. 163, pp. 496–507, Feb. 2018.

[55] L. Wang *et al.*, “Consolidating recycled concrete aggregates using phosphate solution,” *Constr. Build. Mater.*, vol. 200, pp. 703–712, Mar. 2019.

[56] Z. Zhao, S. Wang, L. Lu, and C. Gong, “Evaluation of pre-coated recycled aggregate for concrete and mortar,” *Constr. Build. Mater.*, vol. 43, pp. 191–196, Jun. 2013.

[57] A. I. Kareem, H. Nikraz, and H. Asadi, “Evaluation of the double coated recycled concrete aggregates for hot mix asphalt,” *Constr. Build. Mater.*, vol. 172, pp. 544–552, May 2018.

[58] L. P. Singh, V. Bisht, M. S. Aswathy, L. Chaurasia, and S. Gupta, “Studies on performance enhancement of recycled aggregate by incorporating bio and nano materials,” *Constr. Build. Mater.*, vol. 181, pp. 217–226, Aug. 2018.

[59] J. Wang, B. Vandevyvere, S. Vanhessche, J. Schoon, N. Boon, and N. De Belie, “Microbial carbonate precipitation for the improvement of quality of recycled aggregates,” *J. Clean. Prod.*, vol. 156, pp. 355–366, Jul. 2017.

[60] A. M. Grabiec, J. Klama, D. Zawal, and D. Krupa, “Modification of recycled concrete aggregate by calcium carbonate biodeposition,” *Constr. Build. Mater.*, vol. 34, pp. 145–150, Sep. 2012.

[61] A. H. Zaben, “Mechanical Properties of Green Recycled Aggregate Concrete Using Construction and Demolition Waste in Saudi Arabia.,” King Fahd University of Petrolium and Minerals, Dhahran, 2017.

[62] M. Tuyan, A. Mardani-Aghabaglou, and K. Ramyar, “Freeze–thaw resistance, mechanical and transport properties of self-consolidating concrete incorporating coarse recycled concrete aggregate,” *Mater. Des.*, vol. 53, pp. 983–991, Jan. 2014.

[63] M. S. Choi, S. B. Park, and S.-T. Kang, “Effect of the Mineral Admixtures on Pipe Flow of Pumped Concrete,” *J. Adv. Concr. Technol.*, vol. 13, no. 11, pp. 489–499, 2015.

[64] J. Afsar, “Effect of Mixing time On Concrete Workability | Effect On Slump | Conclusion | Engineering Intro,” 2012. [Online]. Available: http://www.engineeringintro.com/concrete/workability/effect-of-mixing-time-on-workability-of-concrete-effect-on-slump-conclusion/. [Accessed: 26-Feb-2019].

[65] M. Thomas, *Optimizing the Use of Fly Ash in Concrete*, vol. 5420. Portland Cement Association Skokie, IL, 2007.

[66] G. Li, H. Xie, and G. Xiong, “Transition zone studies of new-to-old concrete with different binders,” *Cem. Concr. Compos.*, vol. 23, no. 4–5, pp. 381–387, Aug. 2001.

[67] V. W. Y. Tam, X. F. Gao, and C. M. Tam, “Microstructural analysis of recycled aggregate concrete produced from two-stage mixing approach,” *Cem. Concr. Res.*, vol. 35, no. 6, pp. 1195–1203, Jun. 2005.

[68] S. Sarkar, A. Halder, and S. Bishnoi, “Shrinkage in Concretes Containing Fly Ash,” in *UKIERI Concrete Congress*, 2013.

[69] F. Collins and J. . Sanjayan, “Effect of pore size distribution on drying shrinking of alkali-activated slag concrete,” *Cem. Concr. Res.*, vol. 30, no. 9, pp. 1401–1406, Sep. 2000.

[70] T. Ayub, S. U. Khan, and F. A. Memon, “Mechanical characteristics of hardened

concrete with different mineral admixtures: a review.," *ScientificWorldJournal.*, vol. 2014, p. 875082, 2014.

[71] R. S. Ghosh and J. Timusk, "Creep of Fly Ash Concrete," *ACI J. Proc.*, vol. 78, no. 5, pp. 351–357, Sep. 1981.

[72] Almusallam TH., "Effect of fly ash on the mechanical properties of concrete," in *4th Saudi Engineering Conference*, 1995, pp. 187–192.

[73] P. Nath and P. Sarker, "Effect of Fly Ash on the Durability Properties of High Strength Concrete," *Procedia Eng.*, vol. 14, pp. 1149–1156, 2011.

[74] M. Mazloom, A. A. Ramezanianpour, and J. J. Brooks, "Effect of silica fume on mechanical properties of high-strength concrete," *Cem. Concr. Compos.*, vol. 26, no. 4, pp. 347–357, May 2004.

[75] D. D. L. L. Chung, "Review: Improving cement-based materials by using silica fume," *J. Mater. Sci.*, vol. 37, no. 4, pp. 673–682, Feb. 2002.

[76] J. Newman and B. Choo, *Advanced Concrete Technology : Processes*, 3rd ed. Butterworth-Heinemann, 2003.

[77] A. M. Neville, "Concretes with particular properties," in *Properties of Concrete*, 5th ed., Harlow, 2011, p. 666.

[78] A. A. Ramezanianpour and V. M. Malhotra, "Effect of curing on the compressive strength, resistance to chloride-ion penetration and porosity of concretes incorporating slag, fly ash or silica fume," *Cem. Concr. Compos.*, vol. 17, no. 2, pp. 125–133, Jan. 1995.

[79] M. H. F. Medeiros *et al.*, "Corrosion potential: influence of moisture, water-cement ratio, chloride content and concrete cover," *Rev. IBRACON Estruturas e Mater.*, vol. 10, no. 4, pp. 864–885, Aug. 2017.

[80] M. I. Khan and R. Siddique, "Utilization of silica fume in concrete: Review of durability properties," *Resour. Conserv. Recycl.*, vol. 57, pp. 30–35, Dec. 2011.

[81] S.-S. Park, Y. Y. Kim, B. J. Lee, and S.-J. Kwon, "Evaluation of Concrete Durability

Performance with Sodium Silicate Impregnants," *Adv. Mater. Sci. Eng.*, vol. 2014, pp. 1–11, Aug. 2014.

[82] C. Plowman and J. G. Cabrera, "The use of fly ash to improve the sulphate resistance of concrete," *Waste Manag.*, vol. 16, no. 1–3, pp. 145–149, Jan. 1996.

Vitae

Name	:Rayhan Md. Faysal
Nationality	:Bangladeshi
Date of Birth	:10/13/1990
Email	:rayhanfaysal24@gmail.com
Address	:215/B, Khilgoan, Dhaka-1219, Bangladesh
Academic Background	:Civil Engineering

- B.Sc. Degree from Civil Engineering Department, College of Engineering, Bangladesh University of Engineering and Technology, Dhaka, Bangladesh, February 2013.
- M.Sc. Degree in Civil Engineering from the Civil Engineering Department, College of Engineering, King Fahd University of Petroleum and Minerals, Dhahran, Saudi Arabia, June 2019.